

Dissertation zur Erlangung des Doktorgrades  
der Fakultät für Chemie und Pharmazie  
der Ludwig-Maximilians-Universität München



**Identification of novel mechanisms of action  
contributing to the biological activity of cytotoxic  
natural compounds**

Nancy López Antón

aus

Sabadell / Barcelona

2006



### Erklärung

Diese Dissertation wurde im Sinne von § 13 Abs. 3 bzw. 4 der Promotionsordnung vom 29. Januar 1998 von Frau Prof. Dr. A. M. Vollmar betreut.

### Ehrenwörtliche Versicherung

Diese Dissertation wurde selbständig, ohne unerlaubte Hilfe erarbeitet.

München, am 02.03.2006

---

(Nancy López Antón)

Dissertation eingereicht am: 02.03.2006

1. Gutachter: Frau Prof. Dr. A. M. Vollmar

2. Gutachter: Herr PD. Dr. C. Culmsee

Mündliche Prüfung am: 03.04.2006



dedicated to my family



“Life is pleasant. Death is peaceful.  
It’s the transition that’s troublesome”  
Isaac Asimov



# I. CONTENTS

<b>I. CONTENTS .....</b>	<b>1</b>
<b>II. ABBREVIATIONS .....</b>	<b>2</b>
<b>III. INTRODUCTION .....</b>	<b>8</b>
1 BACKGROUND – NATURAL PRODUCTS IN CANCER THERAPY .....	8
2 CEPHALOSTATINS.....	9
3 SESQUITERPENE LACTONES .....	12
4 AIM OF THE WORK.....	14
5 PROGRAMMED CELL DEATH, APOPTOSIS AND NECROSIS.....	15
6 SIGNAL TRANSDUCTION IN APOPTOSIS.....	17
6.1 CASPASES .....	18
6.1.1 Classification and structure.....	18
6.1.2 Substrate cleavage.....	20
6.1.3 Mechanism of caspase activation and regulation.....	20
6.2 THE EXTRINSIC PATHWAY.....	22
6.3 INTRINSIC PATHWAYS .....	24
6.3.1 Mitochondria.....	24
6.3.2 Endoplasmic reticulum .....	27
6.3.3 Pathways originated in other organelles .....	31
7 ELIMINATION OF APOPTOTIC CELLS .....	32
7.1 PHAGOCYTOSIS.....	32
7.1.1 Importance .....	32
7.1.2 “Eat-me” signals on the apoptotic cell.....	33
7.1.3 Interaction phagocyte-target cell and phagocytosis .....	33
7.1.4 Inhibition of phagocytosis.....	36
7.2 CYTOKINE RESPONSE AND BIOLOGICAL CONSEQUENCES.....	36
7.3 ROLES OF APOPTOTIC CELL CLEARANCE IN DISEASE .....	39
<b>IV. MATERIALS AND METHODS .....</b>	<b>42</b>
1 MATERIALS.....	42
1.1 COMPOUNDS .....	42
1.2 BIOCHEMICALS, INHIBITORS, DYES AND CELL CULTURE REAGENTS .....	42
1.3 TECHNICAL EQUIPMENT.....	43
2 CELL CULTURE .....	44
2.1 CELL LINES.....	44
2.2 CULTURE AND SPLITTING .....	44
2.3 SEEDING FOR EXPERIMENTS.....	45

2.4	FREEZING AND THAWING .....	45
3	FLOW CYTOMETRY.....	46
3.1	INTRODUCTION.....	46
3.2	DETERMINATION OF CELL VIABILITY (PI EXCLUSION ASSAY) .....	48
3.3	QUANTIFICATION OF DNA FRAGMENTATION BY PI STAINING (NICOLETTI METHOD).....	49
3.4	MEASUREMENT OF ROS GENERATION .....	50
4	ANALYSIS OF OTHER CELL DEATH FEATURES .....	51
5	MICROSCOPY .....	52
5.1	LIGHT MICROSCOPY .....	52
5.2	CONFOCAL LASER SCANNING MICROSCOPY .....	52
6	LUMINOMETRIC CASPASE-9 ACTIVITY ASSAY .....	53
7	WESTERN BLOTT .....	54
7.1	PREPARATION OF SAMPLES.....	54
7.2	PROTEIN QUANTIFICATION .....	56
7.3	SDS-PAGE.....	56
7.4	WESTERN BLOTTING AND DETECTION.....	58
7.5	MEMBRANE STRIPPING .....	61
7.6	STAINING OF GELS AND MEMBRANES.....	61
8	MEASUREMENT OF Ca <sup>2+</sup> .....	62
9	CASPASE-4 siRNA.....	64
9.1	INSERT DESIGN AND CLONING INTO psiRNA-h7SKneo G1 VECTOR.....	65
9.2	TRANSFORMATION OF LyoComp GT116.....	66
9.3	MINI PREPARATION OF PLASMIDS .....	66
9.4	SEQUENCING OF THE siRNA INSERT .....	67
9.5	MAXI PREPARATION OF PLASMIDS .....	67
9.6	AMPLIFICATION OF psiRNA-h7SKneo AND psiRNA-h7SKnScr VECTORS.....	67
9.7	TRANSFECTION AND SELECTION OF JURKAT CELLS.....	68
9.8	EFFECT OF CASPASE-4 SILENCING IN CASPASE-9 ACTIVATION AND APOPTOSIS .....	68
10	PHAGOCYTOSIS ASSAY AND CYTOKINE RELEASE .....	69
10.1	EVALUATION OF PHAGOCYTOSIS.....	69
10.2	CYTOKINE QUANTIFICATION .....	70
10.3	ANALYSIS OF PHAGOCYTOSIS BY CONFOCAL MICROSCOPY .....	71
11	STATISTICS .....	72

## **V. RESULTS ..... 74**

A.	CEPHALOSTATIN 1.....	74
1	IMPORTANCE OF CASPASE-9 IN CEPHALOSTATIN 1-INDUCED APOPTOSIS .....	74
2	SIGNAL TRANSDUCTION IN CEPHALOSTATIN-INDUCED ENDOPLASMIC RETICULUM (ER) STRESS AND APOPTOSIS .....	75

2.1	CEPHALOSTATIN INDUCES ER STRESS .....	75
2.1.1	Influence on ER stress markers.....	75
2.1.2	Cephalostatin does not induce $\text{Ca}^{2+}$ release into cytosol.....	77
2.1.3	ROS production is not increased by cephalostatin 1 treatment.....	79
2.1.4	Ubiquitinated proteins accumulate upon cephalostatin 1 treatment.....	80
2.2	INVOLVEMENT OF THE ASK1/JNK SIGNALLING PATHWAY .....	81
2.2.1	Activation of ASK1 and JNK .....	81
2.2.2	Importance of ASK1 in cephalostatin 1-induced apoptosis .....	82
2.3	ROLE OF CASPASES IN CEPHALOSTATIN 1-INDUCED ER APOPTOTIC PATHWAY .....	83
2.3.1	Cephalostatin 1-induced activation of caspase-4 is necessary for apoptosis .....	84
2.3.2	Caspase-2 participation in apoptosis.....	87
2.3.3	Caspase-4 and caspase-2 are activated upstream of caspase-9 .....	88
2.3.4	Caspase-4 and caspase-2 are required for caspase-9 activation and apoptosis .....	90
2.4	ASK1/JNK AND CASPASE-4 PATHWAYS ACT INDEPENDENTLY.....	93
<b>B.</b>	<b>SESQUITERPENE LACTONES (SQL).....</b>	<b>94</b>
1	CHARACTERISTICS OF SQL-INDUCED CELL DEATH.....	94
1.1	CYTOTOXIC ACTIVITY .....	94
1.2	MORPHOLOGIC CHANGES OF THE NUCLEUS (DNA CONDENSATION AND FRAGMENTATION).....	95
1.3	CHANGES IN CELL MORPHOLOGY, PHOSPHATIDYL SERINE EXPOSURE AND MEMBRANE INTEGRITY .....	97
1.3.1	Light microscopic analysis of SQL-treated cells.....	97
1.3.2	Flow cytometric analysis of cell morphology, membrane permeability and translocation of phosphatidylserine .....	98
1.3.3	Analysis of membrane integrity by measure of LDH activity .....	99
1.4	CASPASE ACTIVATION .....	100
2	MACROPHAGE RESPONSE.....	101
2.1	ANALYSIS OF PHAGOCYTOSIS BY FLOW CYTOMETRY.....	101
2.1.1	Increase in macrophages cell size .....	101
2.1.2	Quantification of phagocytosis by analysis of cell fluorescence (FL1) .....	102
3	CONFOCAL MICROSCOPY .....	104
4	CYTOKINE RELEASE.....	106
<b>VI.</b>	<b>DISCUSSION .....</b>	<b>110</b>
<b>A.</b>	<b>CEPHALOSTATIN 1.....</b>	<b>110</b>
1	REQUIREMENT OF CASPASE-9 .....	110
2	INDUCTION OF ER STRESS .....	110
3	ASK1/JNK PATHWAY .....	112
4	INITIATOR CASPASES.....	112

4.1	CASPASE-4 .....	113
4.2	CASPASE-2 .....	114
5	CONCLUDING REMARKS AND FUTURE DIRECTIONS .....	115
<b>B.</b>	<b>SESQUITERPENE LACTONES .....</b>	<b>116</b>
1	INDUCTION OF PCD BY SESQUITERPENE LACTONES .....	116
2	ANTI-INFLAMMATORY EFFECT .....	117
2.1	EFFICIENT REMOVAL OF DYING CELLS.....	118
2.2	RELEASE OF CYTOKINES BY MACROPHAGES .....	119
3	CONCLUDING REMARKS .....	120
<b>VII.</b>	<b>SUMMARY .....</b>	<b>124</b>
<b>A.</b>	<b>CEPHALOSTATIN 1.....</b>	<b>124</b>
<b>B.</b>	<b>SESQUITERPENE LACTONES .....</b>	<b>125</b>
<b>VIII.</b>	<b>REFERENCES .....</b>	<b>128</b>
<b>IX.</b>	<b>APPENDIX .....</b>	<b>148</b>
1	ALPHABETICAL LIST OF COMPANIES .....	148
2	PUBLICATIONS .....	149
2.1	ABSTRACTS .....	149
2.2	ORIGINAL PUBLICATIONS .....	149
3	CURRICULUM VITAE .....	150
4	ACKNOWLEDGEMENTS .....	151

## INDEX OF FIGURES

FIGURE III.1: CEPHALODISCUS SP. (FAMILY CEPHALODISCIDAE). ....	10
FIGURE III.2: FINGERPRINT OF GROWTH INHIBITORY PROFILE OF CEPHALOSTATIN 1 EVALUATED BY THE NCI-60 IN VITRO CANCER SCREEN.....	11
FIGURE III.3: CHEMICAL STRUCTURE OF CEPHALOSTATIN 1 AND 2.....	12
FIGURE III.4: ILLUSTRATION AND PHOTOGRAPH OF <i>ARNICA MONTANA</i> . ....	13
FIGURE III.5: SESQUITERPENE LACTONES FROM <i>ARNICA MONTANA</i> .....	13
FIGURE III.6: SCHEMATIC REPRESENTATION OF APOPTOTIC AND NECROTIC CELL DEATH AND ELECTRON MICROGRAPHS OF A NECROTIC AND AN APOPTOTIC CELL.....	17
FIGURE III.7: CASPASE STRUCTURE. ....	19
FIGURE III.8: SCHEMATIC REPRESENTATION OF THE PROTEOLYTIC ACTIVATION OF CASPASES.....	19
FIGURE III.9: IAPs IN MAMMALS .....	22
FIGURE III.10: THE EXTRINSIC APOPTOTIC PATHWAY. ....	23
FIGURE III.11: THE MITOCHONDRIAL APOPTOTIC PATHWAY.....	25
FIGURE III.12: BCL-2 FAMILY MEMBERS .....	26
FIGURE III.13: THE UNFOLDED PROTEIN RESPONSE (UPR) PATHWAY. ....	28
FIGURE III.14: ER APOPTOTIC PATHWAYS. ....	30
FIGURE III.15: SIMPLIFIED MODEL FOR THE PHAGOCYTIC SYNAPSE. ....	35
FIGURE III.16: SUPPRESSION OF INFLAMMATION BY MACROPHAGES INGESTING APOPTOTIC CELLS. ....	38
FIGURE IV.1: CLOSE UP OF THE FLOW CHAMBER .....	47
FIGURE IV.2: OPTICAL BENCH DIAGRAM OF THE FACSCALIBUR BENCHTOP FLOW CYTOMETER .....	48
FIGURE IV.3. LSM 510 META BEAM PATH.....	53
FIGURE IV.4. psiRNA-h7SKNEO G1 VECTOR .....	64
FIGURE IV.5: SCHEMATIC ILLUSTRATION OF THE PHAGOCYTOSIS CO-CULTURE MODEL. ....	69
FIGURE V.1: CASPASE-9 IS ESSENTIAL FOR CEPHALOSTATIN 1-INDUCED APOPTOSIS. ....	74
FIGURE V.2: CEPHALOSTATIN 1 INDUCES ER STRESS IN JURKAT LEUKEMIA T CELLS. ....	76
FIGURE V.3: ER STRESS IS OBSERVED IN HE LA CARCINOMA CELLS TREATED WITH CEPHALOSTATIN 2. ....	77
FIGURE V.4: CEPHALOSTATIN 1 DOES NOT INDUCE $Ca^{2+}$ RELEASE INTO CYTOSOL.....	78
FIGURE V.5: HE LA CELLS DO NOT INCREASE INTRACELLULAR $Ca^{2+}$ CONCENTRATION IN RESPONSE TO CEPHALOSTATIN TREATMENT. ....	79
FIGURE V.6: ROS LEVELS ARE NOT INCREASED UPON CEPHALOSTATIN 1 TREATMENT.....	80
FIGURE V.7: ACCUMULATION OF UBIQUITIN-CONTAINING PROTEINS UPON CEPHALOSTATIN 1 TREATMENT. ....	81
FIGURE V.8: ACTIVATION OF ASK1 AND JNK BY CEPHALOSTATIN 1.....	82
FIGURE V.9: THE ASK1/JNK PATHWAY IS IMPORTANT FOR CEPHALOSTATIN 1-INDUCED APOPTOSIS. ....	83
FIGURE V.10: CASPASE-4 ACTIVATION BY CEPHALOSTATIN 1. ....	84
FIGURE V.11: CASPASE-4 IS NECESSARY FOR APOPTOSIS.....	85
FIGURE V.12 : CASPASE-4 IS INVOLVED IN APOPTOSIS IN HE LA CELLS. ....	86
FIGURE V.13 : CEPHALOSTATIN 1 ACTIVATES CASPASE-2.....	87

FIGURE V.14: CASPASE-4 AND CASPASE-2 ARE ACTIVATED UPSTREAM OF CASPASE-9 IN CEPHALOSTATIN 1-INDUCED APOPTOSIS.....	89
FIGURE V.15: CASPASE-4 AND CASPASE-2 ARE REQUIRED FOR CEPHALOSTATIN 1-INDUCED CASPASE-9 ACTIVATION.....	91
FIGURE V.16: CASPASE-4 AND -2 ACTIVATION ARE ESSENTIAL FOR CEPHALOSTATIN 1-INDUCED APOPTOSIS.....	92
FIGURE V.17: NEITHER ASK1 NOR JNK ARE INVOLVED IN CASPASE-4 ACTIVATION.....	93
FIGURE V.18: CHEMICAL STRUCTURE AND CYTOTOXIC ACTIVITY OF THE SQTL IN STUDY.....	95
FIGURE V.19: INDUCTION OF DNA FRAGMENTATION AND CONDENSATION, RESPECTIVELY, BY SQTL.....	96
FIGURE V.20: LIGHT MICROSCOPIC PICTURES OF SQTL-TREATED JURKAT T CELLS.....	97
FIGURE V.21: TEMPORAL CHANGES IN CELL MORPHOLOGY, MEMBRANE PERMEABILITY AND TRANSLOCATION OF PS DUE TO SQTL TREATMENT.....	99
FIGURE V.22: LDH LEVELS IN CULTURE MEDIUM OF SQTL-TREATED JURKAT CELLS.....	99
FIGURE V.23: CASPASES ARE ACTIVATED AND RESPONSIBLE FOR CHANGES IN NUCLEAR MORPHOLOGY IN RESPONSE TO SQTL TREATMENT.....	100
FIGURE V.24: QUANTIFICATION OF THE INCREASE IN THP-1-DERIVED MACROPHAGES CELL SIZE AFTER PHAGOCYTOSIS OF JURKAT CELLS.....	102
FIGURE V.25: PHAGOCYTOTIC ACTIVITY OF DIFFERENTIATED THP-1 CELLS FED WITH SQTL-TREATED JURKAT CELLS.....	103
FIGURE V.26: QUANTIFICATION OF PHAGOCYTOSIS BY DIFFERENTIATED THP-1 CELLS FED WITH SQTL-TREATED JURKAT CELLS BY FLOW CYTOMETRY.....	104
FIGURE V.27: REPRESENTATIVE PICTURES SHOWING CO-LOCALISATION OF MACROPHAGES AND TARGET CELLS FLUORESCENCE.....	105
FIGURE V.28: 3D PROJECTIONS OF MACROPHAGES THAT HAVE ENGULFED JURKAT CELLS.....	106
FIGURE V.29: CONCENTRATION OF TNF- $\alpha$ AND TGF-B IN CULTURE SUPERNATANTS OF THP-1 CELLS FED WITH SQTL-TREATED JURKAT CELLS.....	107
FIGURE VII.1: SCHEMATIC ILLUSTRATION OF CEPHALOSTATIN 1-INDUCED ER STRESS MARKERS AND APOPTOTIC PATHWAYS.....	124

## **INDEX OF TABLES**

TABLE III.1: REPRESENTATIVE ANTICANCER DRUGS FROM NATURAL ORIGIN IN DEVELOPMENT OR CLINICAL USE .....	9
TABLE III.2: CLASSIFICATION OF PCD ACCORDING TO THE MORPHOLOGY OF THE DYING CELL .....	16
TABLE IV.1: FREEZING MEDIUM. ....	46
TABLE IV.2: EMISSION WAVELENGTH AND DETECTORS.....	47
TABLE IV.3: SEPARATING GEL CONCENTRATIONS. ....	57
TABLE IV.4: PRIMARY ANTIBODIES. ....	60
TABLE IV.5: SECONDARY ANTIBODIES.....	60
TABLE IV.6: INSERT OLIGONUCLEOTIDES CONTAINING siRNA SEQUENCES. ....	65
TABLE VII.1: CELL DEATH CHARACTERISTICS OF 11 $\alpha$ ,13-DIHYDROHELENALIN ACETATE (DHA) AND 7-HYDROXYCOSTUNOLIDE (HC). ....	125



## **II. ABBREVIATIONS**

## II. ABBREVIATIONS

17-AAG	17-(allylamino)-17-demethoxygeldanamycin
AIDS	Acquired immune deficiency syndrome
AIF	Apoptosis inducing factor
ANOVA	Analysis of variance between groups
ANT	Adenine nucleotide translocator
Apaf-1	Apoptotic-protease-activating factor-1
APS	Ammonium persulfate
ASK1	Apoptosis signal-regulating kinase-1
ASK1-DN	Apoptosis signal-regulating kinase-1 dominant negative
ATF-4 / ATF-6	Activating transcription factor 4 / 6
ATP / dATP	Adenosine-5'-triphosphate / 2'-desoxyadenosine-5'-triphosphate
BAP31	B-cell receptor associated protein 31
Bcl	B-cell lymphoma
$\beta_2$ GP1	$\beta_2$ glycoprotein 1
BH	Bcl-2 homology
BiP	Binding protein
BIR	Baculoviral IAP repeat
bp	Base pair
BP	Band pass
BSA	Bovine serum albumin
CAD	Caspase-activated DNase
Carboxy-H <sub>2</sub> DCFDA	Carboxy-2',7'-dichlorodihydrofluorescein diacetate
CARD	Caspase recruitment domain
CCFSE	5-(and-6)-carboxy-2',7'-dichlorofluorescein diacetate, succinimidyl ester
Cdc42	Cell division cycle 42
CED	Cell-death abnormality
c-FLIP	Cellular FLICE-inhibitory protein
CHOP	C/EBP homologous protein
CI	Confidence interval
c-IAP1 / c-IAP2	Cellular inhibitor of apoptosis 1 / 2
CR3 / CR4	Complement receptor 3 / 4
CrmA	Cytokine response modifier A
CRP	C-reactive protein
3D	Three-dimensional
DCF	2',7'-dichlorofluorescein
DD	Death domain

DED	Death effector domain
DHA	11 $\alpha$ ,13-dihydrohelenalin acetate
DIABLO	Direct IAP-binding protein with low pI
DISC	Death-inducing signalling complex
DMSO	Dimethyl sulfoxide
DNA	Deoxyribonucleic acid
DR4 / DR5	Death receptor 4 / 5
DTT	Dithiothreitol
ECL	Enhanced chemoluminescence
EDTA	Ethylenediaminetetraacetic acid
EGTA	Ethylene glycol-bis(2-aminoethylether) tetraacetic acid
eIF2 $\alpha$	Eukaryotic translation initiation factor-2, $\alpha$ -subunit
ELISA	Enzyme-linked immunosorbent assay
EM	4 $\beta$ ,15-epoxymiller-9Z-enolide
EndoG	Endonuclease G
EOR	ER-overload response
ER	Endoplasmic reticulum
ERAD	ER-associated degradation
ERK	Extracellular signal-regulated kinase
ERSE	ER stress response element
FACS	Fluorescence-activated cell sorter
FADD	Fas-associated death domain
FasL	Fas ligand
FCS	Foetal calf serum
FITC-VAD-fmk	Fluorescein isothiocyanate- Val-Ala-Asp(OMe)-fluoromethylketone
FL	Fluorescence
FSC	Forward scatter
Fura-2-AM	Fura-2 acetoxyethyl ester
GADD153	Growth arrest and DNA damage-inducible gene 153
Gas-6	Growth-arrest-specific 6
GI <sub>50</sub>	Growth inhibition of 50%
GM-CSF	Granulocyte macrophage-colony stimulating factor
GRP78 / GRP94	Glucose-regulated protein of 78 / 94 kDa
HC	7-hydroxycostunolide
H <sub>2</sub> DCF	2',7'-dichlorodihydrofluorescein
HEPES	N-(2-hydroxyethyl)piperazine-N'-(2-ethanesulfonic acid)
HFS	Hypotonic fluorochrome solution
HMGB-1	High-mobility group box chromosomal protein-1
HtrA2	High-temperature-requirement protein A2

## II Abbreviations

---

IAP	Inhibitor of apoptosis
ICAD	Inhibitor of caspase-activated DNase
ICAM-3	Intercellular adhesion molecule-3
ICE	Interleukin-1 $\beta$ converting enzyme
IL	Interleukin
INF	Interferon
IPTG	Isopropyl- $\beta$ -D-thigalactopyranoside
IRE1	Inositol requiring-1
ITIMs	Immuno-receptor tyrosine-based inhibitory motifs
JNK	c-Jun N-terminal kinase
kDa	Kilo Dalton
LB	Lysogeny broth
LDH	Lactate dehydrogenase
LDL	Low density lipoproteins
$\lambda_{em}$	Emission wavelength
LOX1	Lectin-like oxLDL-receptor 1
LP	Long pass
LPS	Lipopolysaccharide
LTC <sub>4</sub>	Leukotriene C <sub>4</sub>
MBL	Mannose-binding lectin
MFG-E8	Milk fat globule epidermal growth factor (EGF) factor 8
MKP-1	MAPK phosphatase-1
MMP	Mitochondrial membrane permeabilisation
mRNA	Messenger ribonucleic acid
MTT	3-(4,5-dimethylthiazol-2-yl)-2,5-diphenyl tetrazolium bromide
NADH	Nicotinamide adenine dinucleotide
NAIP	Neuronal apoptosis inhibitory protein
NCI	National cancer institute
NF- $\kappa$ B	Nuclear factor kappa B
nt	Nucleotide
p-	Phospho-
p38 MAPK	p38 mitogen-activated protein kinase
PAA	Polyacrylamide
PAF	Platelet activating factor
PAK2	p21 (CDKN1A)-activated kinase 2
PARP	Poly(ADP-ribose) polymerase
PBS	Phosphate buffered saline
PCD	Programmed cell death
PDI	Protein disulfide isomerase

PECAM-1	Platelet-endothelial cell adhesion molecule-1
PERK	PKR-like ER-localised eIF2 $\alpha$ kinase
PGE <sub>2</sub>	Prostaglandin E <sub>2</sub>
PI	Propidium iodide
PIDD	p53-induced protein with a DD
PKR	Double-stranded RNA-activated protein kinase
PMA	Phorbol myristate acetate
PMSF	Phenylmethylsulphonylfluoride
PS	Phosphatidylserine
PSR	Phosphatidylserine receptor
PTPC	Permeability transition pore complex
RAIDD	RIP associated ICH-1/CED-3-homologous protein with DD
RNAi	RNA interference
ROCK-1	Rho-associated coiled-coil forming kinase 1
ROS	Reactive oxygen species
sCD95	Soluble CD95
SDS	Sodium dodecyl sulfate
SDS-PAGE	Sodium dodecyl sulfate polyacrylamide gel electrophoresis
SEM	Standard error of the mean
shRNA	Short hairpin RNA
siRNA	Short interfering RNA
SLE	Systemic lupus <i>erythematosus</i>
Smac	Second mitochondria-derived activator of caspases
SP-A / SP-B	Surfactant protein A / B
SQTL	Sesquiterpene lactones
SR-A / SR-B	Scavenger receptor A / B
SSC	Side scatter
TBS-T	Tris-buffered saline with Tween
TEMED	N, N, N' N' tetramethylethylene diamine
TGF	Transforming growth factor
TLR2 / 4	Toll-like receptor 2 / 4
TNF	Tumour necrosis factor
TNF-R1	Tumour necrosis factor receptor 1
TRAIL	TNF-related apoptosis-inducing ligand
TRAIL-R1 / TRAIL-R2	TNF-receptor associated apoptosis inducing ligand receptor 1 / 2
TRAF2	TNF receptor-associated factor 2
TSP	Thrombospondin
TXB <sub>2</sub>	Thromboxane B <sub>2</sub>
UPR	Unfolded protein response

## II Abbreviations

---

UV	Ultraviolet
VDAC	Voltage-dependent anion channel
WB	Western Blot
XBP-1	X-box binding protein
x-Gal	5-bromo-4-chloro-3-indolyl-β-D-galactopyranoside
XIAP	X-linked inhibitor of apoptosis
zLEVD-fmk	N-benzyloxycarbonyl-Leu-Glu-Val-Asp-fluoromethylketone
zVAD-fmk	N-benzyloxycarbonyl-Val-Ala-Asp(OMe)-fluoromethylketone
zVDVAD-fmk	N-benzyloxycarbonyl-Val-Asp-Val-Ala-Asp-fluoromethylketone

### **III. INTRODUCTION**

## III. INTRODUCTION

### 1 BACKGROUND – NATURAL PRODUCTS IN CANCER THERAPY

Cancer is the second-biggest cause of death in developed countries despite the global efforts and the major advances achieved in the last decades. Surgery is most frequently the first line of therapy. It may be used alone or in combination with radiotherapy, a valuable tool for the control of local tumours. However, more effective anticancer therapies are required for most patients. The use of drugs (chemotherapy) and/or other additional treatments as anti-angiogenic and immune therapies are needed to treat disseminated cancer and achieve eradication of the disease.

The chemotherapy of cancer started with the discovery of nitrogen mustard sixty years ago but in spite of the successful advances the main problems observed at that time still exist: the acute and long-term toxicities and probability of relapses [1,2].

A wide range of chemotherapeutic drugs induce death in malignant cells by inducing apoptosis [3,4] though other forms of programmed cell death (see III.5) seem to be involved in the killing of certain tumour cells [5]. Inactivation of apoptosis is one of the fundamental hallmarks of cancer and also the major contributor to drug resistance developed by many cancer cells [6]. Compounds employing novel mechanisms of action, different from conventional chemotherapeutic drugs, can certainly help to resensitise tumour cells to cancer therapy. In this respect, nature provides us with esoteric structures that may have unusual modes of action and help to combat chemoresistance.

In fact, natural products or their structural relatives comprise about 50% of the drugs used for cancer chemotherapy. Plants, microorganisms and marine organisms have been screened by the NCI (National Cancer Institute, USA) since almost 50 years and have given us exceptional drugs and very promising antineoplastic agents (Table III.1 shows some examples).

**Table III.1: Representative anticancer drugs from natural origin in development or clinical use (adopted from [7-9]).**

<b>Drug (class)</b>	<b>Source</b>
Etoposide, teniposide (Lignans)	<i>Podophyllum peltatum</i> (plant)
Vincristine, vinblastine (Vinca alkaloids)	<i>Catharanthus roseus</i> ( <i>Vinca rosea</i> ) (plant)
Paclitaxel, docetaxel (Taxanes)	<i>Taxus brevifolia</i> , <i>Taxus baccata</i> (plant)
Topotecan, irinotecan (Camptothecins)	<i>Camptotheca accuminata</i> (plant)
Combretastatin A-4	<i>Combretum caffrum</i> (plant)
Geldanamycin, 17-AAG	<i>Streptomyces hygroscopicus</i> (microorganism)
Epothilones A-D	<i>Sorangium cellulosum</i> (microorganism)
Bleomycin	<i>Streptomyces verticillus</i> (microorganism)
Daunomycin, doxorubicin (Anthracyclines)	<i>Streptomyces</i> sp. (microorganism)
Bryostatin 1	<i>Bugula neritina</i> (marine organism)
Aplidin™	<i>Aplidium albicans</i> (marine organism)
Dolastatin 10	<i>Dolabella auricularia</i> (marine organism)
Spongistatin 1	<i>Hyrtios altum</i> (marine organism)

None of the compounds isolated from marine organisms has been accepted to commercialisation yet. However, several drugs as Aplidin™ and Bryostatin 1 are in clinical development.

The NCI introduced in 1990 a new programme in which extracts from plants, animals and microorganisms are screened against a rationally designed panel of 60 human tumour cell lines, derived from different solid human cancer types (colon, brain, lung, melanoma, ovary, kidney, breast, and prostate) and leukaemia. Interestingly, the growth-inhibitory patterns ( $GI_{50}$ ) of anticancer drugs against the cell lines correlate with their mechanism of action.

## 2 CEPHALOSTATINS

The family of cephalostatins has been isolated by Prof. G. R. Pettit from various collections of the South African marine tube worm *Cephalodiscus gilchristi* Ridewood (family Cephalodiscidae) (Figure III.1). Up to now 19 members of this family have been characterised [10-18], all of which have shown remarkable activity in the NCI-60 panel with differences in their overall toxicity.

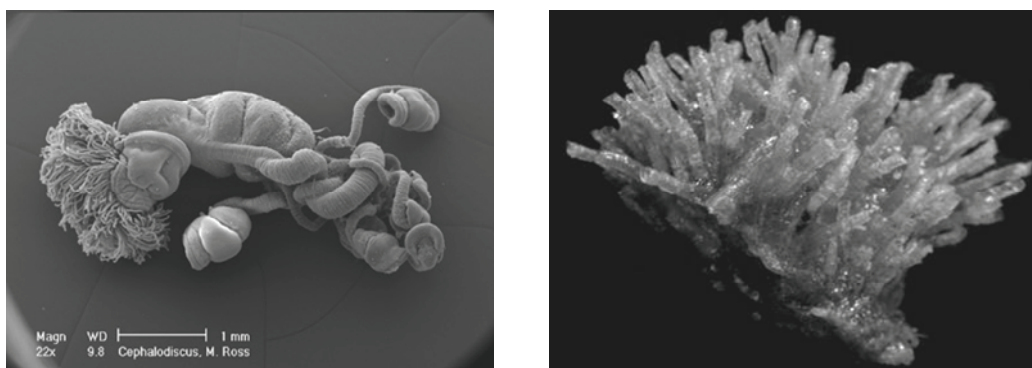


**Figure III.1: Cephalodiscus sp. (family Cephalodiscidae).**  
Left panel, scanning electron microscopy micrograph of a zooid. Right panel, general view of a whole colony [19].

Cephalostatins possess a similar and unique growth-inhibitory fingerprint (Figure III.2), which suggests that they may employ a novel mechanism of action different from any other anticancer agent. The first studies destined to elucidate the mechanism of action of cephalostatin 1 support this notion [20]. Cephalostatin 2 potency is comparable to cephalostatin 1 (Figure III.3) and employs the same signalling pathways than cephalostatin 1 (research performed in our group by Anita Rudy).

The main limitation of cephalostatins is their low yield (0.0008% w/w) in the worm. A total synthesis has been achieved [9,21], but it is not a suitable alternative to the isolation from *C. gilchristi* yet. The complexity and unprecedent nature of their structures makes synthesis a difficult and long process, not feasible for the future from an industrial and economic point of view.

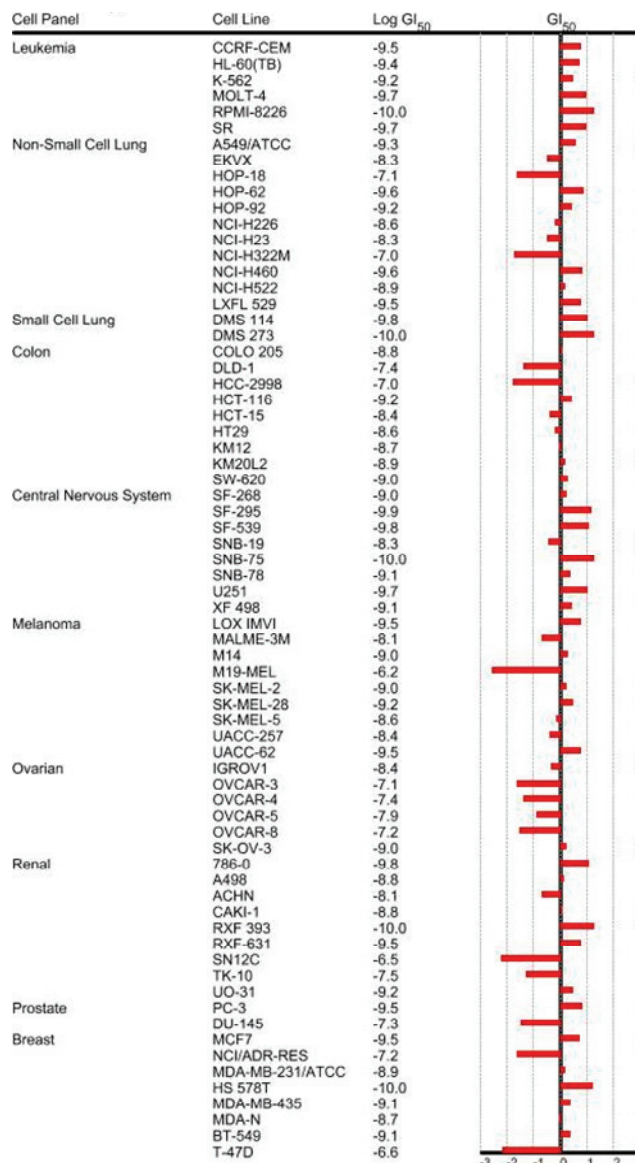


**Figure III.2: Fingerprint of growth inhibitory profile of cephalostatin 1 evaluated by the NCI-60 in vitro cancer screen (September 2005, [22]).**

The zero value represents the mean of all cell lines. Bars indicate the deviation of the mean data obtained from the individual cell line from the overall mean. Negative bars correspond to less sensitive cell lines and positive bars, to more sensitive. Average GI<sub>50</sub> (growth inhibition of 50%) of cephalostatin 1 was 1.8 nM.

Due to this complexity, the structure of cephalostatin 1 (Figure III.3), the first isolated and the most potent member of the family was not reported until 1988. Cephalostatin 1 is 400-fold more active *in vitro* than paclitaxel and one of the most powerful cytostatics ever to be tested by the NCI with a mean GI<sub>50</sub> of 1.8 nM [9]. Structure-activity studies on cephalostatins and their analogues revealed that the Northern part (see Figure III.3) is not only the most common unit in the cephalostatin family but is also strongly associated with the most

potent antitumour activity. An increased hydroxylation in the Southern part results in a reduction in the human cancer cell growth inhibition [9].

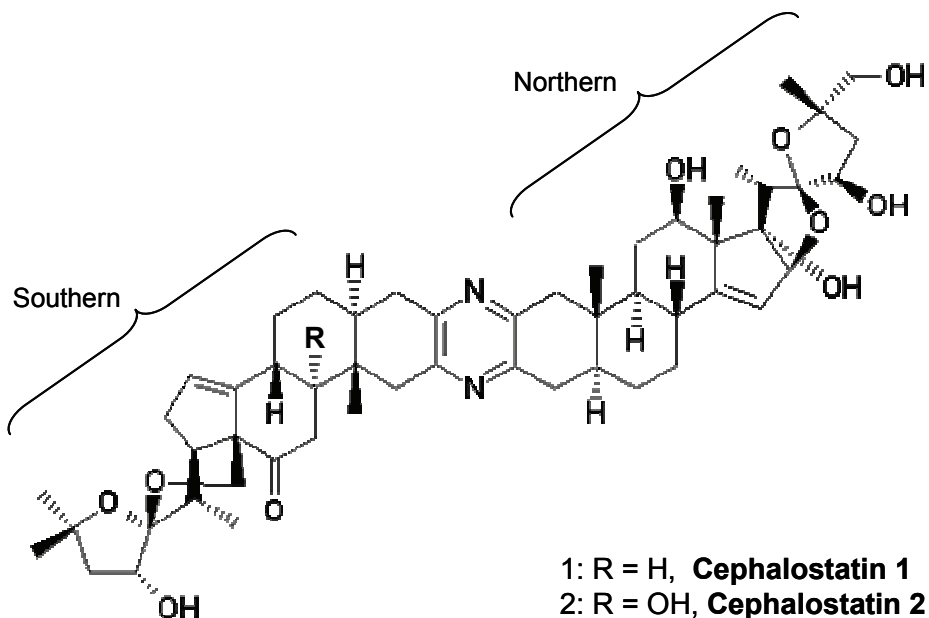


**Figure III.3: Chemical structure of cephalostatin 1 and 2.**

The biological activity of cephalostatin 1 is being evaluated by *in vivo* screenings in the NCI employing models of melanoma, in sarcoma, mammary carcinoma and P388 leukaemia in mice.

### 3 SESQUITERPENE LACTONES

Sesquiterpene lactones (SQL) are secondary plant metabolites found predominantly in the sunflower family (Asteraceae). Since decades these compounds are recognised to have cytotoxic [23-27] as well as an anti-inflammatory potential [28-33], accompanied by antibacterial and analgesic properties. In traditional medicine, preparations from flowers of *Arnica montana* (Figure III.4) are used externally to treat various inflammatory diseases.



**Figure III.4: Illustration and photograph of *Arnica montana*.**

The leaves from *A. montana* form a flat rosette, from the center of which rises a flower stalk, 1 to 2 feet high, bearing orange-yellow flowers. The rhizome is dark brown, cylindrical, usually curved (*left panel*, from [34,35]). *Right panel*, photograph of a flower [36].

SQTL of pseudoguaianolide type are the most potent compounds found in preparations of *A. montana*, with helenalin, dihydrohelenalin and their acetate and fatty acids esters as prominent representatives (Figure III.5). The most common structural feature of biologically active SQTL is an  $\alpha$ -methylene- $\gamma$ -lactone. In addition or alternatively, other  $\alpha,\beta$ -unsaturated carbonyl structures, such as  $\alpha,\beta$ -unsaturated cyclopentenones are found. These structural elements are thought to mediate the biological effects of SQTL by alkylating biological macromolecules, in particular enzymes with sulphydryl groups [23,24,26,37].

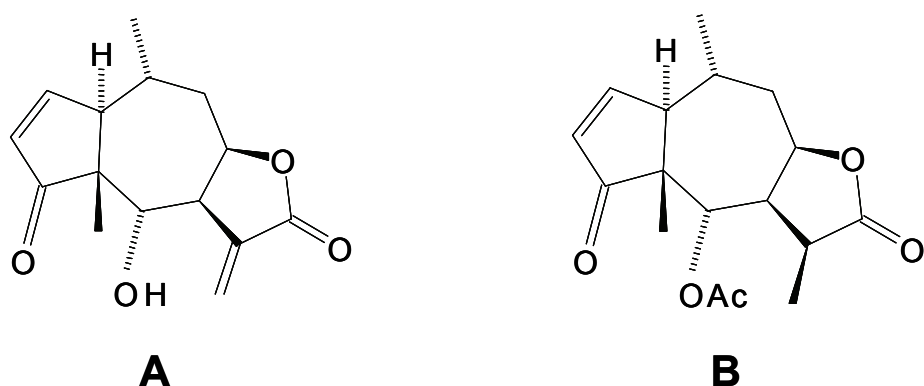


**Figure III.5: Sesquiterpene lactones from *Arnica montana*.**

Chemical structure of helenalin (**A**) and dihydrohelenalin acetate (**B**).

The anti-inflammatory activity of SQTL has been linked mainly to an inhibition of the activity of the transcription factor nuclear factor kappa B (NF- $\kappa$ B), although there is some controversy about the exact mechanism of inhibition [28,38,39]. Several studies have shown that SQTL with both kinds of  $\alpha,\beta$ -unsaturated groups were the most active in *in vivo* and *in vitro*, but the  $\alpha$ -methylene- $\gamma$ -lactone moiety seemed the most important property [31,33].

The antitumoral activity of helenalin, possessing two  $\alpha,\beta$ -unsaturated carbonyl structural elements (Figure III.5 A) was first reported in 1967. It proved to be the most active constituent of a collection of *Helenium autumnale* screened by the NCI in an *in vivo* assay employing the murine P388 lymphocytic leukaemia [7]. Toxic activities of SQTL have been explained by the covalent binding to sulphhydryl groups of biological molecules (such as endogenous glutathione) by Michael addition of their  $\alpha,\beta$ -unsaturated carbonyl structures [23,37,40]. Early structure-activity relationships reported that the presence of the  $\alpha$ -methylene- $\gamma$ -lactone group was essential for their cytotoxic activity and an  $\alpha,\beta$ -unsaturated ester or cyclopentenone strengthened this property [24,25]. On the contrary, studies on helenalin derivatives have shown that the contribution of a cyclopentenone group to cytotoxicity is considerably higher than that of the methylene lactone group (summarized in [41]). In addition, a correlation between lipophilicity and cytotoxic activity could be shown [42].

However, the mode of cell death induced by SQTL and the signalling pathways involved were not investigated until recently. Our group reported that programmed cell death induced by helenalin differs considerably from that of classical chemotherapeutic drugs. Importantly, helenalin is capable to overcome mitochondrial apoptosis resistance mechanisms [43].

#### 4 AIM OF THE WORK

The aim of the present work was to investigate mechanisms of action contributing to the biological activity of the natural compounds cephalostatin 1 and selected sesquiterpene lactones, heading at identifying exceptional or unusual signalling. The project can be dislodged in two parts:

- A. Characterisation of cephalostatin 1-induced apoptosis: contribution of endoplasmic reticulum signalling pathways
- B. Investigation of whether the mode of cell death induced by sesquiterpene lactones with different reactive groups influences macrophage response and a putative anti-inflammatory effect

## 5 PROGRAMMED CELL DEATH, APOPTOSIS AND NECROSIS

In multicellular organisms, programmed cell death (PCD) is an essential physiological process required for the maintenance of proper tissue homeostasis. PCD can be defined as a coordinated sequence of events based on cellular metabolism that leads to cell destruction and occurs at a specific point in development [44,45]. Dispensable or potentially dangerous cells are forced to die and are removed by phagocytes to avoid negative consequences for the organism such as inflammation or autoimmune responses. The most classical form of PCD is referred to as apoptosis, term first employed by Kerr et al. in 1972 [46] to describe a form of cell death in mammals distinctive to necrosis. Apoptosis is a genetically controlled event required to maintain the balance to mitosis and differentiation, with essential roles in embryogenesis and the homeostasis of the immune system, but also involved in diseases such as cancer, AIDS or neurodegenerative diseases.

“Apoptosis” refers to a particular morphology characterised by cell shrinkage, internucleosomal cleavage of chromatin, blebbing of the plasma membrane and finally fragmentation of the cell into apoptotic bodies. These fragments are enclosed by an intact plasma membrane, avoiding leakage of intracellular contents into the surrounding tissue. A hallmark of apoptosis is the exposure of phosphatidylserine (PS) on the surface of apoptotic cells, which mediates their recognition and phagocytosis by macrophages. Caspases, a family of cysteine proteases, are specifically activated in apoptosis and mediate the series of characteristic morphological changes.

Forms of PCD different than apoptosis have been extensively described [44,47-50]. However, there is a lack of suitable names or classification of these modes of death. Some definitions are overlapping and dying cells may display a mixture of some morphological and/or molecular features associated to more than one of the types of PCD. According to morphological changes PCD can be classified into apoptosis, apoptosis-like PCD, necrosis-like PCD or autophagy (Table III.2) [47]. Biochemically, apoptosis (caspase-dependent) can be differentiated from death controlled by other proteases (caspase-independent cell death) [45]. Now it is accepted that all these forms of cell death exist *in vivo* and can occur under physiologic circumstances, but may be triggered by chemotherapeutic drugs as well [50-52]. In fact, a single stimulus may initiate overlapping death pathways depending on conditions such as the intracellular levels of ATP, nitrative/oxidative stress [53] or caspase inhibition.

**Table III.2: Classification of PCD according to the morphology of the dying cell (adapted from [47,50,51]).**

MODE OF DEATH	CHARACTERISTICS
<b>Apoptosis</b> (type I cell death)	<ul style="list-style-type: none"> <li>• Chromatin condensation into compact figures (stage II)</li> <li>• Internucleosomal DNA fragmentation</li> <li>• Cytoplasm condensation</li> <li>• Activation of caspases</li> <li>• Phosphatidylserine exposure</li> <li>• Zeiosis and formation of apoptotic bodies</li> <li>• Phagocytosis of dying cell</li> </ul>
<b>Apoptosis-like PCD</b>	<ul style="list-style-type: none"> <li>• Chromatin condensation less compact than in apoptosis (stage I)</li> <li>• Caspase-dependent or –independent</li> <li>• Display of phagocytosis-recognition molecules before lysis of the plasma membrane</li> <li>• Induced by AIF (apoptosis inducing factor), endonuclease G, cathepsins, other proteases</li> </ul>
<b>Necrosis-like PCD</b>	<ul style="list-style-type: none"> <li>• Absence of chromatin condensation or chromatin clustering to form loose speckles</li> <li>• Usually caspase-independent</li> <li>• Externalisation of PS might occur before lysis</li> <li>• Result of the interception of active cellular processes by oxygen-radical scavengers, Bcl-2, protease inhibitors or inhibition of autophagosome formation</li> </ul>
<b>Autophagy</b> (type II cell death)	<ul style="list-style-type: none"> <li>• Caspase-independent</li> <li>• Formation of lysosome-derived cytosolic vacuoles containing organelles and cytoplasm.</li> <li>• Can be also classified as necrotic-like PCD.</li> </ul>

Necrosis is the conceptual counterpart to PCD (Figure III.6). It is an accidental, passive and uncontrolled mode of cell death that occurs after exposure to high concentrations of detergents, oxidants, ionophores or high intensities of pathologic insult (hyperthermia, hypoxia, ischemia, direct cell trauma, etc.). Necrosis is characterised by cellular swelling, absence of zeiosis (membrane blebbing), partial degradation of DNA in randomly sized fragments, disruption of organelles and lysis of the plasma membrane, leading to release of the potentially inflammatory cellular contents. Necrosis typically affects groups of contiguous cells and provokes a substantial inflammatory response.

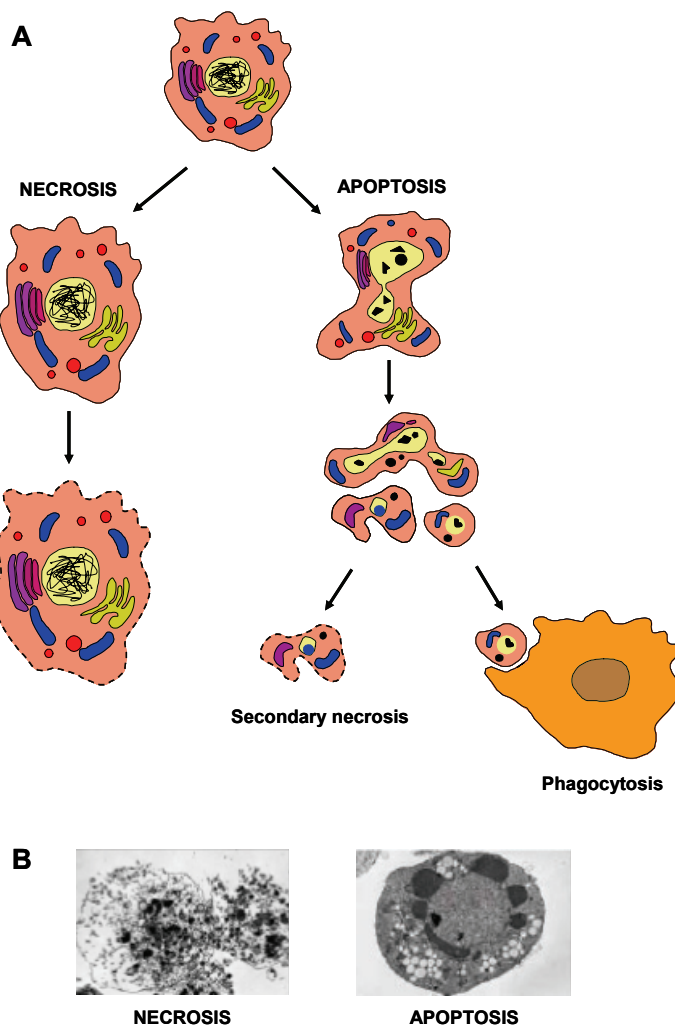


**Figure III.6:** Schematic representation of apoptotic and necrotic cell death (A) and electron micrographs of a necrotic and an apoptotic cell (B, from [54]).

Necrosis is characterised by swelling of the cytoplasm and organelles, followed by a rupture of plasma membrane and release of the cellular contents (*left*). On the contrary, apoptotic death (*right*) is characterised by condensation of the nucleus and the cell followed by fragmentation of the cell into apoptotic bodies with intact membranes, which are rapidly removed by macrophages (*phagocytosis*). Apoptotic cells that have not been removed by phagocytes may lose their integrity and proceed to secondary or apoptotic necrosis.

## 6 SIGNAL TRANSDUCTION IN APOPTOSIS

Cell death with apoptotic morphology can be triggered by several stimuli, including intracellular stress and receptor-mediated signalling. These signals activate an evolutionarily conserved and highly regulated intracellular machinery of execution where caspases play a pivotal role.

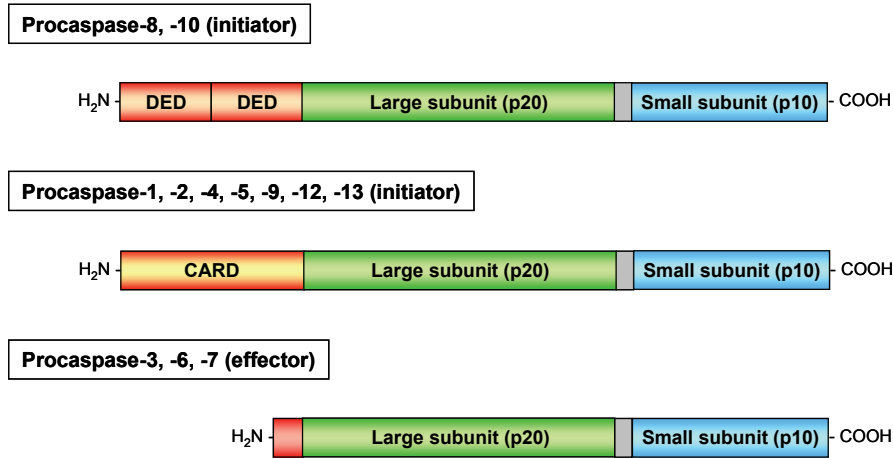
## 6.1 CASPASES

Early pioneering work in the molecular mechanism mediating apoptosis was developed in the worm *Caenorhabditis elegans*, where it was observed that apoptosis was determined by 3 genes, including an inhibitor of apoptosis (*ced-9*), an executor of apoptosis (*ced-3*) and an activator of apoptosis (*ced-4*). The general structure of this death sequence is evolutionarily conserved from nematodes to humans [55]. Identification of interleukin-1 $\beta$ -converting enzyme (ICE, now known as caspase-1) as the mammalian protein related to CED-3 led to the discovery of a whole family of proteases critically involved in apoptosis and today called caspases (cysteinyl-aspartate-cleaving proteases). Apart from caspases, other proteases can lead to the characteristic apoptotic morphology, including other cysteine proteases as calpains, cathepsins (lysosomal proteases) or serine proteases [47]. They contribute to the action of caspases or mediate caspase-independent cell death, and are often mutually activated by caspases in an amplification signal of cell death.

### 6.1.1 Classification and structure

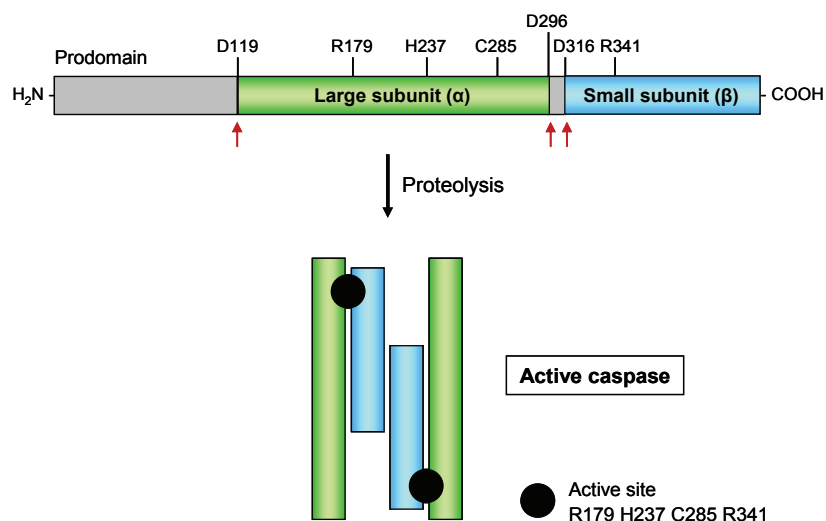
To date, 15 mammalian caspases have been identified, of which there are 11 in humans. Caspases are zymogens (inactive enzyme precursors) that consist of an N-terminal prodomain of variable length followed by a large subunit of about 20 KDa (p20) and a small subunit of about 10 KDa (p10) (Figure III.7). The p20 and p10 subunits are separated by a small linker sequence. Depending on the structure of the prodomain and their function, caspases are typically divided into 3 major groups [56]. Caspases with large prodomains (>90 residues) are classified by their phylogenetic relationship in inflammatory caspases (caspase-1, -4, -5 and -13) and apoptotic initiator caspases (caspase-2, -8, -9, -10 and -12). Caspases with short prodomains (20-30 residues) belong to the group of effector caspases (caspase-3, -6 and -7).

The large prodomain of procaspases contain structural motifs that belong to the death domain (DD) superfamily. The death effector domain (DED) and the caspase recruitment domain (CARD) are responsible for the recruitment of initiator caspases into death- or inflammation-inducing signalling complexes, where they are activated. Procasparase-8 and -10 possess 2 tandem DEDs in their prodomain and the CARD is found in procasparase-1, -2, -4, -5, -9, -12 and -13 [57].

**Figure III.7: Caspase structure.**

Pro caspase-8 and -10 carry two repeats of the DED in their long prodomain, whereas other initiator caspases contain a CARD domain. All effector caspases have short prodomains (red). Prodomains are followed by the large subunit (~20 KDa), a linker region (grey) and the small subunit (~10 KDa).

Except pro caspase-9 and probably some other initiator caspases, all zymogens require proteolytic activation [58,59]. Mature caspases are “homodimers of heterodimers” [60] formed by association of two monomers, with each monomer comprising the large (p20 or  $\alpha$ -) and the small (p10 or  $\beta$ -) subunits (Figure III.8). Each tetramer contains two active sites, positioned at opposite ends of the molecule and comprising amino acid residues from the p20 and p10 subunits.

**Figure III.8: Schematic representation of the proteolytic activation of caspases [59].**

Activation proceeds by cleavage of the N-terminal domain at Asp119, Asp296 and Asp316 (all caspase-1 numbering convention) leading to a large ( $\alpha$ ) and a small ( $\beta$ ) subunit. The activity and specificity determining residues (R179, H237, C285 and R341) are brought into the necessary structural arrangement for catalysis. Cys285 is the catalytic nucleophile. The active caspase is a tetramer of two heterodimers, each comprising a large and a small subunit and an active site.

### 6.1.2 Substrate cleavage

Caspases are specific cysteine proteases that recognise four amino acids (except for caspase-2, five) named P4-P3-P2-P1 and cleave C-terminal to P1, which in most cases is an Asp residue [61]. Interestingly, P3 corresponds to Glu for all known mammalian caspases, leading to a general recognition sequence X-Glu-X-Asp. The cleavage site between the large and small subunits for initiator caspases carries its own tetrapeptide recognition motif, which is consistent with the model proposing that initiator caspases are autoactivated.

To date, more than 280 caspase targets are identified [62]. Many structural and regulatory proteins are inactivated by caspases, while other substrates can be activated to ensure proper induction of cell death. Proteolysis of certain components leads to the morphological changes of cell death. Cleavage of ICAD (inhibitor of caspase-activated DNase) by caspase-3 liberates the active CAD (caspase-activated DNase) nuclease that mediates apoptotic DNA fragmentation while cleavage of PARP [poly (ADP-ribose) polymerase] inhibits DNA repair. The cleavage of gelsolin and the kinases ROCK-1 (Rho-associated coiled-coil forming kinase 1) and PAK2 [p21 (CDKN1A)-activated kinase 2] has been implicated in membrane blebbing. Destruction of nuclear matrix proteins and cytoskeletal proteins (actin, nuclear lamin) results in loss of the cellular architecture. Activation of Bid by caspase-8 is an example of the amplification of a death signal. Moreover, cell-protective mechanisms as c-FLIP (cellular FLICE-inhibitory protein), Bcl-2, Bcl-x<sub>L</sub>, Akt or NF-κB are turned off by caspase cleavage.

### 6.1.3 Mechanism of caspase activation and regulation

All caspases are produced as single-chain inactive proenzymes located in cytosol or cellular compartments and must be tightly regulated to prevent spontaneous cell death. Caspases are subject to transcriptional regulation, post-translational modifications and are eliminated by ubiquitination and degradation by the proteasome system.

The activation of caspases proceeds by limited proteolysis and removal of the N-terminal prodomain and the linker peptide within the protease domain. Effector caspases are activated by initiator caspases through cleavage at specific internal Asp residues that separate the large and small subunits. As a consequence, a conformational change occurs and the catalytic activity of the effector caspase is enhanced by several orders of magnitude [59].

Effector caspases are responsible for the proteolytic cleavage of a broad spectrum of cellular targets, leading ultimately to cell demise.

Activation of initiator caspases occurs upon recruitment to large macromolecular activation complexes and is explained by the induced proximity and proximity-induced dimerisation model [63]. Apoptotic and inflammatory caspases are recruited and brought into close proximity by virtue of their long DED or CARD domains. The dimerisation of inactive monomers is sufficient to trigger the activation and processing of procaspases. Up to now, complexes have been described for the activation of procaspase-8 and -10 (DISC), procaspase-9 (apoptosome), procaspase-2 (PIDDosome) [64] and procaspase-1 and -5 (inflammasome) [65,66].

Endogenous caspase inhibitors inhibit either the activation of caspases or the proteolytic effect of activated caspases. c-FLIP proteins are inhibitors of the extrinsic pathway of apoptosis by blocking activation of procaspase-8 at the death-inducing signalling complex (DISC). The enzymatic activity of mature caspases is inhibited by the IAP (inhibitor of apoptosis) protein family [67]. To date eight distinct mammalian IAPs have been identified (Figure III.9). The BIR (baculoviral IAP repeat) domain is the functional unit in IAPs, responsible for the binding to caspases. XIAP (X-linked inhibitor of apoptosis), c-IAP1 (cellular inhibitor of apoptosis 1), c-IAP2 (cellular inhibitor of apoptosis 2) and NAIP (neuronal apoptosis inhibitory protein) have three of such sequences. XIAP, the most efficient of the family, specifically inhibits active caspase-3, -7 and -9. Survivin controls cell division and inhibits apoptosis selectively in cancer cells. Down-regulation of survivin has emerged as a promising approach for the sensitisation of tumour cells to chemotherapy [68].

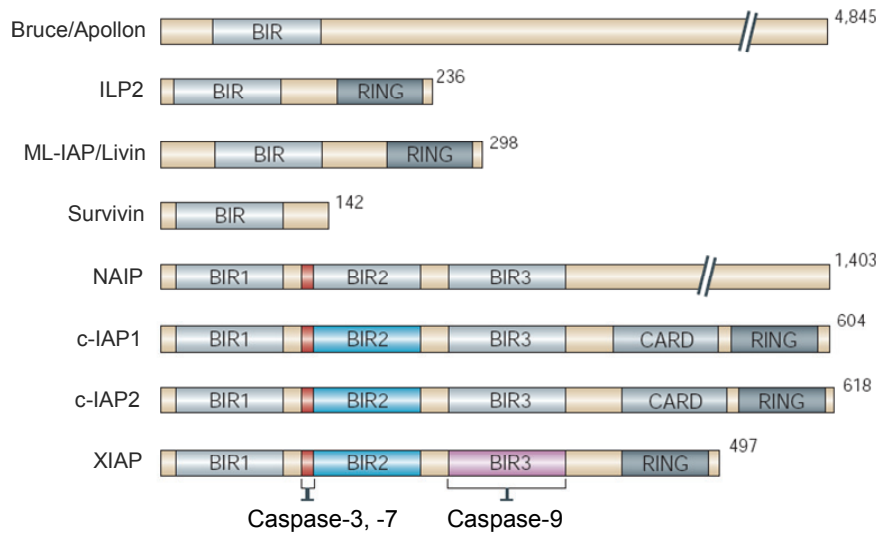


**Figure III.9: IAPs in mammals (adapted from [67]).**

Members of the mammalian IAP family and their domain structure. A conserved linker peptide that precedes the BIR2 domain of XIAP, c-IAP1 or c-IAP2 is responsible for inhibiting caspases-3 and -7. Only the BIR3 domain of XIAP can potently inhibit caspase-9 by interacting with the small subunit. Mammalian IAPs are controlled by binding of Smac and Omi/HtrA2 (see III.6.3.1).

Other natural inhibitors of caspases are viral proteins responsible for the survival of infected mammalian cells. CrmA (cytokine response modifier A) is a serpin that inhibits the activity of caspase-1 and -8 and the baculoviral p35 protein is a pan-caspase inhibitor [69].

## 6.2 THE EXTRINSIC PATHWAY

In mammalian cells, the apoptotic response is initiated through either the intrinsic pathway (see III.6.3) or the extrinsic pathway, depending on the origin of the death stimuli [6,55,67]. The extrinsic pathway is mediated by death receptors on the cell surface and is of particular importance in multicellular systems where signalling is crucial, such as the immune system. Death receptors are members of the TNF (tumour-necrosis factor) receptor superfamily and comprise a subfamily that is characterised by an intracellular death domain and an extracellular ligand-binding domain. Prominent representatives are Fas/CD95, TNF-R1 (tumour-necrosis factor receptor-1), DR4/TRAIL-R1 (death receptor-4/TNF-related apoptosis-inducing ligand receptor-1) or DR5/TRAIL-R2. The “decoy receptors” constitute a negative regulatory mechanism of the extrinsic pathway. These receptors, such as soluble CD95 (sCD95) bind the death ligands but cannot propagate downstream signals due to non-functional or absent death domains [6].

The extrinsic pathway (Figure III.10) is activated by the binding of an extracellular death ligand, such as Fas ligand (FasL), to its death receptor, such as Fas. Binding leads to the formation of a minimally homotrimeric ligand-receptor complex that recruits an intracellular adaptor protein, such as FADD (Fas-associated death domain), and the inactive proforms of caspase-8 or caspase-10, forming the death-inducing signalling complex (DISC). Formation of the DISC leads to the activation and cleavage of the initiator caspase-8, which in turn cleaves and activates downstream effector caspases (caspase-3, -6 and -7) [6]. The DISC complex formation downstream of other death receptors (DR4/5, TNF-R1) is similar to the Fas pathway.

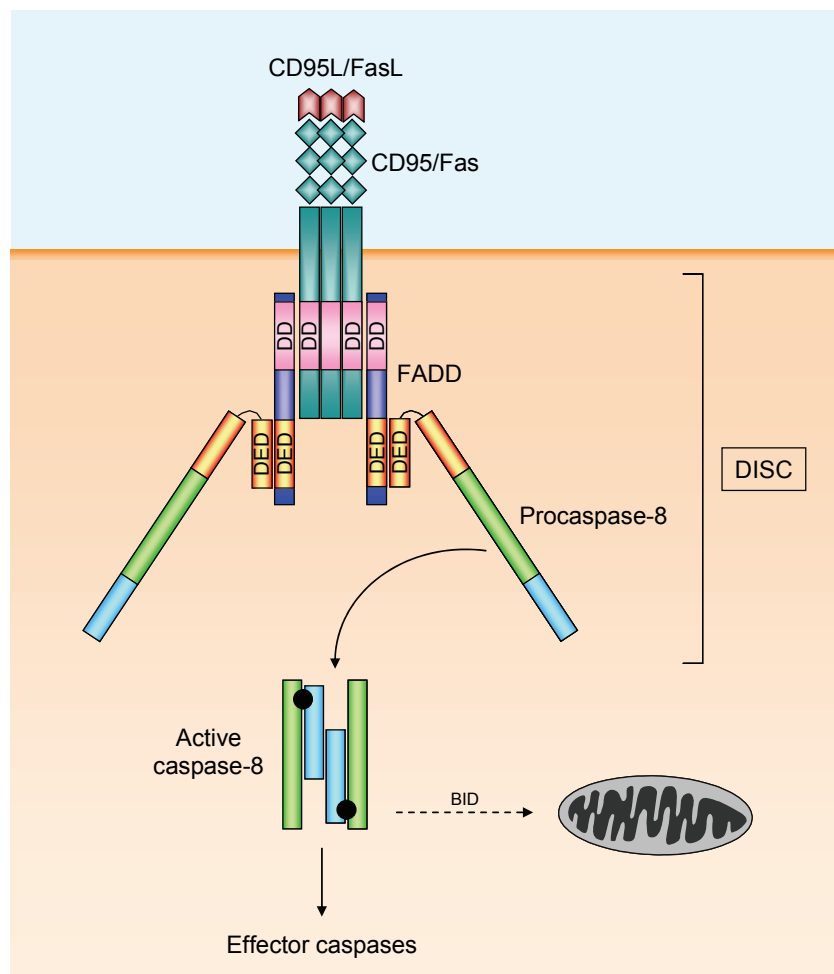


**Figure III.10: The extrinsic apoptotic pathway.**

Binding of death ligands (FasL, in this example) to their preassembled receptor (as a trimer) results in the recruitment of the adaptor protein FADD and procaspase-8, forming the death-inducing signalling complex (DISC). FADD contains a death domain (DD), which enables the association with the intracellular part of the death receptor and a death effector domain (DED), which binds procaspase-8. In the DISC, procaspase-8 is autolytically cleaved and activates effector caspases. Active caspase-8 can also cleave Bid to amplify the apoptotic signal through mitochondria.

In some cells (known as type I cells) the amount of active caspase-8 formed is sufficient to initiate apoptosis directly, but in other cells (type II) the amount is too small and requires amplification of the death signal through mitochondria to generate sufficient effector caspase activity. This cross-talk is mediated through the caspase-8-mediated cleavage of Bid, which then translocates to mitochondria and triggers the release of pro-apoptotic proteins (see III.6.3.1).

## 6.3 INTRINSIC PATHWAYS

### 6.3.1 Mitochondria

Work over the past few years has revealed that, apart from being the cell's powerhouse, mitochondria is a crucial organelle regulating and mediating apoptotic cell death. In response to many apoptotic stimuli, such as chemotherapeutic agents, toxins or cellular stress, mitochondrial membrane integrity is disrupted, process known as mitochondrial membrane permeabilisation (MMP). As a consequence, an arsenal of pro-apoptotic proteins exclusively confined to mitochondria under physiological conditions are released from mitochondria into the cytoplasm and initiate or promote apoptotic pathways (Figure III.11). Some stimuli, as bilirubin,  $\beta$ -amyloid or bacterial toxins can induce MMP directly. Chemotherapeutic drugs induce MMP by mechanisms including generation of reactive oxygen species (ROS), increase of mitochondrial  $\text{Ca}^{2+}$  uptake or translocation of pro-apoptotic Bcl-2 proteins and/or inhibition of anti-apoptotic family members (see the **Bcl-2 family**) [70].

Apoptogenic proteins released from the intermembranal space include cytochrome c, Smac/DIABLO (second mitochondria-derived activator of caspases/direct IAP-binding protein with low pI), AIF (apoptosis-inducing factor), EndoG (endonuclease G) and Omi/HtrA2 (high-temperaturerequirement protein A2).

The most investigated of these proteins is cytochrome c, which binds to and activates the protein Apaf-1 (apoptotic-protease-activating factor-1) in the cytoplasm. The binding of cytochrome c to Apaf-1 induces a conformational change that allows Apaf-1 to bind to ATP/dATP and recruit procaspase-9 to form the apoptosome. The high local concentration of procaspase-9 promotes its activation and self-processing and acts as the initiator of a caspase cascade leading to cell death.

Smac/DIABLO interacts with multiple inhibitor of apoptosis proteins (IAPs) and removes IAP-mediated inhibition of active initiator and effector caspases. A Smac dimer binds the BIR2 domain of XIAP and allows caspase-3 activation. In the monomeric form, Smac binds the BIR3 domain of XIAP and relieves inhibition of processed caspase-9. Omi/HtrA2 contains an IAP-binding tetrapeptide motif and a serine protease domain and induces caspase-independent cell death. The serine protease domain is absolutely essential to the cell killing activity whereas the N-terminal IAP-binding motif appears less critical [61]. AIF translocates to the nucleus and triggers apoptotic-like death characterised by caspase-independent chromatin condensation and the formation of large DNA fragments. Endonuclease G also translocates to the nucleus, where it catalyses both high molecular weight DNA cleavage and oligonucleosomal DNA fragmentation [71].

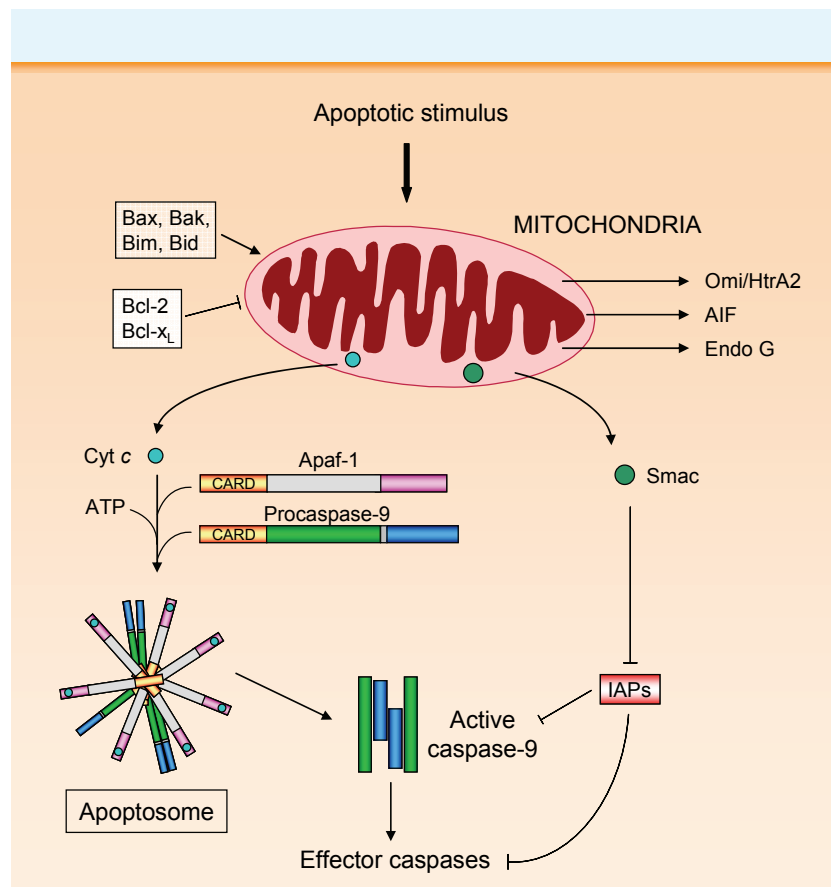


**Figure III.11: The mitochondrial apoptotic pathway.**

Many apoptotic stimuli induce mitochondrial membrane permeabilisation (MMP) and release of apoptogenic factors from mitochondria. Cytochrome c (cyt c) binds and activates Apaf-1, which in turn recruits procaspase-9 to the Apoptosome leading to auto-activation of caspase-9. Then, caspase-9 activates downstream effector caspases. Smac/DIABLO relieves the inhibition of active initiator and effector caspases by the IAPs. AIF, Omi/HtrA2 and endonuclease G initiate own death pathways. Anti-apoptotic Bcl-2 proteins inhibit the release of mitochondrial proteins whereas the pro-apoptotic members contribute to MMP.

## The bcl-2 family

The intrinsic pathway of apoptosis is critically regulated by the Bcl-2 family, an evolutionarily conserved group of proteins including pro-apoptotic as well as anti-apoptotic members [55,72]. The founding member is Bcl-2, first identified as a protooncogene involved in human follicular B cell lymphoma (hence the name *bcl*) and homologue to the *C. elegans ced-9* gene [55]. These proteins have been classified into three functional groups (Figure III.12). Members of the first group, such as Bcl-2 and Bcl-x<sub>L</sub>, possess anti-apoptotic activity and are characterised by four short, conserved Bcl-2 homology (BH) domains (BH1-BH4). They also possess a C-terminal hydrophobic tail, which anchors the proteins to organelles as mitochondria and the endoplasmic reticulum. Group II consists of Bcl-2 proteins with pro-apoptotic activity as Bax and Bak, with an overall structure similar to the first group. Group III is formed by a large and diverse collection of proteins whose common feature is the only presence of the BH3 domain and are also known as “BH3-only” proteins (Bid, Bik, Bim, Bad, among others).

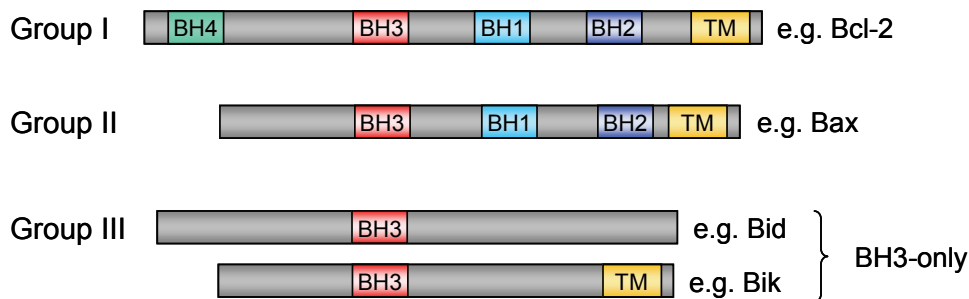


**Figure III.12: Bcl-2 family members (adapted from [72]).**

The group I include anti-apoptotic proteins, characterised by four conserved Bcl-2 homology domains (BH1-BH4) and a hydrophobic domain (TM) responsible for the localisation to membranes. Group II proteins are pro-apoptotic and lack the BH4 domain. Group III consists of the pro-apoptotic “BH3-only” proteins.

The multidomain pro-apoptotic members Bax and Bak are crucially involved in the induction of MMP and release of mitochondrial proteins. Upon receipt of a death signal inactive Bax and/or Bak experience a conformational change, oligomerise and insert into the mitochondrial membrane forming protein-permeable channels. Intermembrane mitochondrial proteins as cytochrome c are released through these channels. Another model proposes that Bax and Bak interact with and regulate the permeability of the permeability transition pore complex (PTPC), formed by the adenine nucleotide translocator (ANT,

inner membrane), the voltage-dependent anion channel (VDAC, outer membrane) and other proteins [72].

The BH3-only members serve as “sensors” that selectively respond to specific death and survival signals. For example, cleavage of Bid by caspase-8 occurs after the activation of death receptors and Bad is switched on and off by its phosphorylation in response to survival factors. Activation of BH3-only molecules results in the activation of Bax, Bak and formation of channels. On the contrary, Bcl-2 and Bcl-x<sub>L</sub> bind and sequester BH3-only proteins, preventing Bax and Bak activation and the release of pro-apoptotic mitochondrial proteins.

### 6.3.2 Endoplasmic reticulum

The endoplasmic reticulum (ER) is the principal site of synthesis and folding of proteins [73,74] destined for secretion, the cell membrane, Golgi apparatus and lysosomes and a site of biosynthesis for steroids, cholesterol and other lipids. The second essential function of the ER is the storage and signalling of calcium ( $\text{Ca}^{2+}$ ).

Chaperone proteins, a high  $\text{Ca}^{2+}$  concentration and an oxidative environment within the ER are required to fulfil these functions efficiently [75,76]. Properly folded proteins exit from the ER and progress down the secretory pathway to the Golgi complex. Any alterations in the ER environment can disrupt ER function, resulting in what has been referred to as “ER stress” [75,77-80]. The two major causes leading to ER stress are an alteration of  $\text{Ca}^{2+}$  homeostasis and the accumulation of unfolded or misfolded proteins. Thus, ER stress can be induced by calcium depletion from the ER lumen, inhibition of protein glycosylation, reduction of disulfide bonds, expression of mutated proteins in the ER or impairment of protein transport to the Golgi, among others. In order to overcome ER stress, this organelle has a specific signalling pathway globally called the “ER stress response” pathway.

The ER responds with activation of the unfolded protein response (UPR) signal transduction pathway, the ER-overload response (EOR) and the ER-associated degradation (ERAD) to survive the stress. These pathways lead to a reduction in the amount of newly synthesised proteins, an increased degradation of misfolded proteins and an augmentation of the protein folding capacity of the ER. However, if the damage is too strong or prolonged, apoptosis is initiated to protect the organism from the damaged cell.

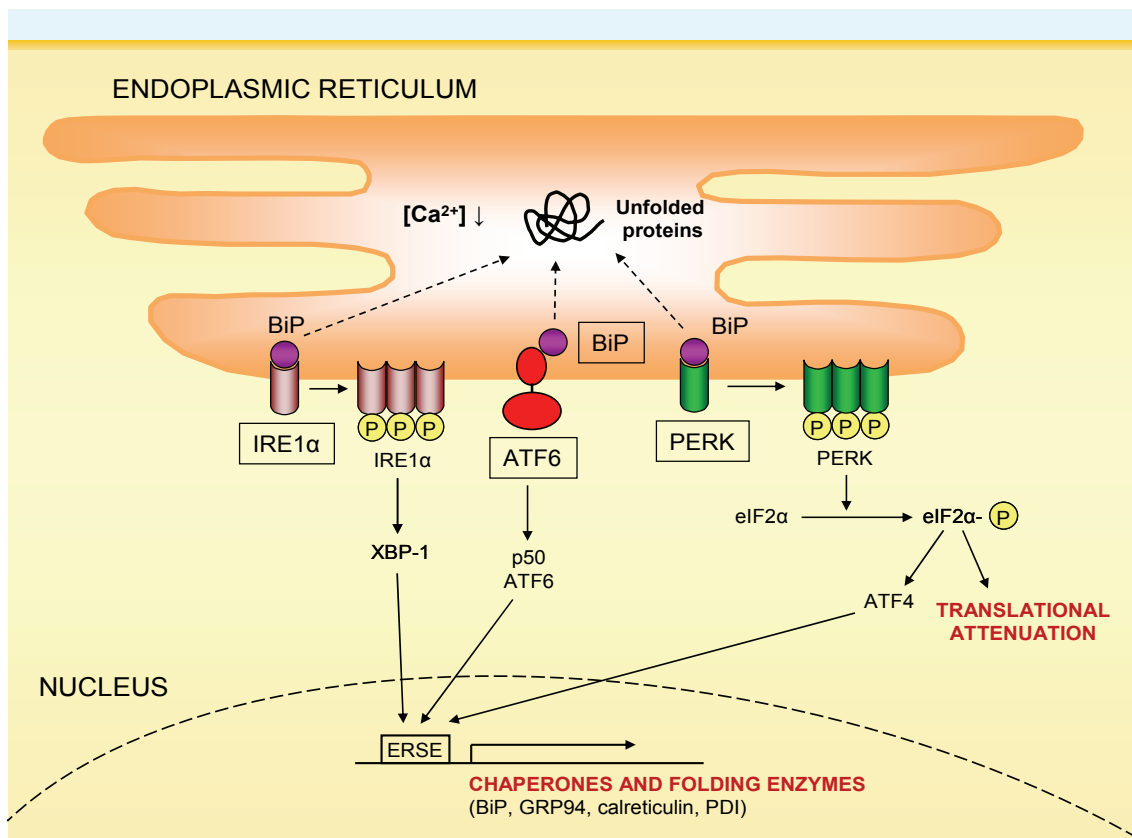


**Figure III.13: The unfolded protein response (UPR) pathway.**

The UPR is activated by the accumulation of unfolded proteins in the ER. The transmembrane proteins IRE1, PERK and ATF6 act as sensors and induce the transcription factors XBP-1, p50ATF6 and ATF4, which in turn stimulate the transcription of their target genes. Target genes of the UPR share a consensus sequence in their promoters, the ER stress response element (ERSE), and code for chaperones and other proteins involved in protein folding as BiP/GRP78, GRP94, calreticulin or PDI (protein disulfide isomerase). Phosphorylation of eIF2 $\alpha$  by PERK leads to an attenuation of general protein synthesis.

The UPR (Figure III.13) is initiated by the activation of three ER transmembrane proteins: IRE1 (inositol requiring-1), ATF6 (activating transcription factor-6) and PERK (PKR-like ER-localised eIF2 $\alpha$  kinase). These proteins are normally kept in an inactive state through an association between their N-terminal luminal domains and the chaperone BiP/GRP78 (binding protein/glucose-regulated protein of 78 kDa). Under accumulation of unfolded proteins in the ER, BiP dissociates from IRE1, PERK and ATF6 to bind unfolded proteins. IRE1 and PERK undergo homooligomerisation and autophosphorylation within their serine/threonine kinase domains. IRE1 contains a C-terminal endonuclease domain that excises a short sequence from the mRNA of the X-Box binding protein (XB<sup>+</sup>1), generating an active bZIP transcription factor that stimulates transcription of ER chaperones and other folding enzymes. PERK phosphorylates the translation initiation factor eIF2 $\alpha$ , leading to an attenuation

of general translational initiation and protein synthesis but to a stimulation of the translation of the mRNA of the transcription factor ATF4. ATF6 translocates from the ER to the Golgi, where it is processed to generate an N-terminal cytosolic domain, p50ATF6, which translocates to the nucleus and induces UPR target genes including BiP and XBP1.

The EOR is triggered by accumulation of membrane proteins in the ER. It is believed that  $\text{Ca}^{2+}$  release from ER and sequent production of reactive oxygen intermediates activates NF- $\kappa$ B, a transcription factor mediator of anti-apoptotic responses. The ERAD pathway eliminates misfolded proteins in the ER by the ubiquitin-proteasome system [81,82].

When these stress modulators are unable to rescue cells, at least three pathways can induce apoptosis (Figure III.14). The cytosolic domain of activated IRE1 recruits the adaptor molecule TRAF2 (TNF receptor-associated factor 2) and activates the apoptosis signal-regulating kinase 1 (ASK1)/c-Jun N-terminal kinase (JNK) cascade [79]. In addition, the transcription factors activated by the UPR, but most notably ATF4, increase the transcription of CHOP (C/EBP homologous protein), a transcription factor that induces cell cycle arrest and apoptosis by modulation of Bcl-2 and many other proteins [82,83]. Furthermore, caspases participate in ER-triggered apoptosis [80]. Caspase-12 (a murine caspase) aggregates at the ER membrane surface through the complex IRE1-TRAF2, resulting in its cleavage and activation, followed by activation of caspase-9 independent of cytochrome c and Apaf-1 [80,84,85]. Caspase-7 can translocate to the ER surface upon ER stress and participate in caspase-12 activation [86]. In humans, caspase-4 has been proposed to play a role as ER stress-specific caspase similarly to caspase-12 [87], and also caspase-2 can be activated by ER stress [88,89]. Caspase-8 cleavage of the transmembrane protein BAP31 (B cell receptor associated protein 31) generates a p20 fragment that probably induces a pro-apoptotic  $\text{Ca}^{2+}$  flux between the ER and mitochondria [75,77].

On the other hand, an increase in cytosolic free  $\text{Ca}^{2+}$  as the primary mechanism causing ER stress or as a consequence of the ER dysfunction can activate many proteins involved in cell death pathways [90-92]. For instance, the  $\text{Ca}^{2+}$ -activated protein phosphatase calcineurin dephosphorylates the BH3-only protein BAD, promoting mitochondrial targeting of BAD and apoptosis [93].

Calpains are a family of cysteine proteases that require  $\text{Ca}^{2+}$  for their activity [94-96]. An increasing number of cellular proteins are dually susceptible to cleavage by calpain and caspases, especially in neuronal death. The activation of calpains can facilitate or inhibit apoptotic cell death and switch to necrosis depending on the cellular context [92,97,98]. Notably, caspase-12 has been reported to be activated upon cleavage by calpain [99].

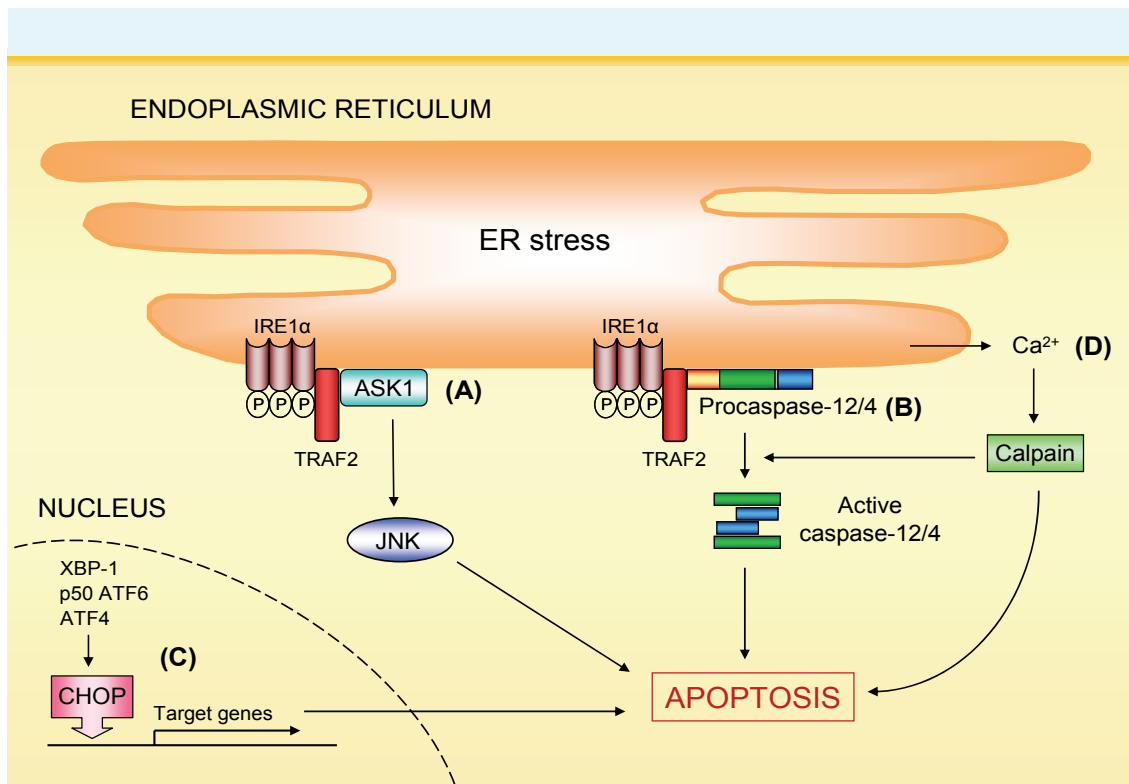


**Figure III.14: ER apoptotic pathways.**

ER stress-activated IRE1 recruits TRAF2 and ASK1 to the ER membrane surface, leading to activation of ASK1 and its downstream kinase JNK (A). The initiator caspase-12 and probably caspase-4 can also aggregate at the ER through TRAF2, resulting in the activation of caspase-12/4 (B). In addition, the UPR-activated transcription factors ATF4, XBP-1 and p50ATF6 activate the pro-apoptotic transcription factor CHOP (C).  $\text{Ca}^{2+}$  released from the ER lumen can activate the cysteine protease calpain, which may activate caspase-12/4 or induce cell death on its own (D).

Besides their role in mitochondria, Bcl-2 family members participate in the regulation of apoptosis at the ER. Bcl-2, Bcl-x<sub>L</sub>, Bax, Bak and some BH3-only proteins can localise to the ER membrane. Bax, Bak and Bcl-2 exert a critical control of the  $\text{Ca}^{2+}$  homeostasis in the ER and subsequent cross-talk to mitochondria. Bcl-2 reduces the quantity of  $\text{Ca}^{2+}$  released after a pro-apoptotic stimulus arrives by increasing the leak of  $\text{Ca}^{2+}$  under resting conditions, thus lowering mitochondrial  $\text{Ca}^{2+}$  uptake [90,100,101]. The pro-apoptotic proteins

Bax and Bak exert the contrary effect and, in fact, are required for the induction of apoptosis by some apoptotic stimuli whose primary target is not the ER [102,103]. Furthermore, the interaction of the BH3-only protein Bim with Bcl-x<sub>L</sub> has been reported to induce caspase-12 activation and apoptosis [104].

### Caspase-4 and caspase-2

Caspase-4 was first described in 1995 as a novel protein with protease and apoptotic activity exhibiting 50% sequence identity with caspase-1. It was classified in the inflammatory caspase family, proteases involved in the processing of pro-inflammatory cytokines as IL-1 (interleukin 1) and IL-18. Many studies have demonstrated that caspase-4 is necessary in Fas-, TRAIL (TNF-related apoptosis-inducing ligand)- and INF (interferon)-induced apoptosis [105-109]. But most importantly, caspase-4 has been proposed to be the human homologue and fulfil the same function than mouse caspase-12. Caspase-4 was recently shown to mediate apoptosis induced specifically by ER stress and amyloid  $\beta$  treatment [87]. Interestingly, a physiological role for caspase-4 in apoptosis has been lately described [110]. During spontaneous plasma cell death, ER stress induces caspase-4 activation upstream of mitochondria that leads to caspase-3 activation and apoptosis.

Even though caspase-2 was the second mammalian caspase identified, its exact role in the regulation of cell death is controversial and relatively unknown, in part due to its different function dependent on cell type and stimulus. Caspase-2 contains a CARD domain, as other initiator caspases, and shares sequence homology with caspase-1, -4, -5 and -9. Caspase-2 can act as initiator caspase (cleavage of itself and golgin-160) but has characteristics of effector caspase (e.g. cleavage of  $\alpha$ -spectrin). It is localised predominantly to the Golgi complex and the nucleus, but also in mitochondria and cytosol [111]. Caspase-2 is activated in response to DNA damage, where it acts as the only initiator caspase, and it appears necessary for apoptosis triggered by UV (ultraviolet) irradiation, trophic factor withdrawal [112,113], cytokine deprivation or administration of TNF and TRAIL. Importantly, caspase-2 has been also implicated in neuronal death induced by  $\beta$ -amyloid [114] and recently in ER stress [88,89].

#### 6.3.3 Pathways originated in other organelles

Besides mitochondria and the endoplasmic reticulum, other organelles have been demonstrated to trigger, or at least to participate in, apoptotic and non-

apoptotic cell death [70]. Examples are the activation of p53 in the nucleus or the role of lysosomes in autophagic and in cathepsins-mediated cell death.

The Golgi apparatus plays an essential role in membrane traffic and is situated in an ideal position to sense and integrate information about the state of the cell. Even though its role has not been deeply investigated so far, some studies evidence a potential and specific role in cell death. The Golgi complex contains several apoptosis-signalling proteins: caspase-2, death receptors (TNF-R1, Fas), beclin (protein involved in autophagy) and GD3 synthase, which converts ceramide into the mitochondria-targeting GD3 ganglioside [70]. Moreover, recent reports demonstrate that the calpain/calpastatin network is associated with the cytosolic surface of the Golgi apparatus and ER membranes and calpains can be activated at the interface between these organelles [115,116]. Accordingly, both the Golgi apparatus and the endoplasmic reticulum contribute to the rise in cytosolic  $\text{Ca}^{2+}$  observed upon agonist stimulation [117]. The role of caspase-2 is particularly interesting. After delivery of a pro-apoptotic signal, caspase-2 is locally activated at the Golgi complex and cleaves golgin-160 at a unique site not susceptible to cleavage by other caspases. This initial event is entirely responsible for the disintegration of the Golgi complex [118].

## 7 ELIMINATION OF APOPTOTIC CELLS

### 7.1 PHAGOCYTOSIS

#### 7.1.1 Importance

Extensive studies over the last decades have provided deeper insights in the characteristics and signalling pathways of apoptosis, but only recently apoptosis research focused also on the importance of self debris clearance. Phagocytosis of dying cells constitutes the last step of programmed cell death *in vivo* and should occur before cells undergo severe damage and spill their contents into surrounding tissues. Dead cells are continuously generated but are immediately removed from the organism by neighbouring cells or professional phagocytes, mainly macrophages, to avoid tissue damage and inflammatory or autoimmune responses.

### 7.1.2 “Eat-me” signals on the apoptotic cell

During the apoptotic process cells mark themselves for the recognition and engulfment by phagocytes. The surface of apoptotic cells exhibits molecules that are absent in normal cells and existing molecules are modified in sugar chains or by oxidation processes [119,120].

The most prominent “eat-me” signal is the phospholipid phosphatidylserine (PS), which is externalised by essentially all apoptotic cells during apoptosis. In a resting cell, PS is normally confined to the inner leaflet of the membrane bilayer by two mechanisms. First, an aminophospholipid translocase, i.e. a Mg<sup>2+</sup>-ATPase inhibited by Ca<sup>2+</sup>, transfers PS from the external to the inner layer. Second, PS is bound to proteins of the membrane-associated cytoskeleton. PS translocation requires the concomitant inhibition of the aminophospholipid translocase and activation of a plasma membrane phospholipid scramblase [121-123]. Activation of the scramblase requires phosphorylation processes and Ca<sup>2+</sup>, whereas the translocase is inactivated probably due to the decrease in ATP and increase in Ca<sup>2+</sup> often associated with the apoptotic process. PS exposure has been linked to caspase activation [47,121] but there are also reports that PS externalisation occurs independent of caspases [124,125] and even in necrotic cells [126].

The modification of membrane structures with carbohydrate chains has not been very extensively studied but is suggested to be another important signal in apoptotic cells. ICAM-3 (intercellular adhesion molecule-3), a highly glycosylated protein expressed in leukocytes, is somehow modified during apoptosis. Another example is the CD43 glycoprotein, which undergoes a transient capping with sialylpolylactosaminyl sugar chains at early stages of apoptosis [127,128]. Oxidation of proteins and lipids at the apoptotic cell surface is also important for engulfment. Phosphatidylserine oxidation is required for its externalisation [129-131] and for efficient phagocytosis [120].

### 7.1.3 Interaction phagocyte-target cell and phagocytosis

The engulfment of apoptotic cells is explained by the “tether and tickle” two step model. In a first step, recognition molecules on the phagocytic cell bind to structures on the apoptotic cell to tether it to the surface of the phagocyte. Following, the structures of the phagocyte participating in tethering and/or additional receptors are engaged to enclose the target cell and initiate uptake.

In the past years, a vast array of receptors and factors that participate in the recognition and engulfment of apoptotic cells in mammals have been identified [119,120,132-137]. Even though there are still obscure points and some controversy, there is agreement about the critical role of PS in cell removal. A receptor specific for PS was identified [138] and called phosphatidylserine receptor (PSR). Engagement of the PSR leads to macropinocytosis and uptake of tethered apoptotic cells. Numerous *in vitro* and *in vivo* experiments have demonstrated that the PSR is essential for cell uptake and for the clearance of apoptotic cells in the early stages of mammalian organogenesis [139]. However, it requires the collaboration of other receptors for the first step of cell tethering. Members of the scavenger receptor family, integrins ( $\alpha_v\beta_3$  and  $\alpha_v\beta_5$ ), lectins and CD14 are considered tethering receptors [140,141].

One of the systems best characterised after the PSR is the recognition by the vitronectin receptor ( $\alpha_v\beta_3$ ). Non-activated macrophages recognise an unknown ligand on apoptotic cells through a complex formed by  $\alpha_v\beta_3$ , CD36 and secreted thrombospondin, whereas activated macrophages form a tripartite PS/MFG-E8/ $\alpha_v\beta_3$ . MFG-E8 [milk fat globule epidermal growth factor (EGF) factor 8] is a soluble glycoprotein secreted by activated macrophages that acts as a bridge between aminophospholipids (such as PS) on the apoptotic cell and the integrins  $\alpha_v\beta_3$  or  $\alpha_v\beta_5$  on the macrophage [142,143]. Other receptors in the macrophage are the receptor tyrosine kinase Mer [144],  $\beta_2$ GP1 ( $\beta_2$  glycoprotein 1) receptor, CD14, lectins, annexin I and II and scavenger receptors, among others. Scavenger receptors include CD36 [145], CD68, LOX1 (lectin-like oxLDL-receptor 1, that recognises oxidised sites on the apoptotic cell) and the scavenger receptors A and B (SR-A, SR-B).

Adding a level of complexity, several bridging molecules linking specific receptors on the phagocyte to ligands on the dying cell appear to increase the efficiency of uptake. In many cases, these are known PS-binding proteins, such as the serum proteins  $\beta_2$  glycoprotein 1 ( $\beta_2$ GP1) and protein S, the gene product of Gas-6 (growth-arrest-specific 6), annexin I, thrombospondin and the milk fat globule protein MFG-E8.  $\beta_2$ GP1 and protein S receptors are not been identified yet, whereas Gas-6 is a ligand for the receptor tyrosine kinase Mer. Annexin I may facilitate the recognition of PS by the PSR [146].

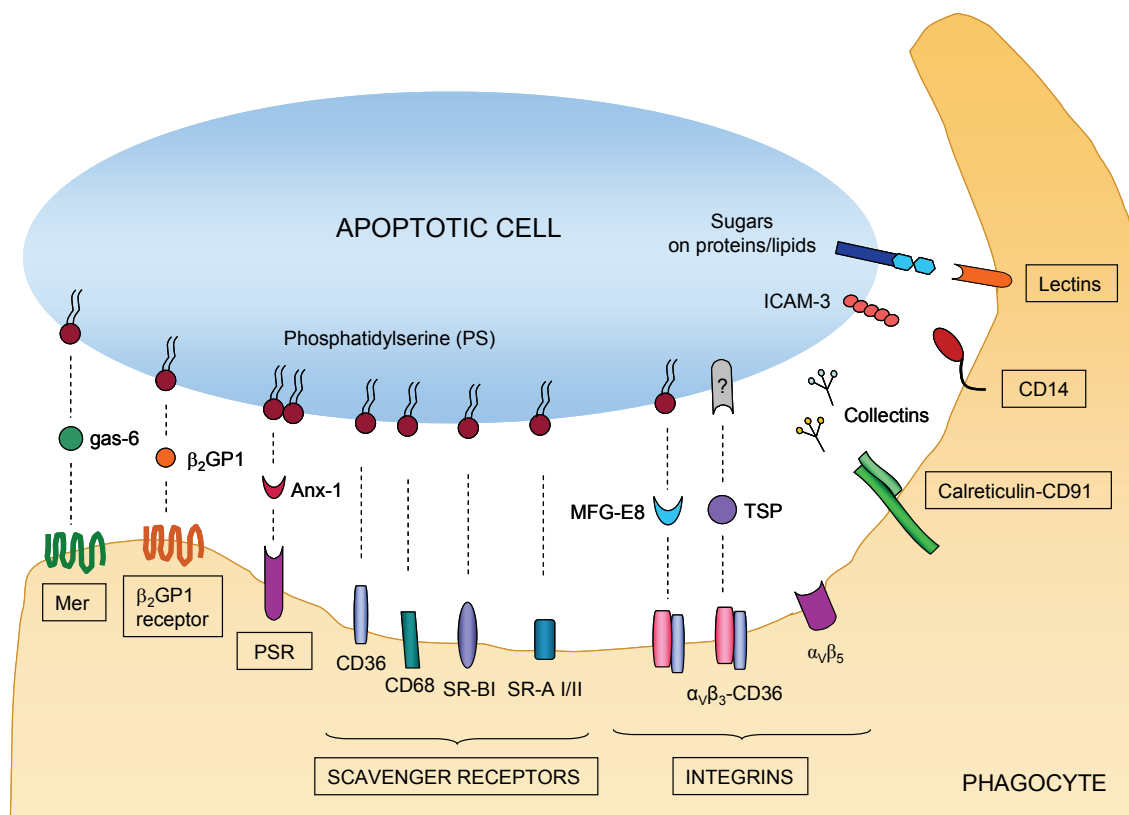


**Figure III.15: Simplified model for the phagocytic synapse.**

Phosphatidylserine (PS) on the surface of apoptotic cells is recognised by the tyrosine kinase receptors Mer and β<sub>2</sub> glycoprotein 1 (β<sub>2</sub>GP1) receptor, the phosphatidylserine receptor (PSR) scavenger receptors and some integrins. The vitronectin receptor (α<sub>v</sub>β<sub>3</sub>) recognises apoptotic cells through the bridging molecules milk fat globule epidermal growth factor 8 (MFG-E8) and thrombospondin (TSP). Some members of the innate immunity, as collectins, bridge the apoptotic cell to the calreticulin-CD91 receptor. Sugar chains and intercellular adhesion molecule-3 (ICAM-3) on the apoptotic cell are recognised by lectins and CD14.

Recognition molecules of the innate immune system play a pivotal role in the clearance of apoptotic cells [147]. This group includes soluble proteins such as collectins, C-reactive protein (CRP), complement proteins (C3b/bi) and the membrane-bound receptors calreticulin-CD91, Toll-like receptors and complement receptors 3 and 4 (CR3, CR4) [148]. The collectin family is a group of serum opsonins that includes mannose-binding lectin (MBL), surfactant proteins A and D (SP-A, SP-D) and the complement component C1q. These molecules are especially effective at recognising components of late apoptotic cells, necrotic cells and cell debris, and bind to ligands different than PS exposed late in the apoptotic process. Collectins seem to be the mechanism of removal of dying cells that have not been engulfed by macrophages in the early apoptosis phase. The receptor to collectins corresponds to cell-surface calreticulin, which together with its partner signalling molecule CD91 initiates macropinocytosis of dead cells [149,150].

One of the requirements for proper phagocytosis is the polymerisation and reorganisation of the actin cytoskeleton underneath bound particles. Binding of apoptotic cells induces actin polymerisation and protein phosphorylation at nascent phagocytic cups, crucial for the formation of membrane extensions around, and engulfment of the target particle [151]. The intracellular signalling in the phagocytosis of apoptotic cells may depend on the receptor involved. In mammals, the small GTPases of the Rho family Rac and Cdc42 (cell division cycle 42) are required for the organisation of actin filaments leading to uptake of apoptotic cells [120,141].

#### **7.1.4 Inhibition of phagocytosis**

In general, removal of apoptotic corpses is a beneficial process for the organism. However, too much phagocytosis can produce undesirable results, as the production of ROS and tissue injury. Molecules displayed on the target cell and macrophage participate in a negative regulation of phagocytosis.

Normal cells present molecules that promote detachment from phagocytes or that inhibit phagocytic activity, the so-called “don’t eat-me” signals. They are lost by apoptotic cells and allow macrophages to discriminate between viable and apoptotic cells. CD31 (PECAM-1, platelet-endothelial cell adhesion molecule-1) is a demonstrated “don’t eat-me” signal. The encounter of a viable cell with a phagocyte via the homophilic interaction of CD31 on both cell surfaces leads to the viable cell’s active repulsion from the phagocyte. Upon induction of apoptosis, the inside-out signalling of CD31 is somehow disabled and the apoptotic cell is not able to detach [152]. Moreover, a range of inhibitory receptors on the macrophage attenuate activation signals initiated by other receptors. Inhibitory receptors contain immuno-receptor tyrosine-based inhibitory motifs (ITIMs), which recruit phosphatases that in turn transduce inhibitory signals [120].

## **7.2 CYTOKINE RESPONSE AND BIOLOGICAL CONSEQUENCES**

Macrophages do not simply engulf and degrade dying cells acting as scavengers, but also respond actively modulating immune responses. In general, monocytes and macrophages react to apoptotic cells releasing anti-inflammatory cytokines as IL-10, TGF- $\beta_1$  (transforming growth factor  $\beta_1$ ), PGE<sub>2</sub> (prostaglandin E<sub>2</sub>) and PAF (platelet activating factor) and down-regulating the production of pro-inflammatory factors including TNF- $\alpha$  (tumour necrosis factor- $\alpha$ ), IL-1 $\beta$ , IL-12, IL-8, GM-CSF (granulocyte macrophage-colony stimulating

factor), INF- $\gamma$  (interferon- $\gamma$ ) and eicosanoids [TXB<sub>2</sub> (thromboxane B<sub>2</sub>) and LTC<sub>4</sub> (leukotriene C<sub>4</sub>) [119,153-155], leading to an overall anti-inflammatory and immunosuppressive response.

It has been proposed that, in fact, TGF- $\beta$  is the main cytokine responsible for all the anti-inflammatory effects of apoptotic cells, by modulating the others at the level of gene transcription or protein translation [156]. It is explained by a mechanism involving TGF- $\beta$  activation of ERK (extracellular signal-regulated kinase), which in turn up-regulates MKP-1 (MAPK phosphatase-1), thereby inactivating the kinase p38 MAPK (p38 mitogen-activated protein kinase) [157]. *In vivo*, TGF- $\beta$  secretion follows a biphasic response: early increase corresponding to release of preformed TGF- $\beta$  and a late increase corresponding to *de novo* protein synthesis [153].

Phosphatidylserine exposed on apoptotic cells and its major counterpart, the PSR, have been implicated as the major players in the anti-inflammatory effect. *In vitro* and *in vivo* studies support this notion. Specific stimulation of the PSR mimics the effect of apoptotic cells, increasing TGF- $\beta$  and reducing TNF- $\alpha$  release [138]. But phagocyte receptors other than PSR can also mediate the immunosuppressive effects of apoptotic cells. Ligation of the vitronectin receptor  $\alpha_V\beta_3$ -CD36 by apoptotic lymphocytes has been reported to mediate an increase in IL-10 and decrease in TNF- $\alpha$ , IL-1 $\beta$  and IL-12 [154]. A recent study clearly demonstrates that the tripartite PS/MFG-E8/ $\alpha_V\beta_3$  is required for the inhibitory signal of the phagocytosis of apoptotic B cells in the germinal centres of the spleen and lymph nodes [142,143]. The kinase domain of the Mer receptor has shown ability to down-regulate the production of cytokines such as TNF- $\alpha$  after the ligation of PS on apoptotic cells via gas-6 [158].

Necrotic or lysed cells are also efficiently removed and can expose PS on their membranes, but their uptake is normally pro-inflammatory. Even though they can be recognised by the PSR, the anti-inflammatory effect is overridden by other mechanisms. Necrotic cells release proteins that stimulate macrophage production of pro-inflammatory mediators, as HMGB-1 (high-mobility group box chromosomal protein-1), heat shock proteins [137] and double-stranded DNA. HMGB-1 is recognised by TLR2 and TLR4 (toll-like receptor-2 and -4), acting similarly to LPS [159]. The effect may also be due to the blocking of PS by cytoplasmic proteins as annexins [140] or cleavage of the PSR by proteases contained in cell lysates such as neutrophil elastases [160,161].

However, a body of investigations demonstrates that it is not that simple. Apoptotic cells have elicited pro-inflammatory responses in several studies [162-165]. The uptake mediated by some molecules of the innate immunity such as the receptor calreticulin-CD91 is pro-inflammatory [147]. Under some conditions, apoptotic debris can be opsonised with antibodies and recognised by macrophages via Fc receptors that trigger pro-inflammatory responses in the phagocyte [166]. In addition, necrotic cells are not necessarily pro-inflammatory. The membranes of either necrotic or apoptotic cells are recognised through PS and are an anti-inflammatory stimulus [126,161,167].

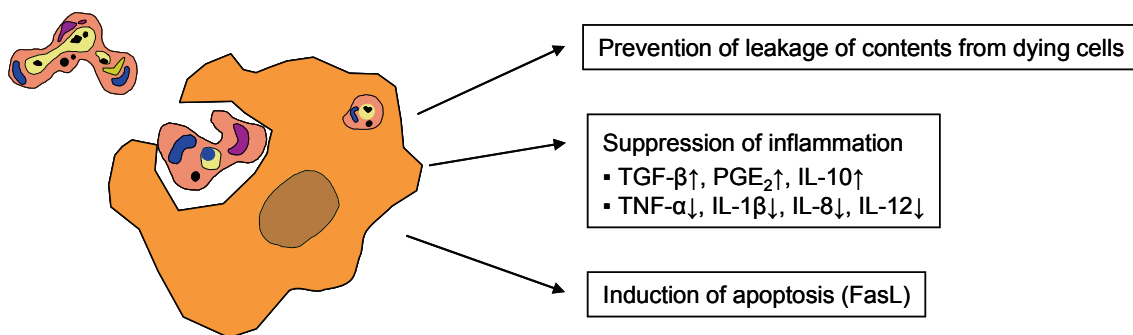


**Figure III.16: Suppression of inflammation by macrophages ingesting apoptotic cells.**

Macrophages that have engulfed apoptotic cells contribute to an anti-inflammatory effect by several mechanisms. Uptake avoids the leakage of potentially immunogenic contents from dying cells and induces an active suppression of inflammation through an increase of anti-inflammatory cytokines and a down-regulation of pro-inflammatory. Phagocytosis triggers release of the death-inducing ligand FasL by macrophages, resulting in the apoptosis of bystander cells.

The recognition and engulfment of apoptotic cells by professional phagocytes plays an active and necessary role in the resolution of inflammation (Figure III.16). In inflammatory sites, neutrophils need to be removed prior to their lysis, as their contents would otherwise expel into the extracellular milieu and perpetuate inflammation. A primary mechanism is the modulation of the macrophage production of anti- and pro-inflammatory cytokines [153-155]. Uptake of apoptotic cells promotes an increased survival and decreased proliferation of macrophages, which may aid the macrophage in its role as scavenger during resolution of inflammation [168]. Furthermore, macrophages are not only scavengers of apoptotic debris, but can induce apoptosis actively. Deficiencies in the apoptosis of inflammatory cells or in the removal of dead cells are involved in the development of autoimmune diseases as cystic fibrosis [160], rheumatoid arthritis [169] or systemic lupus erythematosus (SLE) [170].

### 7.3 ROLES OF APOPTOTIC CELL CLEARANCE IN DISEASE

Autoimmune diseases can result from impairment of apoptotic cell clearance or due to defective signalling in the anti-inflammatory response that apoptotic cells elicit. Apoptotic cells are a rich source of autoantigens that can drive autoimmune responses.

Deficiencies of the complement component C1q are linked with the development of autoimmune disorders as SLE [170]. Mutations in the Mer gene seem to be associated with retinitis pigmentosa. MFG-E8 deficient mice develop high titres of autoantibodies and consequent glomerulonephritis [143]. Importantly, defects in apoptotic cell clearance has been observed in the airways of patients with cystic fibrosis, characterised by accumulation of inflammatory cells into the airways and release of neutrophil elastases that cleave the PSR [160]. An *in vivo* study has demonstrated the beneficial effects of apoptotic cells [153]. The instillation of apoptotic cells into LPS-stimulated lungs induced a reduction in the pro-inflammatory chemokine levels and in the infiltration of inflammatory cells in the bronchoalveolar lavage fluid. The beneficial effects were attributed to the secretion of TGF- $\beta$  by macrophages after ligation of the PSR.

On the contrary, the beneficial consequences of apoptotic cells uptake are turned into negative in circumstances where suppression of inflammation or immunity is harmful, as in infectious diseases, sepsis and cancer. The uptake of apoptotic cells by macrophages infected with *Trypanosoma cruzi*, an intracellular parasite, can enhance parasite growth through macrophage production of TGF- $\beta$  and PGE<sub>2</sub> [171]. In an *in vivo* mouse sepsis model, adoptive transfer of apoptotic cells worsened the survival of mice whereas necrotic cells improved survival via modulation of INF- $\gamma$  [172,173]. Tumour cells killed by chemotherapy treatment are normally apoptotic and expose PS (some of them as malignant melanoma cells even when they are viable), provoking a tolerance of the organism to tumour cells that attenuates immune reactions against tumours and favours the growth of cancer. A study demonstrates that the release of the anti-inflammatory cytokine IL-10 is negative in renal cell carcinoma [174]. Furthermore, the phagocytosis of apoptotic tumour cells contributes to genetic instability and diversity within tumours [175].

The modulation of the process of programmed cell clearance may yield novel strategies for therapeutic intervention, especially in autoimmune diseases and cancer.



## **IV. MATERIALS AND METHODS**

## IV. MATERIALS AND METHODS

### 1 MATERIALS

#### 1.1 COMPOUNDS

Cephalostatin 1 and cephalostatin 2, isolated as described in [10,11], were obtained from Prof. G. R. Pettit (Cancer Research Institute, Arizona State University, Tempe, USA).

Sesquiterpene lactones were isolated as described previously: 11 $\alpha$ ,13-dihydrohelenalin acetate (DHA) was isolated from flower heads of *Arnica montana* [176], 7-hydroxycostunolide (HC) was isolated from *Podachaenium eminens* [177] and 4 $\beta$ ,15-epoxymiller-9Z-enolide (EM) was isolated from *Milleria quinqueflora* [178]. They were kindly provided by Prof. Irmgard Merfort (Department of Pharmaceutical Biology and Biotechnology, University of Freiburg, Freiburg, Germany).

#### 1.2 BIOCHEMICALS, INHIBITORS, DYES AND CELL CULTURE REAGENTS

Carboxy-H <sub>2</sub> DCFDA	Molecular Probes, Eugene, OR, USA
CCFSE	Molecular Probes, Eugene, OR, USA
Complete™	Roche, Mannheim, Germany
DMEM	PAN Biotech, Aidenbach, Germany
Etoposide	Calbiochem, Schwalbach, Germany
FCS gold	PAN Biotech, Aidenbach, Germany
FITC-VAD-fmk	Promega, Heidelberg, Germany
Fura-2, AM	Biotrend, Cologne, Germany
G418 sulfate	PAA Laboratories, Cölbe, Germany
Hoechst 33342	Sigma, Taufkirchen, Germany
MTT	Sigma, Taufkirchen, Germany
PKH26	Sigma, Taufkirchen, Germany
PMA	Sigma, Taufkirchen, Germany
Probenecid	Sigma, Taufkirchen, Germany
Propidium iodide	Sigma, Taufkirchen, Germany
Pyruvate	Merck, Darmstadt, Germany
RPMI 1640	PAN Biotech, Aidenbach, Germany
SP600125	Calbiochem, Schwalbach, Germany

Staurosporine	Calbiochem, Schwalbach, Germany
Thapsigargin	Sigma, Taufkirchen, Germany
TNF- $\alpha$	Sigma, Taufkirchen, Germany
Tunicamycin	Sigma, Taufkirchen, Germany
zLEVD-fmk	MBL, Woburn, Massachusetts, USA
zVAD-fmk	Calbiochem, Schwalbach, Germany
zVDVAD-fmk	MBL, Woburn, Massachusetts, USA

**PBS (pH 7.4)**

NaCl	7.20 g
Na <sub>2</sub> HPO <sub>4</sub>	1.48 g
KH <sub>2</sub> PO <sub>4</sub>	0.43 g
H <sub>2</sub> O	ad 1,000 ml

**Trypsin/EDTA (T/E)**

Trypsin	0.50 g
EDTA	0.20 g
PBS	ad 1,000 ml

**1.3 TECHNICAL EQUIPMENT**

Vi-CELL™ (Beckman Coulter)	Cell viability analyser
FACSCalibur (Becton Dickinson)	Flow cytometer
Axiovert 25 (Zeiss)	Inverted microscope
Axiovert 200 (Zeiss)	Inverted microscope
LSM 510 Meta (Zeiss)	Confocal laser scanning microscope
Sunrise™ (Tecan)	Microplate absorbance reader
SpectraFluor Plus™ (Tecan)	Plate-reading multifunction photometer
Curix 60 (Agfa)	Tabletop film processor
Lambda Bio 20 (Perkin Elmer)	Photometer
RF-1502 spectrofluorophotometer (Shimadzu)	Spectrofluorophotometer
Thermoshake THO 500 (Gerhardt)	Incubator shaker
Nucleofector™ II (Amaxa)	Electroporation device

## **2 CELL CULTURE**

### **2.1 CELL LINES**

The human leukemia Jurkat T cells (J16) (kindly provided by Prof. Dr. P.H. Krammer and Dr. H. Walczak, Heidelberg, Germany) as well as Jurkat T cells stably expressing an inactive form of ASK1 (ASK1-DN, clones A2-1 and A2-3 [179]) (kindly provided by Prof. M. Lienhard Schmitz, Giessen, Germany) were cultured in RPMI 1640 containing 2 mM L-glutamine (PAN Biotech, Aidenbach, Germany) supplemented with 10% foetal calf serum (FCS) (PAA Laboratories, Cölbe, Germany) and 1% pyruvate (Merck, Darmstadt, Germany). Caspase-9-deficient Jurkat cells (courtesy of Prof. Klaus Schulze-Osthoff, Düsseldorf, Germany) were cultured in the medium described above containing heat-inactivated FCS. Medium of transfected cells was supplemented with 1 mg/ml G418 (PAA Laboratories, Cölbe, Germany) every fifth passage for antibiotic selection. Cells exposed to G418 were not used for experiments.

As an additional model for the study of apoptosis the human HeLa cervix carcinoma cell line was employed. HeLa cells were obtained from the German Collection of Microorganisms and Cell Cultures (DSMZ, Braunschweig, Germany) and cultured in DMEM (PAN Biotech, Aidenbach, Germany) supplemented with 10% FCS (PAA Laboratories, Cölbe, Germany).

The human monocytic leukemia cell line THP-1, usually employed in phagocytosis assays after differentiation into macrophages, was obtained from the German Collection of Microorganisms and Cell Cultures (DSMZ, Braunschweig, Germany). Cells were cultured in RPMI 1640 medium (PAN Biotech, Aidenbach, Germany) supplemented with 10% FCS (PAA Laboratories, Cölbe, Germany).

### **2.2 CULTURE AND SPLITTING**

Jurkat cells were split three times a week (to a concentration of  $1 \times 10^5$  cells/ml but  $0.8 \times 10^5$  cells/ml before weekends) in order to maintain them under a concentration of  $1 \times 10^6$  cells/ml and thus reduce the probability of mutations. Cells were not used after passage number twenty for the same reason. THP-1 cells were cultured exactly as Jurkat cells.

The HeLa carcinoma cell line growths in monolayer adhered to plastic surfaces. Cells were split when reaching 85-90% confluence. Cells were shortly washed with PBS and detached by incubation with a solution of trypsin/EDTA at 37°C. The process was stopped as soon as cells detached by addition of medium. The cell suspension was centrifuged (180 x g, 10 min, 25°C) and resuspended in fresh medium before transferring to culture flasks.

All cell lines were cultured in tissue culture flasks at 37°C in a humidified atmosphere and 5% CO<sub>2</sub>. Cell concentration and viability was determined in the Vi-CELL™ cell viability analyser (Beckman Coulter, Krefeld, Germany).

### **2.3 SEEDING FOR EXPERIMENTS**

Jurkat cells were seeded approximately 16 h before experiments (alternatively, at a higher cell concentration 2-3 h before). The cell suspension was centrifuged (180 x g, 10 min, 25°C), resuspended in prewarmed medium, and analysed in the Vi-CELL™ cell viability analyser. The desired cell density was adjusted by addition of the required volume of medium. Except for the MTT and caspase-9 activity assays (96-well), cells were seeded in 24-well tissue culture plates.

HeLa cells were detached and centrifuged as described in IV.2.2. The cell suspension was analysed in the Vi-CELL™ and concentration was adjusted. Cells were seeded in 12-well tissue culture plates 8-16 h before experiments.

### **2.4 FREEZING AND THAWING**

Cryogenic preservation of cell lines is necessary to maintain reserves of cells. Frozen cells can be stored almost indefinitely in liquid nitrogen. Some advantages of this process are that cells are protected from microbial contamination, genetic and morphological changes are avoided and experiments can be conducted using cells of similar passage number, increasing reproducibility.

Cells are frozen in a special medium (freezing medium, Table V.1) that contains a higher percentage of serum than culture medium and 10% (v/v) of DMSO as a cryoprotector. Some cell lines such as THP-1 cells are more sensitive to DMSO and are stored in freezing medium containing a high concentration of serum.

After centrifugation (180 x g, 10 min, 4°C) cells were resuspended in the appropriate freezing medium at a concentration of  $2 \times 10^6$  cells/ml. The cell suspension was transferred to cryovials (1.5 ml) and frozen overnight at -20°C. Cells were then kept at -80°C and if desired, transferred to liquid nitrogen (-196°C) after two days for long-term storage.

**Table IV.1: Freezing medium.**

	Jurkat	THP-1	HeLa
RPMI 1640	70 %	45 %	-
DMEM	-	-	80 %
FCS gold	20 %	45 %	10 %
DMSO	10 %	10 %	10 %

Cells were thawed in a water bath (37°C), diluted 1:10 with medium and centrifuged (200 x g, 5 min) to remove dead cells and DMSO. Cells were resuspended in fresh medium and cultured for at least five days before conducting any experiment.

### 3 FLOW CYTOMETRY

#### 3.1 INTRODUCTION

##### FACS buffer

NaCl	8.12 g
KH <sub>2</sub> PO <sub>4</sub>	0.26 g
Na <sub>2</sub> HPO <sub>4</sub>	2.35 g
KCl	0.28 g
Na <sub>2</sub> EDTA	0.36 g
LiCl	0.43 g
Na-azide	0.20 g
H <sub>2</sub> O	ad 1,000 ml, pH 7.37

Flow cytometry is a method that allows for the analysis of various properties of single cells or particles suspended in a fluid. This technology is ideally suited for the rapid, reliable and accurate quantitative analysis of selected physical properties of cells of interest, even (or especially) when these form a small population within a mixture of cell types. Flow cytometers can be used for the analysis of cell cycle, viability, apoptosis, calcium influx, membrane potential or amounts of surface receptors or intracellular proteins.

In the flow chamber (Figure IV.1) the suspension of single cells emerges from the sample needle into a surrounding sheath fluid liquid that is moving with a greater velocity. The resulting acceleration at the orifice forces the particles to travel one by one in the central portion of the fluid jet that emerges from the flow chamber. This principle is called hydrodynamic focusing.

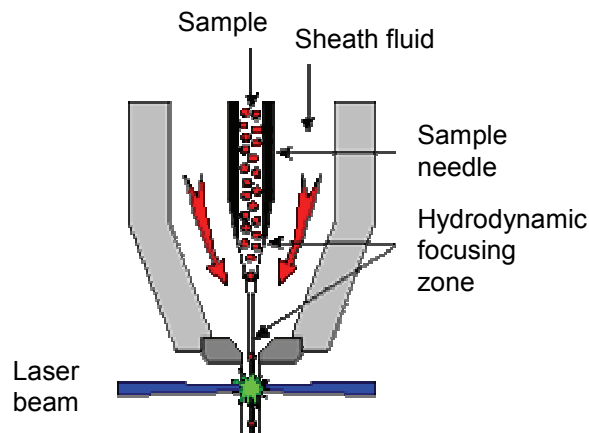


**Figure IV.1: Close up of the flow chamber (adapted from [180]).**

The cells flow past the detector point and are illuminated by a focused laser beam. The illuminating light is scattered and simultaneously, if particles have been previously stained with a fluorescent dye capable of absorbing the illuminating light, fluorescence emission occurs. Scattered light and emitted fluorescence is collected and sent to different detectors by using optical filters. The relative size and granularity of a cell influence the way in which light is scattered as the cell passes through the laser beam. Low angle scattered light depends on cell size and is recorded as a parameter called forward scatter (FSC). Similarly, cell granularity and surface convolutions scatter light at higher angles. For convenience the signal is measured orthogonal to the stream and is referred to as side scatter (SSC). Fluorescence (FL) measurements are also made in the orthogonal direction with detectors appropriate to the specific emission spectrum of the fluorochrome used (Table IV.2).

**Table IV.2: Emission wavelength and detectors.**

Fluorochrome	$\lambda_{em}$	Detector
Propidium iodide	617 nm	FL2
CCFSE	525 nm	FL1
Carboxy-H <sub>2</sub> DCFDA (oxidized dye)	525 nm	FL1

All measurements were performed on a FACSCalibur (Becton Dickinson, Heidelberg, Germany) (Figure IV.2). Cells are illuminated by a 488 nm argon-ion laser. Scattered light and emitted fluorescence are filtered and the last is measured with several detectors: FL1 (530 nm), FL2 (585 nm), FL3 (650 nm) or FL4 (optional, in this case FL3 detects >670 nm).

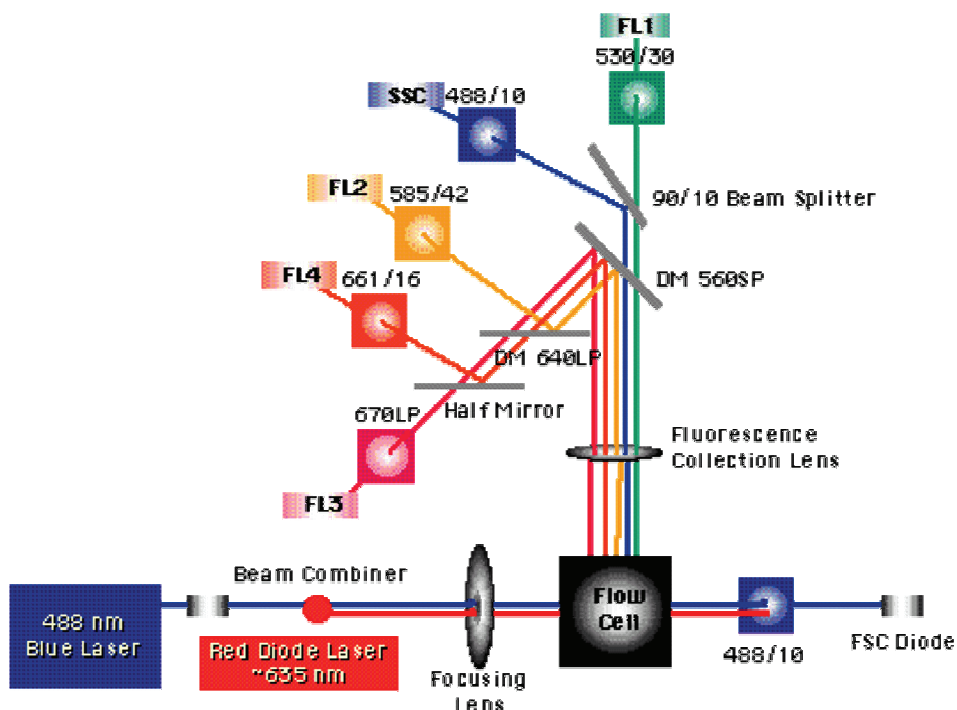


**Figure IV.2: Optical bench diagram of the FACSCalibur benchtop flow cytometer (from [181]).**

### 3.2 DETERMINATION OF CELL VIABILITY (PI EXCLUSION ASSAY)

Propidium iodide (PI) is a red fluorescent dye which binds to DNA and RNA by intercalating between the bases. Its absorption and emission wavelengths are 535 and 617 nm respectively when bound to nucleic acids. Cells with an intact membrane are impermeable to PI and do not take it up when incubated in a solution of this dye. On the contrary, dead or damaged cells (late apoptotic or necrotic) that have lost membrane integrity are stained and can be quantified by flow cytometry.

$5 \times 10^5$  untreated, stimulated with SQTL/etoposide or necrotic Jurkat cells were harvested by centrifugation ( $600 \times g$ , 10 min,  $4^\circ C$ ) and washed once with phosphate buffered saline (PBS).

Pellets were resuspended in 500 µl of a PI solution (1 µg/ml in PBS) and incubated for 10 min at room temperature in the dark. Probes were stored shortly on ice and analysed by flow cytometry using a FACSCalibur. Fluorescence intensity of cells was recorded with the fluorescence channel 2 (FL2,  $\lambda_{em}$  585 nm). Cells from 0 to  $10^1$  (histogram plot, logarithmic scale) were regarded as viable while cells with a fluorescence ranging from  $10^1$  to  $\sim 10^4$  were considered dead.

### 3.3 QUANTIFICATION OF DNA FRAGMENTATION BY PI STAINING (NICOLETTI METHOD)

During the apoptotic process endogenous endonucleases become activated and cause the fragmentation of nuclear DNA into oligonucleosomal-size fragments. Thus an easy and widely used assay to quantify apoptotic cell death is the counting of nuclei with a subdiploid DNA content after staining with PI. The method described by Nicoletti et al. [182] is one of the most widely used for the quantification of apoptosis because of its rapidness and simplicity. Cells are permeabilised in a hypotonic buffer that contains PI and red fluorescence is measured by flow cytometry.

The whole DNA content of cells is stained independently from their viability or membrane integrity. Most cells of normal untreated cell populations are in G<sub>0</sub>/G<sub>1</sub> phase with 2n DNA content and emit a homogenous fluorescence after binding of PI to DNA. Cells in G<sub>2</sub>/M phase (DNA content of 4n) peak at higher fluorescence intensity and cells in S phase appear between the G<sub>0</sub>/G<sub>1</sub> and G<sub>2</sub>/M peaks. DNA fragments of apoptotic cells respectively apoptotic bodies have a lower fluorescence and thus appear “left” to the G<sub>0</sub>/G<sub>1</sub> peak in the FL2 histogram.

7 × 10<sup>5</sup> Jurkat cells/ml (500 µl, 24-well plate) or 2 × 10<sup>5</sup> HeLa cells were left untreated or stimulated with the required substances. In some experiments, caspase inhibitors were added 1 h before stimulation at a concentration of 20 µM. After different incubation times cells were harvested by centrifugation (600 × g, 10 min, 4°C) and washed once with PBS. Cells were incubated in a hypotonic buffer containing PI [hypotonic fluorochrome solution (HFS) buffer] overnight at 4°C and analysed by flow cytometry on a FACSCalibur. The logarithmic mode of FL2 was recorded and the instruments settings were adjusted in each experiment by assigning a fluorescence intensity of 10<sup>3</sup> to the G<sub>0</sub>/G<sub>1</sub> peak. Events to the left of the “G1-peak” containing hypodiploid DNA were quantified as apoptotic cells.

HFS

---

Propidium iodide	50 µg
Sodium citrate	0.1 % (w/v)
Triton X-100	0.1 % (v/v)
PBS	ad 1 ml

Propidium iodide was added under light protection just before use.

### 3.4 MEASUREMENT OF ROS GENERATION

The fluorogenic probe carboxy-2',7'-dichlorodihydrofluorescein diacetate (carboxy-H<sub>2</sub>DCFDA) is commonly used for measuring the production of reactive oxygen species (ROS) in both flow cytometric and spectrofluorometric systems, mainly due to its simplicity, high sensitivity, and low cost relative to traditional approaches to the measurement of ROS.

Carboxy-H<sub>2</sub>DCFDA is a nonfluorescent compound capable of crossing the plasma membrane to enter the cell, where cellular esterases hydrolyse its acetyl moieties to produce 2',7'-dichlorodihydrofluorescein (H<sub>2</sub>DCF) which is trapped in the cells. The de-acetylated form of the probe is then susceptible to oxidation, generating a fluorescent product, 2',7'-dichlorofluorescein (DCF). Accumulation of DCF indicates the production of redox-active substances.

Jurkat cells were centrifuged (180 x g, 10 min, 25°C), washed once in PBS and resuspended at 10<sup>6</sup> cells/ml in PBS containing 0.1% bovine serum albumine (BSA). Carboxy-H<sub>2</sub>DCFDA was added to a final concentration of 5 µM, and cells were incubated for 30 min at 37°C in the dark. Cells were subsequently washed once with 0.1% BSA-PBS solution, resuspended in fresh medium (without phenol red) at a concentration of 8 x 10<sup>5</sup> cells/ml and transferred to FACS tubes. Cells were left untreated or stimulated with cephalostatin-1 (1 µM) or staurosporine (0.5 µM) as a positive control, placed into a water bath (37°C) and measured at different points of time by flow cytometry. Fluorescence intensity of cells was recorded with the fluorescence channel 1 (FL1,  $\lambda_{em}$  530 nm) and analysed employing histogram plots.

## 4 ANALYSIS OF OTHER CELL DEATH FEATURES

In addition to the quantification of DNA fragmentation (Nicoletti) other features of SQTL-induced cell death were investigated (appearance of small granular cells, visualisation of apoptotic nuclei after staining with Hoechst 33342, translocation of phosphatidylserine to the cell surface and total caspase activity) as well as overall cytotoxicity (MTT assay) as described in [183].

Late apoptotic and necrotic cells usually lose membrane integrity as a result of the deterioration of cellular function. Plasma membrane rupture can be analysed by quantifying the activity of lactate dehydrogenase (LDH), a cytosolic enzyme, in the culture supernatant of treated cells. This assay is based on the conversion of pyruvate to lactate. This reaction is catalysed by LDH and accompanied by an oxidation of NADH/H<sup>+</sup> to NAD<sup>+</sup>. The activity of LDH is proportional to the decrease of NADH/H<sup>+</sup> measured [184].

---

### Phosphate buffer

---

Adequate volumes of KH<sub>2</sub>PO<sub>4</sub> (6.80 g/l) and K<sub>2</sub>HPO<sub>4</sub> (8.74 g/l) solutions were mixed until a pH of 7.5 was achieved. Subsequently 66 mg of pyruvate were added to 1 l of this buffer. The final solution can be stored for 14 days at 4°C.

---

### NADH solution (stability 7 days)

---

NADH-Na <sub>2</sub>	10 mg
NaHCO <sub>3</sub> (0.5 % in H <sub>2</sub> O)	1 ml

5 × 10<sup>5</sup> Jurkat cells/ml (1 ml, 24-well plate) were left untreated or stimulated for 24 h with sesquiterpene lactones (DHA 40 μM, HC 20 μM, EM 5 μM) or as control with etoposide (25 μg/ml). Cells were centrifuged (600 × g, 10 min, 4°C) and supernatants were recovered in new tubes. 600 μl of supernatant were mixed with 400 μl of phosphate buffer before addition of 10 μl of NADH solution. Absorbance was recorded with a Lambda Bio 20 photometer (Perkin Elmer, Überlingen, Germany) for 1 min and enzyme concentration was calculated based on the decrease in absorbance due to the conversion of NADH ( $\epsilon_{365\text{nm}} = 3.34 \text{ mM}^{-1} \text{ cm}^{-1}$ ) to NAD<sup>+</sup>.

## 5 MICROSCOPY

### 5.1 LIGHT MICROSCOPY

The characteristic morphological changes of apoptosis as well as other forms of programmed cell death, such as shrinking, swelling or formation of apoptotic bodies can be easily detected by light microscopy.

$7 \times 10^5$  cells/ml (500 µl, 24-well plate) were left untreated or stimulated with the required substances for different periods of time. Cells were viewed with a Zeiss Axiovert 25 microscope (Zeiss, Oberkochen, Germany) at 200 x magnification and pictures were taken with a connected reflex camera.

### 5.2 CONFOCAL LASER SCANNING MICROSCOPY

Confocal microscopes are increasingly used in life sciences due to the many advantages they offer. Among them, the fact that extremely high-quality images are obtained with a maximum resolution, three-dimensional information of thick specimens can be obtained and colocalisations of signals from different fluorochromes can be reliably studied.

Confocal can be defined as “having the same focus”: the final image has the same focus as the point of focus in the object. A confocal microscope is able to filter out the out-of-focus light from above and below the point of focus in the object.

For the visualisation of phagocytosis of Jurkat cells by THP-1-derived macrophages an LSM 510 Meta (Zeiss, Oberkochen, Germany) was used. Figure IV.3 represents schematically the beam path of this confocal laser scanning microscope. The excitation light is reflected by a main dichroic beamsplitter and focused into the specimen by the objective. The focused excitation light is scanned through the specimen point by point. The light returned or the fluorescent radiation emitted by the specimen is collected by the objective and focused on to a confocal pinhole which allows only the in-focus portion of the light to be imaged. Light passing through the image pinhole is detected by a photodetector while out-of-focus interference is rejected.

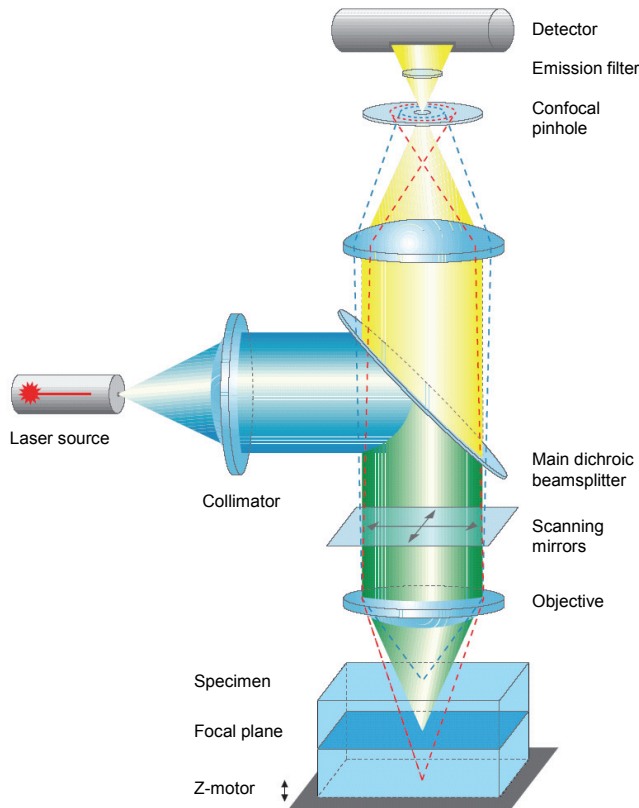


**Figure IV.3. LSM 510 Meta beam path (adapted from [185]).**

## 6 LUMINOMETRIC CASPASE-9 ACTIVITY ASSAY

Activation of caspases is usually demonstrated by the appearance of smaller processed fragments by Western Blot. However, cleavage of caspases does not always correlate with caspase activation and some initiator caspases can be active before or without catalytic processing [58,186]. Thus caspase activity is often quantified by the use of fluorescent or luminescent-labelled specific peptide substrates.

Caspase-9 activity was measured using the Caspase-Glo™ 9 Assay from Promega GmbH (Mannheim, Germany) following manufacturer's protocol. This assay system employs a pro-luminogenic substrate ( $\alpha$ -LEHD-aminoluciferin) containing the LEHD sequence, which has been shown to be selectively recognised by caspase-9. After cleavage of the substrate by caspase-9 aminoluciferin is recognised by luciferase and a luminescent signal (light) is produced. Luminescence is proportional to the amount of caspase-9 activity.

$5 \times 10^5$  cells/ml (100 µl, 96-well plate) were left untreated or treated with 1 µl DMSO (solvent) or cephalostatin 1 for 4 h with or without preaddition of caspase-4 or -2 inhibitors (20 µM, added 1 h before stimulation). After stimulation 100 µl of Caspase-Glo™ 9 Reagent was added to each well and gently mixed. Luminescence was measured immediately in a plate-reading multifunction photometer (SPECTRAFluor PLUS, Tecan, Crailsheim, Germany) using Xflou 4 software and every 10 min for 2 hours. Background luminescence corresponding to the culture medium was subtracted from experimental values. The 100 % of caspase-9 activity was assigned arbitrarily to the luminescence corresponding to untreated cells.

## 7      WESTERN BLOTTING

Western Blot (WB) is a method extensively used by investigators to identify specific proteins present in different protein mixtures (usually samples prepared from cell lysates). Proteins are first separated by electrophoresis, then transferred (“blotted”) to membranes and finally visualised by immunodetection.

### 7.1    PREPARATION OF SAMPLES

#### Lysis buffer for BiP, CHOP and caspases

---

30 mM Tris-HCl, pH 7.5  
150 mM NaCl  
2 mM EDTA  
1 % Triton X-100  
Complete™

#### Lysis buffer for phosphorylated proteins (p-JNK, p-eIF2α)

---

20 mM Tris-Base  
137 mM NaCl  
2 mM Na<sub>4</sub>P<sub>2</sub>O<sub>7</sub>  
2 mM EDTA  
20 mM C<sub>3</sub>H<sub>7</sub>Na<sub>2</sub>O<sub>6</sub>P (Na glycerolphosphate)  
10 mM NaF  
2 mM Na<sub>3</sub>VO<sub>4</sub>  
1 mM PMSF  
1 % Triton-X 100  
10 % Glycerol  
Complete™

---

Lysis buffer for p-ASK1 (modified RIPA buffer, from BioSource)

---

10 mM Tris, pH 7.4  
 100 mM NaCl  
 1 mM EDTA  
 1 mM EGTA  
 1 mM NaF  
 20 mM Na<sub>4</sub>P<sub>2</sub>O<sub>7</sub>  
 2 mM Na<sub>3</sub>VO<sub>4</sub>  
 1 mM PMSF  
 0.1 % SDS  
 0.5 % Sodium deoxycholate  
 1 % Triton-X 100  
 10 % Glycerol  
 Complete™

$7 \times 10^5$  Jurkat cells/ml (1 ml, 24-well plate) or  $4 \times 10^5$  HeLa cells/ml (500 µl, 12-well plate) were left untreated or stimulated with cephalostatin 1 (1 µM), cephalostatin 2 (50 nM) or the respective positive controls. In some experiments, caspase-4 and -2 inhibitors (20 µM) were added 1 h before stimulation or the JNK inhibitor SP600125 (10 µM) was added 30 min before. After the required incubation times cells were harvested (HeLa cells were detached as described in IV.2.2) by centrifugation (1,500 x rpm, 10 min, 4°C) and washed once with cold PBS. Pellets were resuspended in the appropriate lysis buffer (100 µl for three wells) and incubated on ice for 30 min or stored overnight at -80°C. Lysates were homogenized with an ultrasonic device and centrifuged at 10,000 x g, 4°C for 10 min. Supernatants were transferred to new tubes and protein concentration was determined by the Bradford method as described in IV.7.2. Lysates were diluted 1 : 5 with 5 x sample buffer with the exception of the analysis of ASK1, where a 3 x sample buffer containing bromophenol blue was used (dilution 1 : 3). Protein solutions were digested at 95°C for 5 min and stored at -20°C or used immediately for WB analysis.

PMSF, Na<sub>3</sub>VO<sub>4</sub> and Complete™ were added to the lysis buffers immediately before use.

---

Sample buffer (5 x)

---

3.125 M Tris-HCl, pH 6.8	100 µl
Glycerol	500 µl
SDS 20 %	250 µl
DTT 16 %	125 µl
Pyronin Y 5 %	5 µl
H <sub>2</sub> O	ad 1,000 µl

Sample buffer for ASK1 (3 x)

---

0.5 M Tris-HCl, pH 6.8	375 µl
SDS	60 mg
Glycerol	300 µl
Bromophenol blue	0.15 mg
H <sub>2</sub> O	ad 1,000 µl

## 7.2 PROTEIN QUANTIFICATION

The concentration of proteins in a sample can be quantified by different methods. The method developed by Bradford [187] employs the dye Coomassie Brilliant Blue G-250. After binding to proteins, the absorption maximum of this dye shifts from 465 to 595 nm. Probes are incubated with a reagent solution and absorbance is typically measured at 595 nm.

10 µl of a calibration curve containing increasing concentrations of BSA in H<sub>2</sub>O and 10 µl of dilutions 1 : 10 of the cell lysates in H<sub>2</sub>O were incubated with 190 µl of Bradford solution (Bio-Rad, Munich, Germany, diluted 1 : 5 in H<sub>2</sub>O) in enzyme linked immunosorbent assay (ELISA) plates for 5-10 min and absorbance of samples at 592 nm was measured in a microplate absorbance reader (Sunrise™, Tecan, Crailsheim, Germany). Before electrophoresis, the required volumes of 1 x sample buffer were added to the protein solutions in order to achieve the same protein concentration in all samples.

## 7.3 SDS-PAGE

Equal amounts of the protein samples described above were separated by discontinuous SDS-polyacrylamide gel electrophoresis (SDS-PAGE) according to Laemmli [188].

Proteins are denatured in order to ensure reproducibility of the technique. Sodium dodecyl sulfate (SDS) is an anionic detergent which binds to the hydrophobic parts of protein molecules in aqueous solutions. The negative charges on SDS destroy most of the secondary and tertiary structure of proteins. Moreover the reducing agent dithiothreitol (DTT) included in the sample buffer cleaves disulfide bonds inside the proteins. Denatured and negatively charged proteins are strongly attracted and migrate toward the anode in an electric field. The final separation of proteins is dependent almost entirely on the differences in molecular weight of polypeptides. Molecular weight

of proteins is estimated by comparison with commercial solutions containing mixtures of prestained proteins of known molecular weight, as the marker Bio-Rad All Blue® (Bio-Rad, Munich, Germany).

#### Stacking gel

PAA solution 30 %	1.7 ml
1.25 M Tris-HCl , pH 6.8	1 ml
SDS 10 %	100 µl
H <sub>2</sub> O	7 ml
TEMED	20 µl
APS	100 µl

#### Separating gel (10 %)

PAA solution 30 %	5 ml
1.5 M Tris-HCl , pH 8.8	3.75 ml
SDS 10 %	150 µl
H <sub>2</sub> O	6.1 ml
TEMED	15 µl
APS	75 µl

In a discontinuous electrophoresis system the solid support (gel) is formed by two layers. Proteins are applied into the stacking gel (upper layer) where they are compressed in order to have thin bands and correspondingly better resolution. Proteins begin to separate when they reach the separating gel (lower layer). The concentration of acrylamide of the separating gel was adjusted for an optimal protein separation depending on the molecular weight of the proteins to be analysed (Table IV.3). For gel preparation a stock solution of acrylamide 30 % / bis-acrylamide 0.8 % (Rotiphorese™ Gel 30, Roth, Karlsruhe, Germany) was used.

**Table IV.3: Separating gel concentrations.**

Protein	Acrylamide concentration
p-ASK1, ASK1	7.5 %
p-JNK, JNK, p-eIF2α, caspase-9, ubiquitin	10 %
BiP, CHOP, caspase-4, caspase-2	12 %

Electrophoresis was performed using a vertical Mini Protean III system (Bio-Rad, Munich, Germany) connected to a power supply (Biometra, Göttingen, Germany). Electrophoresis was run at 100 V for 21 min for stacking of proteins and at 200 V for 38-40 min for the separation of proteins.

#### Electrophoresis buffer

---

Tris base	3 g
Glycine	14.4 g
SDS	1 g
H <sub>2</sub> O	ad 1,000 ml

#### 7.4 WESTERN BLOTTING AND DETECTION

After separation of the protein mixtures by electrophoresis, proteins are transferred onto blotting membranes which bind them with a high affinity. The blotting process concentrates proteins and thus increases sensitivity of the subsequent detection of proteins by binding to specific antibodies and visualisation by chemiluminescence.

The Western Blot was carried out by the tank blotting technique using freshly prepared tank buffer (1 x). Nitrocellulose membranes (Hybond™-ECL™, Amersham Biosciences, Freiburg, Germany) were activated by soaking in tank buffer for at least 15 minutes. Transfer sandwiches were assembled in a box containing tank buffer by putting first the black piece of the plastic (cathode side), then a wetted pad, a soaked blotting paper, the gel followed by the membrane, a second blotting paper and pad and finally the sandwich was closed with the white piece of the sandwich (anode side). Sandwiches were mounted in a transfer device (Mini Trans-Blot®, Bio-Rad, Munich, Germany), the cubette was filled up with buffer and transfer was performed at 100 V for 80 min or at 23 V overnight, with magnetic stirring.

---

#### Tank buffer (5 x)

---

Tris base	15.2 g
Glycine	72.9 g
H <sub>2</sub> O	ad 1,000 ml

---

#### Tank buffer (1 x)

---

Tank buffer (5 x)	200 ml
Methanol	200 ml
H <sub>2</sub> O	ad 1,000 ml

**TBS-T**

---

Tris base	3 g
NaCl	11.1 g
Tween 20	1 ml
H <sub>2</sub> O	ad 1,000 ml

After transfer, membranes were blocked in 5 % non-fat dry milk in Tris-buffered saline with Tween (TBS-T) for 1 h at room temperature. After a short washing in TBS-T, membranes were incubated in the respective primary antibody solutions (see Table IV.4) in 5 % BSA in TBS-T overnight at 4°C with gently shaking. After four wash steps in TBS-T for 5-10 minutes each, membranes were shaken in appropriate dilutions of secondary antibodies conjugated to horseradish peroxidase (see Table IV.5) in 1 % non-fat dry milk in TBS-T for 1 h at room temperature. Before development of the blot membranes were washed again as described above.

Protein bands of interest were visualised using the ECL Plus™ Western Blotting detection reagent (Amersham Biosciences, Freiburg, Germany). Membranes were exposed to X-ray film for the appropriate time periods and subsequently developed in a tabletop film processor (Curix 60, Agfa, Cologne, Germany).

## IV Materials and methods

---

**Table IV.4: Primary antibodies.**

Antigen	Isotype	Dilution	Provider
ASK1	Rabbit	1 : 1000	Cell Signaling, Frankfurt, Germany
p-ASK1 (Thr845)	Rabbit	1 : 1000	Cell Signaling, Frankfurt, Germany
BiP / GRP78	Mouse IgG <sub>2a</sub>	1 : 250	BD Biosciences, Heidelberg, Germany
Caspase-2	Mouse IgG <sub>1</sub>	1 : 1000	BD Biosciences, Heidelberg, Germany
Caspase-4	Mouse IgG <sub>1</sub>	1 : 1000	MBL, Woburn, USA
Caspase-9	Rabbit	1 : 1000	Cell Signaling, Frankfurt, Germany
CHOP / GADD153	Rabbit	1 : 250	Sigma-Aldrich, Taufkirchen, Germany
p-eIF2α (Ser51)	Rabbit	1 : 1000	Cell Signaling, Frankfurt, Germany
JNK	Rabbit	1 : 1000	Cell Signaling, Frankfurt, Germany
p-JNK (Thr183/Tyr185)	Mouse IgG <sub>1</sub>	1 : 2000	Cell Signaling, Frankfurt, Germany
Ubiquitin	Mouse IgG <sub>1</sub>	1 : 1000	Cell Signaling, Frankfurt, Germany

**Table IV.5: Secondary antibodies.**

Antibody	Dilution	Provider
Goat anti-mouse IgG <sub>1</sub> : HRP	1 : 1000	Biozol, Eching, Germany
Goat anti-mouse IgG : HRP	1 : 1000	Cell Signaling, Frankfurt, Germany
Goat anti-rabbit : HRP	1 : 10,000	Dianova, Hamburg, Germany

## 7.5 MEMBRANE STRIPPING

After carrying out a WB experiment membranes can be re-used for the detection of different proteins. Bound antibodies resulting from the previous experiment must be removed to avoid cross reactions and mistaken results. For this purpose, membranes were washed after development (4 x 5 min) and incubated in stripping buffer for 30 min at 50°C on a shaking platform. Afterwards membranes were thoroughly washed (6 x 5 min) to remove any remnants of stripping buffer and developed with ECL Plus™ solution to confirm stripping effectiveness. After another washing step membranes were blocked and incubated with primary and secondary antibodies as described in IV.7.4.

### Stripping buffer

---

Tris-HCl pH 6.8	62.5 mM
SDS	2 %
2-mercaptoethanol	100 mM

2-mercaptoethanol was added to the stripping buffer immediately before use.

## 7.6 STAINING OF GELS AND MEMBRANES

Equal protein loading and blotting of samples was checked by staining of gels as well as membranes after WB experiments. A commonly used stain for detecting proteins in polyacrylamide gels is Coomassie blue, which penetrates the gel and sticks permanently to the proteins. Excess dye is washed out by 'destaining'. Ponceau S was used to stain reversibly proteins on nitrocellulose membranes.

After transfer gels were stained with Coomassie blue solution for 20 min at room temperature on a shaking platform. Next gels were washed several times in destaining solution until the proteins appeared as blue bands against a clear background.

### Coomassie staining solution

---

Coomassie blue	3 g
Glacial acetic acid	100 ml
Ethanol	450 ml
H <sub>2</sub> O	ad 1,000 ml

Coomassie destaining solution

---

Glacial acetic acid	100 ml
Ethanol	333.3 ml
H <sub>2</sub> O	ad 1,000 ml

Moreover blotting membranes were stained after development by immersion in Ponceau staining solution (0.2 % Ponceau S in 5% acetic acid) and agitation for 5 minutes on a shaking platform. Membranes were washed in H<sub>2</sub>O until the background disappeared.

## 8 MEASUREMENT OF Ca<sup>2+</sup>

Changes in intracellular calcium levels can be analysed with a range of ion-sensitive indicators, whose light emission reflects the local concentration of the ion. Fura-2 is a calcium indicator often used in the esterified form Fura-2 acetoxyethyl ester (fura-2-AM). The acetoxyethyl ester group increases uptake of the dye and is hydrolysed by cytoplasmic esterases to regenerate and trap the dye in cytosol. Fura-2 free of Ca<sup>2+</sup> emits fluorescence upon excitation at 380 nm but after binding to Ca<sup>2+</sup> experiences a shift to 340 nm in its excitation wavelength. Therefore, the ratio of fluorescence intensity obtained by excitation at 340 nm to the intensity obtained by excitation at 380 nm provides an accurate measurement of the free Ca<sup>2+</sup> concentration. If the technical equipment only allows for the excitation with a single wavelength at any time, a measurement of the fluorescence emitted after excitation at 340 nm is an acceptable indicator of the free ion concentration.

Hepes buffer, pH 7.40

---

125 mM NaCl
3 mM KCl
1.25 mM NaH <sub>2</sub> PO <sub>4</sub> x H <sub>2</sub> O
2.5 mM CaCl <sub>2</sub> x 2H <sub>2</sub> O
1.5 mM MgCl <sub>2</sub> x 6H <sub>2</sub> O
10 mM Glucose
10 mM HEPES

Variations in cytosolic calcium were studied in Jurkat and HeLa cells. For this purpose, Jurkat cells were centrifuged (180 x g, 10 min, 25°C), washed once with Hepes buffer and resuspended at 2 x 10<sup>6</sup> cells/ml in Hepes buffer containing 0.1% BSA and supplemented with 2.5 mM probenecid (Sigma-

Aldrich, Taufkirchen, Germany) to avoid Fura-2 leakage. Fura-2-AM was added to a final concentration of 1  $\mu$ M and the cell suspension was incubated for 45 min at 37°C. After two washing steps with Hepes buffer-0.1% BSA, cells were resuspended in Hepes buffer supplemented with 2.5 mM probenecid at 10<sup>6</sup> cells/ml. The cell suspension was then transferred to a 10 mm square quartz cell polished on four sides and temperature was kept at 37°C by placing the cell in a cell holder equipped with a magnetic stirrer and connected to a constant-temperature water circulating device. After 2-3 min cells were stimulated with *cephalostatin 1*, *thapsigargin* or solvent (DMSO). Cytosolic Fura-2 fluorescence was assayed on a Shimadzu RF-1502 spectrofluorophotometer (Shimadzu, Duisburg, Germany) at an emission wavelength of 510 nm and an excitation wavelength of 340 nm. Changes in intracellular calcium concentration were registered with the PC-1501 software (Shimadzu, Duisburg, Germany).

For the analysis of Ca<sup>2+</sup> release in HeLa cells, 6 x 10<sup>5</sup> cells were plated onto 42 mm glass round coverslips and allowed to adhere for 40 h. Cells were then washed two times with 5 ml Hepes buffer and loaded by incubation in 1 ml of Hepes buffer containing 5  $\mu$ M Fura-2-AM for 1 h at 37°C. Loaded cells were washed twice with Hepes buffer and kept in 2 ml buffer until experiments were done. Coverslips containing loaded cells were mounted into a coverslip holder, buffer was then washed away and replaced with 1 ml of fresh Hepes buffer. The coverslip holder was placed on the stage of a Zeiss Axiovert 200 inverted microscope (Zeiss, Oberkochen, Germany) equipped with a Polychrome V monochromator and an IMAGO-QE camera (TILL Photonics GmbH, Gräfelfing, Germany). Chamber temperature was maintained to 37°C by placing the coverslip holder on a heating insert P (Zeiss, Oberkochen, Germany). Cells were stimulated by addition of 100  $\mu$ l of Hepes buffer (control) or buffer containing the adequate concentration of *cephalostatin 2* and *thapsigargin*. Excitation wavelengths were alternately selected at 340 nm and 380 nm and fluorescence filtered at 440 nm (LP filter) was recorded. Images were acquired and analysed with TILLvision Software 4.0.1.2 (TILL Photonics GmbH, Gräfelfing, Germany). Areas of interest corresponding to single cells and to the whole field of vision were selected, the background was subtracted and the average intensity of each area over the course of the experiment was recorded. Data were expressed as the ratio of fluorescence emitted by excitation at 340 and 380 nm and curves representing the change in fluorescence over the course of the experiment were created.

## 9 CASPASE-4 siRNA

RNA interference (RNAi) has emerged as a powerful method for sequence-specific inhibition of gene function. Down-regulation of the gene of interest can be achieved by introduction of double-stranded short interfering RNAs (siRNAs) into the cells or by producing the silencing RNA within the cells employing expression vectors [189].

The psiRNA-h7SKneo G1 expression vector system (Figure IV.4, InvivoGen, San Diego California, USA) was used to decrease expression of caspase-4. The human 7SK promoter provides a continuous expression of short hairpin RNAs (shRNAs) containing a 19-21 double-stranded stem that is identical in sequence to the target mRNA. The two strands of the stem are connected by a short loop which is removed *in vivo* by Dicer to generate siRNAs. The Neo gene encodes an aminoglycoside 3'-phosphotransferase that confers resistance to the antibiotics kanamycin in bacteria and G418 in mammalian cells, enabling the continuous selection of the cells that have taken up the plasmid. The EM7-alpha-peptide enables the white/blue selection of bacteria colonies.

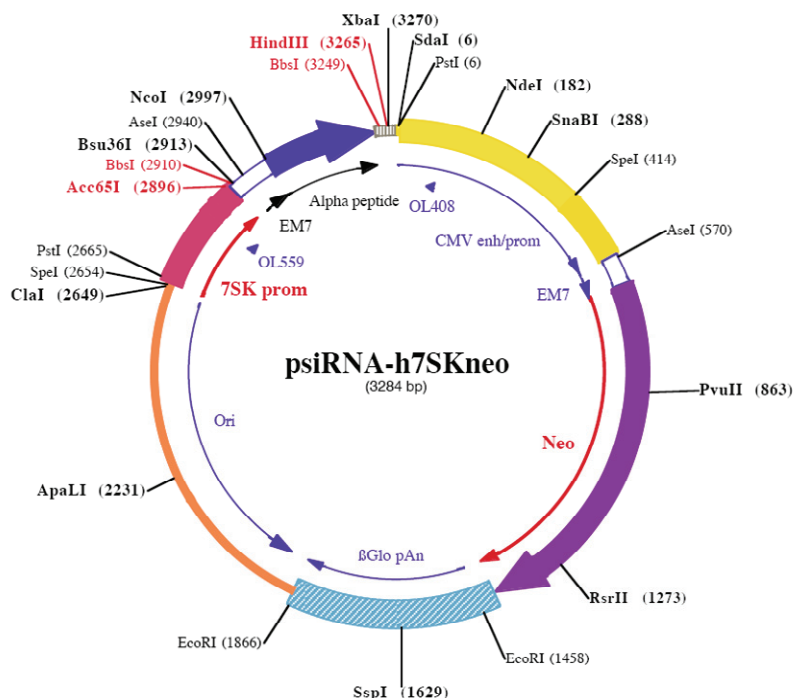


**Figure IV.4. psiRNA-h7SKneo G1 vector (from [190]).**

## 9.1 INSERT DESIGN AND CLONING INTO psiRNA-h7SKneo G1 VECTOR

For the specific targeting of caspase-4 two different oligonucleotides (see Table VI.6) were designed and obtained from Biomers, Ulm, Germany. Sequences encoded respective short hairpin RNAs with a 21 nt complementary region separated by a small loop of 7 nt and flanked by 5'- and 3'- overhangs required for cloning by Bbs I. Target sequences had been described in [87] and designated as caspase-4a and caspase-4b.

DNA oligonucleotides were diluted in nuclease-free H<sub>2</sub>O to a concentration of 25 µM and hybridised by incubation of the annealing solutions (2 µl forward oligo, 2 µl reverse oligo, 6 µl 0.5 M NaCl, 20 µl H<sub>2</sub>O) for 2 minutes at 80°C in a heating block. The annealed oligos were slowly cooled by switching off the heater and waiting until the temperature was about 35°C. Afterwards solutions were stored at -20°C.

**Table IV.6: Insert oligonucleotides containing siRNA sequences.**

### **Caspase-4a**

Forward	5'-acctcAAGTGGCCTTTCACAGTCATcaagagATGACTGT GAAGAGGCCACTTtt-3'
Reverse	5'-aaaaaaAAGTGGCCTTTCACAGTCATctcttgAAAGACTGT GAAGAGGCCACTTg-3'

### **Caspase-4b**

Forward	5'-acctcAAGATTCCCTCACTGGTGTTCcaagagAACACCA GTGAGGAAATCTTtt-3'
Reverse	5'-aaaaaaAAGATTCCCTCACTGGTGTTCtcttgAACACCA GTGAGGAAATCTTg-3'

The psiRNA-h7SKneo G1 plasmid was dissolved in nuclease-free H<sub>2</sub>O to a concentration of 1 µg/ml. The vector was linearised by incubation with the Bbs I restriction enzyme (New England Biolabs, Frankfurt, Germany). For this purpose an appropriate solution was prepared (10 µl plasmid, 2 µl 10 x Bbs I buffer, 1 µl Bbs I, 7 µl H<sub>2</sub>O) and incubated for 2 h at 37°C in a water bath [191]. The large fragment (2945 bp) was eluted using a 0.7% agarose gel and the fragment containing the linearised plasmid was cut using a scalpel. DNA was extracted using a QIAquick® gel extraction kit (QIAGEN, Hilden, Germany) and diluted to obtain a solution 0.1 µg/µl.

Subsequently ligation solutions were assembled (15 µl H<sub>2</sub>O, 2 µl 10 x ligation buffer, 1 µl annealed insert, 1 µl linearised vector, 1 µl T4 DNA ligase) and incubated at 27°C for 2 hours to obtain the recombinant vectors containing caspase-4a and caspase-4b inserts.

## 9.2 TRANSFORMATION OF LyoComp GT116

*E.coli* strain GT116, provided as lyophilized competent cells called LyoComp GT116 (Invivogen, San Diego California, USA) were reconstituted following manufacturer's protocol. 10 µl of the ligation product (see IV.9.1) were incubated with 100 µl of bacteria in ice for 30 min. Then bacteria were incubated at 42°C for 30 seconds and placed back in ice for 1-2 min. 900 µl of room temperature lysogeny broth (LB) medium (Gibco/Invitrogen, Karlsruhe, Germany) were added to each tube and bacteria were incubated in a water bath at 37°C for 90 min.

200 µl of bacteria suspension were spread onto kanamycin (Calbiochem, Schwalbach, Germany)-agar plates [191] containing IPTG (20 µl, solution 100 mM, Calbiochem, Schwalbach, Germany) and X-Gal (30 µl, solution 50 mg/ml, Calbiochem, Schwalbach, Germany). Plates were incubated at 37°C overnight.

### LB agar-kanamycin

---

Lennox L Broth Base	20 g
Agar	15 g
Kanamycin 100 mg/ml	1 ml
H <sub>2</sub> O	ad 1,000 ml

### LB medium-kanamycin

---

Lennox L Broth Base	20 g
Kanamycin 100 mg/ml	1 ml
H <sub>2</sub> O	ad 1,000 ml

Kanamycin was added to LB medium freshly before use.

## 9.3 MINI PREPARATION OF PLASMIDS

Five white colonies each of bacteria transformed with recombinant vectors were picked and inoculated in 2 ml of LB medium containing 100 µg/ml of kanamycin.

Bacteria were grown under agitation at 200 rpm in an orbital incubator shaker (Thermoshake THO 500, Gerhardt, Königswinter, Germany) for 10-12 h at 37°C. Thereafter plasmid DNA was isolated using a QIAprep® Miniprep kit (QIAGEN, Hilden, Germany) according to the manufacturer's protocol and dissolved in nuclease-free H<sub>2</sub>O. Presence of plasmids was confirmed by running probes in 1% agarose gels.

Liquid bacteria cultures can be stored for a long time in glycerol stocks. These were prepared by mixing 775 µl of an overnight bacteria culture with 225 µl of 80% glycerol and frozen at -80°C [191].

#### **9.4 SEQUENCING OF THE siRNA INSERT**

The presence as well as the sequences of the siRNA inserts within 2 clones containing the recombinant plasmids were confirmed (Medigenomics GmbH, Martinsried, Germany) using the sequencing primers provided in the kit (OL559 and OL408) before maxi preparation and transfection in Jurkat cells.

#### **9.5 MAXI PREPARATION OF PLASMIDS**

2 ml of transformed bacteria containing unaltered inserts were added to 600 ml of LB medium-kanamycin and cultures were grown overnight as described in IV.9.3. Plasmids containing caspase-4a and caspase-4b inserts were obtained employing an EndoFree® Plasmid Maxi Kit (QIAGEN, Hilden, Germany) following manufacturer's instructions and dissolved in nuclease- and endotoxin-free H<sub>2</sub>O. Purified plasmids were directly used for transfection.

#### **9.6 AMPLIFICATION OF psiRNA-h7SKneo AND psiRNA-h7SKnScr VECTORS**

The psiRNA-h7SKneo (empty vector) and psiRNA-h7SKnScr (containing the scramble sequence 5'-GCATATGTGCGTACCTAGCAT-3') plasmids provided in the kit were used as controls in the siRNA experiments. In order to obtain enough quantities of these plasmids, competent *E.coli* DH5α bacteria were transformed [191] and grown on kanamycin-agar plates.

Several colonies were picked and grown in LB medium-kanamycin. Mini preparations were performed as described above and presence of plasmids was checked by running probes in 1% agarose gels.

Maxi preparations of the colonies containing the plasmid of interest were used to obtain purified DNA, which was likewise dissolved in nuclease- and endotoxin-free H<sub>2</sub>O and directly used for transfection.

### **9.7 TRANSFECTION AND SELECTION OF JURKAT CELLS**

Jurkat T cells (clone J16) were transfected by electroporation with the Nucleofector™ II device (Amaxa, Cologne, Germany) employing the Cell Line Nucleofector™ Kit V. For each transfection, 4 x 10<sup>6</sup> Jurkat cells from passages four to seven in exponential growing phase were centrifuged for 10 min at 200 x g and resuspended in 100 µl of room temperature Nucleofector™ Solution V. The cell suspension was mixed with 3 µg of psiRNA-h7SKneo, 3 µg of psiRNA-h7SKnScr or 3-4 µg of a 1:1 mixture of the caspase-4a and caspase-4b shRNA constructs. The mixture of cells and DNA was transferred to an amaxa certified cuvette and transfection was performed using the program C19. 500 µl of pre-warmed culture medium were added to the cuvette and cells were immediately seeded in 12-well plates and further cultured or used for experiments 24 h after transfection.

Control cell lines expressing psiRNA-h7SKneo and psiRNA-h7SKnScr were obtained by addition of 1 mg/ml G418 to the culture medium 2 days after transfection and selection for 4 weeks. It was not possible to obtain cell lines with a long-term down-regulation of caspase-4.

### **9.8 EFFECT OF CASPASE-4 SILENCING IN CASPASE-9 ACTIVATION AND APOPTOSIS**

To study the influence of caspase-4 down-regulation in apoptosis, 3 µg of shRNA-generating plasmids (caspase-4a and caspase-4b 1:1) were transfected into Jurkat cells as described above. Cells were incubated at 37°C for 24 h, seeded in 24-well plates and stimulated with cephalostatin 1 for 16 h. DNA fragmentation was quantified by flow cytometry (see IV.3.3).

To investigate caspase-9 activation in cells with silenced caspase-4 expression, Jurkat cells were transfected with 4 µg of shRNA constructs (caspase-4a and caspase-4b 1:1) and 1 mg/ml G418 was added to the culture medium 2 days thereafter. 48 h later, cells were seeded in G418-free medium and stimulated for the required times. Cell lysates were prepared and caspase-9 protein was analysed by Western Blot as described in IV.7.

In both cases cells stably expressing psiRNA-h7SKneo and psiRNA-h7SKnScr vectors were used as controls. Efficiency of RNAi in transfected cells was checked for each experiment by Western Blot analysis using antibodies against caspase-4.

## 10 PHAGOCYTOSIS ASSAY AND CYTOKINE RELEASE

### 10.1 EVALUATION OF PHAGOCYTOSIS

Phagocytosis of Jurkat cells was investigated employing a co-culture model with human macrophages and flow cytometric analysis. For this purpose, THP-1 cells were differentiated to macrophages and Jurkat cells were fluorescently labelled (green) before the induction of cell death. Figure IV.5 represents schematically the co-culture model employed.

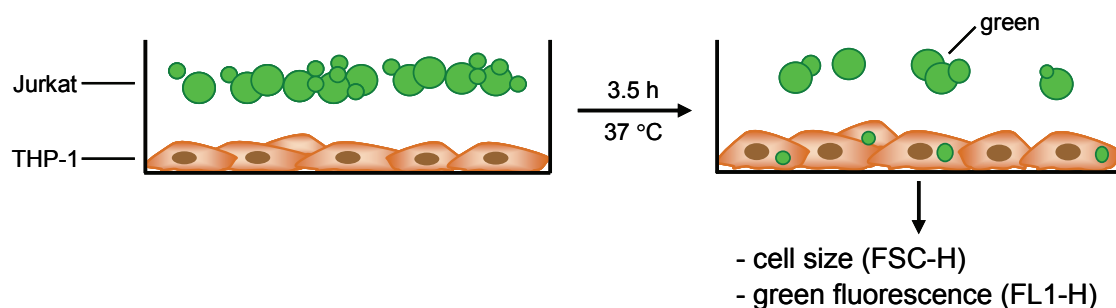


**Figure IV.5: Schematic illustration of the phagocytosis co-culture model.**

THP-1 cells were centrifuged ( $180 \times g$ , 10 min,  $25^\circ\text{C}$ ), washed twice with PBS and resuspended at a concentration of  $5 \times 10^5$  cells/ml in 10% FCS-RPMI containing 160 nM phorbol myristate acetate (PMA). Cells were seeded (1 ml, 24-well plate) and incubated for 72 h at  $37^\circ\text{C}$  [162]. PMA-treated THP-1 cells were washed with PBS three times and maintained in 10% FCS-RPMI until the phagocytosis assay. PMA is an activator of protein kinase C widely used to induce differentiation of several cell lines.

Jurkat cells were labelled with 5-(and-6)-carboxy-2',7'-dichlorofluorescein diacetate, succinimidyl ester (CCFSE), a non-toxic cell-permeable fluorescent dye that binds covalently to the amine groups of proteins.

Cells were centrifuged ( $180 \times g$ , 10 min,  $25^{\circ}\text{C}$ ), washed once with PBS and resuspended at  $10^6$  cells/ml in PBS containing 0.1% BSA. CCFSE was added to a final concentration of 10  $\mu\text{M}$  and the cell suspension was incubated for 10 min at  $37^{\circ}\text{C}$  (protocol adapted from [192]). After a washing step with 0.1% BSA-PBS solution, cells were resuspended in fresh medium and seeded at  $5 \times 10^5$  cells/ml in 24-well tissue culture plates for the induction of apoptosis / PCD or at  $10^6$  cells/ml in tissue culture dishes for the induction of necrosis. Fluorescent labeled Jurkat cells were left untreated or treated with DHA (40  $\mu\text{M}$ ), HC (20  $\mu\text{M}$ ), EM (5  $\mu\text{M}$ ) or etoposide (1.5  $\mu\text{M}$ ) for 4 h at  $37^{\circ}\text{C}$ . Subsequently cells were pooled, centrifuged ( $600 \times g$ , 10 min,  $25^{\circ}\text{C}$ ), washed once with PBS and resuspended in 10% FCS-RPMI at  $10^6$  cells/ml. Necrosis was induced by incubation of cells for 15 min at  $55^{\circ}\text{C}$  [126].

Target cells (SQTL-, etoposide-treated, necrotic or untreated Jurkats) were added to the differentiated THP-1 cells at a ratio of 2:1 and culture plates were incubated for 3.5 h at  $37^{\circ}\text{C}$ . Wells were then gently washed three times with cold PBS to remove uningested cells. Adherent cells were recovered by trypsinisation and analysed by flow cytometry. The fluorescence intensity (FL1) as well as scatter parameters of macrophages were acquired. For the quantification of phagocytosis a region including macrophages was set up and the mean size (linear mode) and fluorescence (logarithmic mode) of gated cells was recorded. Moreover a dot plot representing FSC versus FL1 was used to calculate the percentage of macrophages that had acquired green fluorescence [126,162].

## 10.2 CYTOKINE QUANTIFICATION

The possible influence of the removal of apoptotic cells in the cytokine secretion pattern of co-culture macrophages was investigated by quantifying tumor necrosis factor-alpha (TNF- $\alpha$ ) and transforming growth factor-beta (TGF- $\beta$ ) in cell culture supernatants.

THP-1 cells were differentiated to macrophages at a density of  $1 \times 10^5$  cells/ml (200  $\mu\text{l}$ , 96-well plates) as described in IV.10.1. Macrophages were stimulated with 0.1  $\mu\text{g}/\text{ml}$  lipopolysaccharide (LPS) (*E. coli*) for 3 h and washed with prewarmed PBS after this incubation time. Jurkat cells were stimulated with SQTL/etoposide or incubated for 30 min at  $55^{\circ}\text{C}$  (necrosis) and prepared for phagocytosis as described above. Untreated, apoptotic or necrotic cells were given to macrophages at a ratio of 10:1. Culture supernatants were collected in ice after 3.5 and 18 h of co-culture, centrifuged ( $1,000 \times g$ , 10 min,  $4^{\circ}\text{C}$ ) to

eliminate particulates and stored at –80°C before quantification of cytokines [126,155].

TNF- $\alpha$  and TGF- $\beta$  concentrations in the supernatants were quantified by means of ELISA techniques at the Department of Biochemical Pharmacology, University of Konstanz (Konstanz, Germany). TNF- $\alpha$  was determined by self-made ELISA using TNF- $\alpha$  Antibodies von Pierce – Endogen (Biot. Prod. Nr.: M 302B, Coat. Prod. Nr.: M 303) and TGF- $\beta$  using the human TGF- $\beta_1$  DuoSet® ELISA kit from R&D Systems. TNF- $\alpha$  concentrations were normalised to the value corresponding to LPS-stimulated macrophages which did not receive Jurkat cells. For TGF- $\beta$  analysis, TGF- $\beta$  concentration found in culture medium was subtracted from experimental values.

### 10.3 ANALYSIS OF PHAGOCYTOSIS BY CONFOCAL MICROSCOPY

In order to visualise and confirm phagocytosis, confocal microscopy experiments were carried out. For this purpose, macrophages were stained with the red fluorescent substance PKH26 before co-culture with CCFSE-stained Jurkat cells.

THP-1 cells were differentiated in 24-well plates with glass coverslips as described in IV.10.1. Macrophages were fluorescently labelled with PKH26 by adapting the manufacturer's instructions. Cells were washed once with RPMI 1640 and incubated with 200  $\mu$ l of staining solution (2  $\mu$ M PKH26 in diluent B, freshly prepared) per well for 3 min at room temperature. The staining reaction was stopped by addition of 200  $\mu$ l of FCS. One minute later, 400  $\mu$ l of complete medium were added and cells were finally washed 3 times with RPMI or medium. Labelled cells were kept in medium until addition of target cells.

Jurkat cells were labelled with the fluorescent marker CCFSE and cell death (apoptosis or necrosis) was induced as described in IV.10.1. After 3.5 h of co-culture at a ratio 2:1, uningested Jurkat cells were removed by several washings with cold PBS. Samples were fixed with 1 ml of 4 % para-formaldehyde in PBS for 10 min at room temperature and washed three times with PBS. Glass coverslips were then covered with a droplet of fluorescent mounting medium (DakoCytomation GmbH, Hamburg, Germany) and mounted on a microscope slide. Probes were allowed to solidify for at least 2 h.

Dual-channel fluorescence and transmitted light images were taken by the confocal microscope LSM 510 Meta (Zeiss, Oberkochen, Germany). PKH26 fluorescence was obtained by excitation with the HeNe1 laser (543 nm) and

detection with a 560 nm LP filter. Simultaneously, the argon laser (488 nm) was used to excite samples and emitted light recorded with a 505-530 BP filter corresponded to CCFSE fluorescence.

To perform three-dimensional analysis of the samples, a set of dual-channel z-stack images of each macrophage of interest was captured. Thickness of slices ranged between 10 and 15  $\mu\text{M}$ . Three-dimensional projections of the z-stacks were created with the microscope software and rotated to observe localisation of engulfed cells.

## 11 STATISTICS

All experiments were performed at least three times. Results are expressed as mean value  $\pm$  SEM. Statistical analysis was performed with GraphPad PRISM™ version 3.03 for Windows (GraphPad Software, San Diego, California, USA). Statistical comparisons were made by one-way ANOVA with Bonferroni or Dunnett multiple comparison post-test or by unpaired two-tailed Student's t test. P values  $< 0.05$  were considered significant.

## **V. RESULTS**

## V. RESULTS

### A. CEPHALOSTATIN 1

#### 1 IMPORTANCE OF CASPASE-9 IN CEPHALOSTATIN 1-INDUCED APOPTOSIS

Our group has previously shown that the experimental chemotherapeutic agent cephalostatin 1 induces apoptosis in Jurkat T cells without cytochrome c release and apoptosome formation or requirement of active caspase-8 but involving activation of caspase-9 [20]. To clarify the role of this caspase in cephalostatin 1-induced apoptosis, a Jurkat cell line deficient in caspase-9 was used and compared to normal Jurkat T cells. Interestingly, apoptosis induced by cephalostatin 1 was almost completely inhibited in caspase-9-deficient cells (Figure V.1) pointing to a crucial role of this caspase. As expected, mutant cells did not show any signs of apoptosis in response to etoposide, a drug that induces apoptosis through the intrinsic mitochondrial pathway and used as positive control. These data asked for clarifying the mechanism underlying the apoptosome-independent activation of caspase-9 by cephalostatin and subsequent apoptosis.

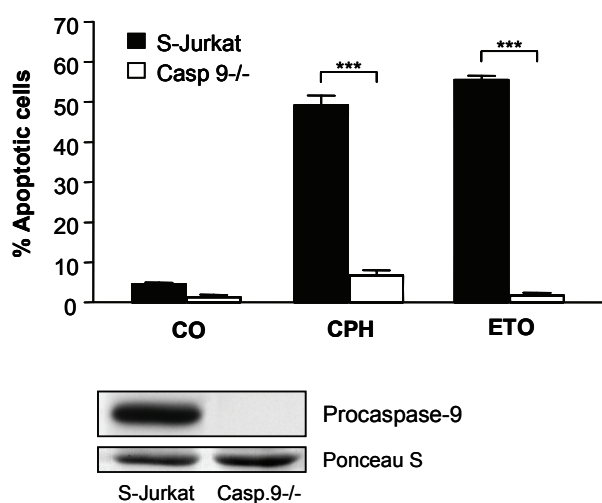


**Figure V.1: Caspase-9 is essential for cephalostatin 1-induced apoptosis.**

Parental Jurkat cells (*S-Jurkat*) and Jurkat cells lacking caspase-9 (*Casp.9-/-*) were left untreated (CO) or treated for 24 hours with cephalostatin 1 (CPH; 1  $\mu$ M) or etoposide (ETO; 2  $\mu$ M). Apoptotic cells were quantified by flow cytometry as described in "Materials and Methods" (upper panel). Protein extracts from *S-Jurkat* and caspase-9-/- cells were prepared and caspase-9 protein levels were analysed by Western Blot (lower panel). Equal protein loading was controlled by staining membranes with Ponceau S (a representative fragment of the stained membrane is shown). Bars, the mean  $\pm$  SEM of three independent experiments performed in triplicate. \*\*\*,  $P < 0.001$  (unpaired two-tailed *t* test).

## 2 SIGNAL TRANSDUCTION IN CEPHALOSTATIN-INDUCED ENDOPLASMIC RETICULUM (ER) STRESS AND APOPTOSIS

### 2.1 CEPHALOSTATIN INDUCES ER STRESS

#### 2.1.1 Influence on ER stress markers

In search of the initial event leading to caspase-9 activation and apoptosis, it was sought to investigate whether cephalostatin 1 induces an ER stress response which could lead to an apoptosome-independent activation of caspase-9. A cytochrome c and Apaf-1-independent but ER-dependent activation of caspase-9 has been described [84,85]. In addition, the cellular morphological changes caused by cephalostatin 1 treatment supported the theory of induction of ER stress. These include the enlargement of ER membranes and the appearance of ER-derived vesicles in the cytoplasm [193].

First, it was studied whether the expression of an ER stress sensor (BiP/GRP78) and an ER stress-induced cell death modulator (CHOP/GADD153) were affected by cephalostatin 1. As shown in Figure V.2 cephalostatin 1 (1 µM) increases expression of the ER chaperone BiP/GRP78 and the transcription factor CHOP/GADD153 as does the known ER stress-inducer tunicamycin. The increase of BiP showed a biphasic pattern, with an early increase (30 min-1 h) followed by a plateau and a second strong elevation after 16-24 h. CHOP protein level increased rapidly (15 min-1 h) and decreased slowly thereafter. The α-subunit of eukaryotic translation initiation factor-2 (eIF2α) is phosphorylated by the kinase PERK in response to ER stress leading to an attenuation of translational initiation and protein synthesis and activation of pathways leading to cell death or survival [75]. Indeed, cephalostatin 1 induced a very early and strong eIF2α phosphorylation as the known ER stress-inducer thapsigargin (Figure V.2) further supporting the assumption of ER stress induction by cephalostatin.

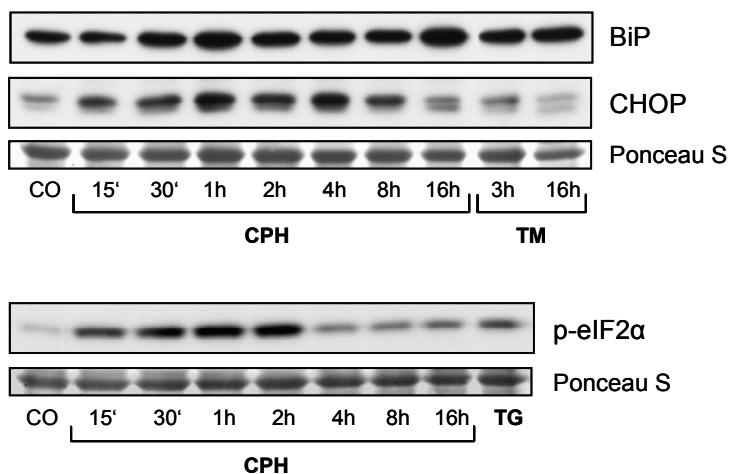


**Figure V.2: Cephalostatin 1 induces ER stress in Jurkat leukemia T cells.**

Cells were either left untreated (CO), treated with cephalostatin 1 (CPH; 1  $\mu$ M) or as a positive control with tunicamycin (TM; 1  $\mu$ g/ml) or thapsigargin (TG; 3  $\mu$ M, 2h) for the indicated times. Western Blot analysis was performed as described in "Materials and Methods" using antibodies against BiP, CHOP and the phosphorylated form of eIF2 $\alpha$ . One representative blot out of three is shown. Equal protein loading was controlled by staining membranes with Ponceau S (a representative fragment of the stained membrane is shown).

Cephalostatin 2 shows a similar cytotoxicity profile and induces apoptosis via mechanisms common to cephalostatin 1 (experiments performed by Anita Rudy). To find out whether ER stress is a phenomenon restricted to Jurkat cells or could be a general mechanism involved in apoptosis, HeLa cells were treated with cephalostatin 2 (50 nM) and the expression of ER stress markers was investigated. As shown in Figure V.3, BiP, CHOP and eIF2 $\alpha$  phosphorylation were early induced by cephalostatin 2 treatment, suggesting that ER stress may be a general initial event in cephalostatin-induced cellular effects.

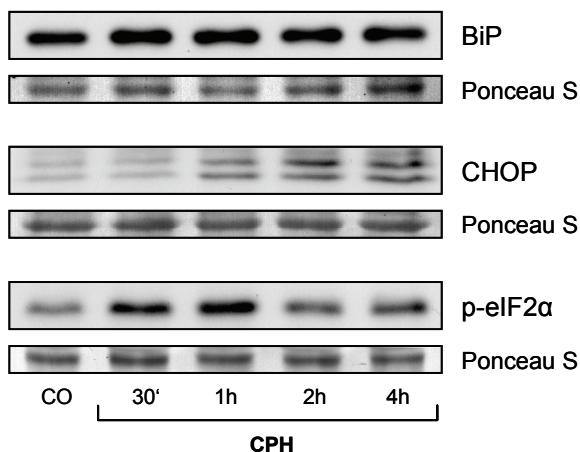


**Figure V.3: ER stress is observed in HeLa carcinoma cells treated with cephalostatin 2.**  
HeLa cells were left untreated (CO) or treated with cephalostatin 2 (CPH; 50 nM) for the indicated times. Cell lysates were prepared as described in "Materials and Methods" and analysed by Western Blot for the expression of BiP, CHOP and p-eIF2 $\alpha$ . One representative Western blot is shown. Protein loading was controlled by staining with Ponceau S.

### 2.1.2 Cephalostatin does not induce Ca<sup>2+</sup> release into cytosol

ER stress can be induced, among many other mechanisms, by alterations in calcium homeostasis [75,92,194]. Moreover, an early (1 h) and notable cleavage of  $\mu$ -calpain, a Ca<sup>2+</sup>-dependent cysteine protease, to its active form upon cephalostatin 1 treatment has been observed [193]. Thus, possible variations in intracellular Ca<sup>2+</sup> concentration were measured to find out whether an increase in cytosolic free Ca<sup>2+</sup> could be responsible for the induction of ER stress by cephalostatin.

First, the Fura-2 fluorescence of Jurkat cells treated with cephalostatin 1 (1  $\mu$ M) or as a positive control with thapsigargin (3  $\mu$ M), an inhibitor of the endoplasmic reticulum Ca<sup>2+</sup> ATPase that induces Ca<sup>2+</sup> leakage into the cytosol, was recorded. Unexpectedly, cephalostatin 1 did not increase the intracellular free Ca<sup>2+</sup> concentration, showing no effect or a slight reduction in Fura-2 fluorescence (Figure V.4). Very similar results were obtained when the dye Calcium Green-1, with different spectral properties, was used (data not shown).

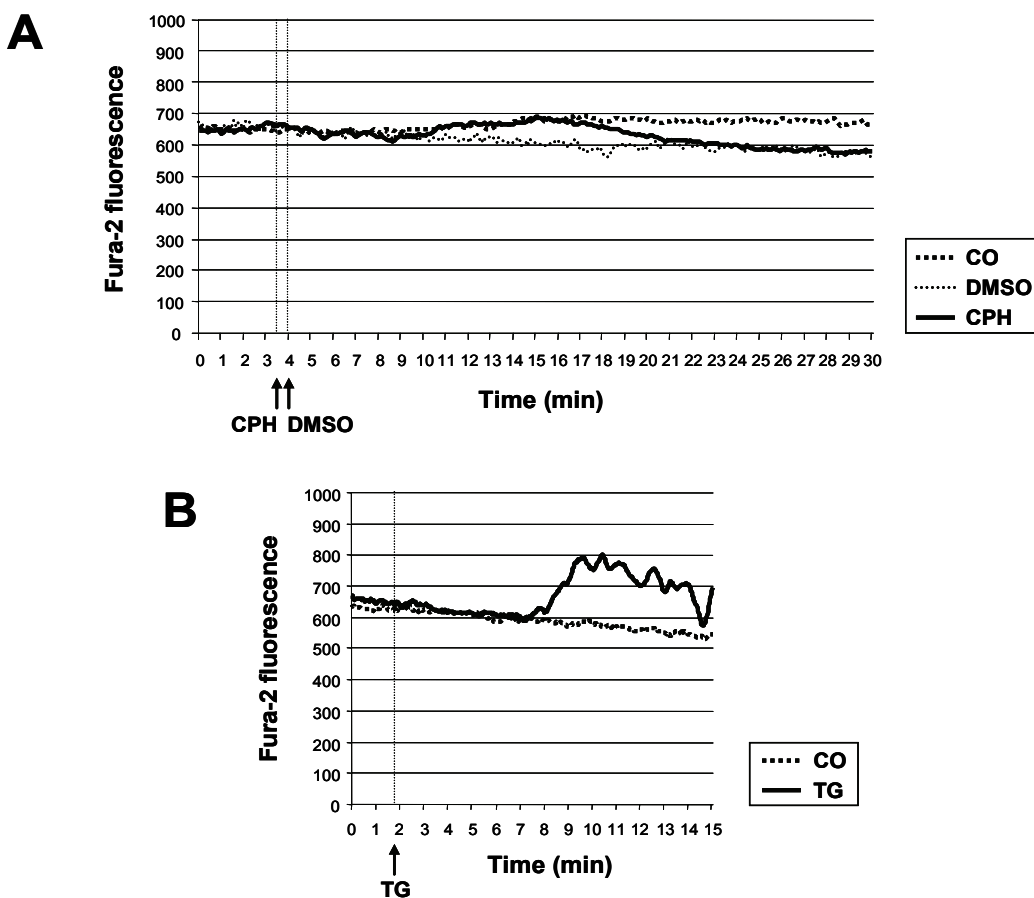


**Figure V.4: Cephalostatin 1 does not induce  $\text{Ca}^{2+}$  release into cytosol.**  
 Jurkat cells were loaded with 1  $\mu\text{M}$  Fura-2-AM as described in "Materials and Methods". Subsequently, cell suspensions were either left untreated (CO) or exposed to solvent (DMSO), 1  $\mu\text{M}$  cephalostatin 1 (CPH) (A) or as a positive control with 3  $\mu\text{M}$  thapsigargin (TG) (B) and Fura-2 fluorescence was monitored with a spectrofluorophotometer. Cells were excited at 340 nm and fluorescence emitted at 510 nm, corresponding to the portion of Fura-2 bound to free  $\text{Ca}^{2+}$ , was recorded and results of one representative experiment are here represented. Experiments were performed three times with similar results.

To confirm these observations, HeLa cells were treated with cephalostatin 2 (50-500 nM) or thapsigargin (3  $\mu\text{M}$ ) and changes in intracellular  $\text{Ca}^{2+}$  were followed. Cephalostatin-treated cells behaved as control cells even at concentrations 10-fold higher than the normally used whereas thapsigargin induced a prominent increase in  $\text{Ca}^{2+}$  concentration (Figure V.5).

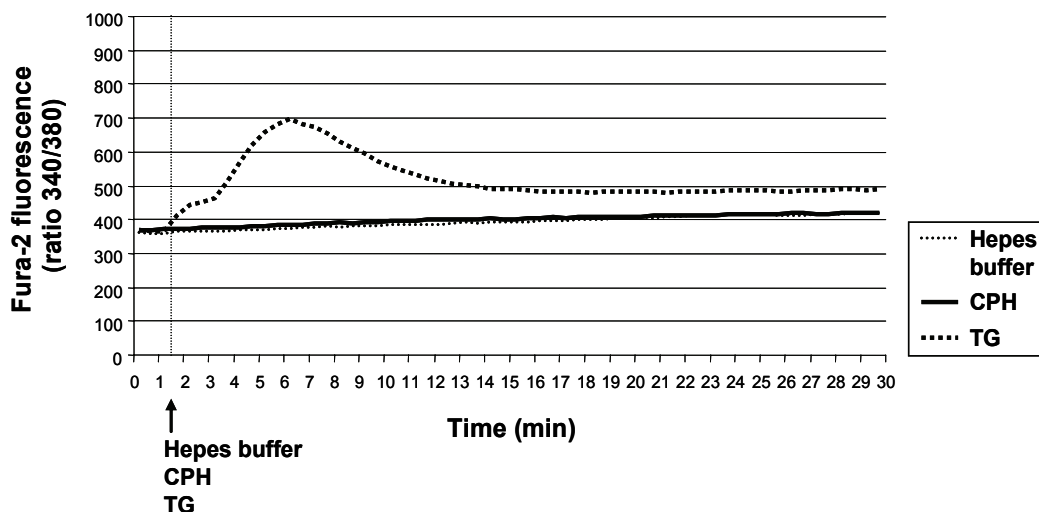


**Figure V.5: HeLa cells do not increase intracellular  $\text{Ca}^{2+}$  concentration in response to cephalostatin treatment.**

Fura-2 preloaded HeLa cells were placed on a Zeiss Axiovert 200 inverted microscope and sequential images were taken. Cells were stimulated by addition of Hepes buffer (control) or buffer containing adequate pre-dilutions of cephalostatin 2 (CPH; final concentration 500 nM) or thapsigargin (TG; final concentration 3  $\mu\text{M}$ ). Excitation wavelengths were alternately selected at 340 nm and 380 nm and fluorescence filtered at 440 nm was recorded. Curves represent the change in the ratio of fluorescence emitted by excitation at 340 and 380 nm over the course of the experiment. The figure shows one representative experiment.

### 2.1.3 ROS production is not increased by cephalostatin 1 treatment

It has been recently described that ROS production can be associated with induction of ER stress [195,196]. In search of the mechanism responsible for triggering ER stress, the possibility that cephalostatin 1 might influence ROS levels was studied.

Figure V.6 provides clear evidence that cephalostatin 1 does not increase ROS levels whereas the positive control staurosporine induces a significant production of ROS.

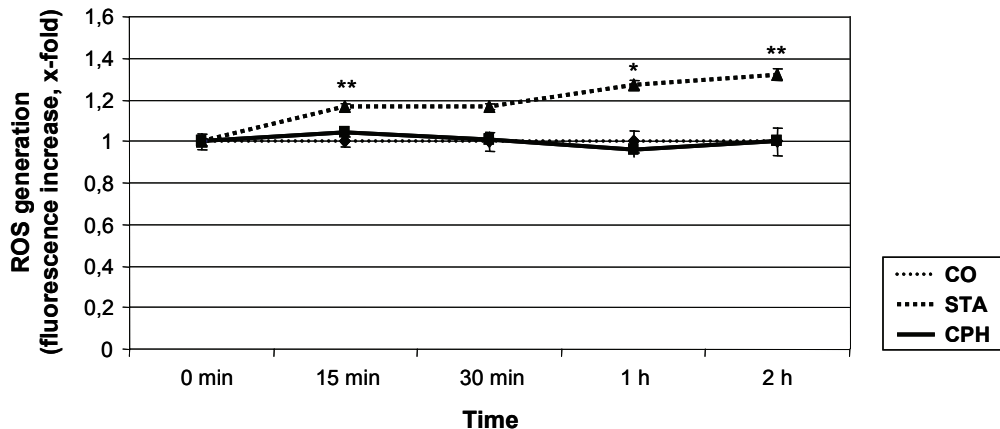


**Figure V.6: ROS levels are not increased upon cephalostatin 1 treatment.**

Jurkat cells were pre-loaded with carboxy-H<sub>2</sub>DCFDA as described in “Materials and Methods” and left untreated (CO) or exposed to 1  $\mu$ M cephalostatin 1 (CPH) or 500 nM staurosporine (STA). At indicated time points, the intracellular fluorescence was quantified by flow cytometry. Bars, the mean  $\pm$  SEM of three independent experiments. \*, P < 0.05; \*\*, P < 0.01 (Anova/Dunnett’s test).

#### 2.1.4 Ubiquitinated proteins accumulate upon cephalostatin 1 treatment

Neither an intracellular increase in calcium levels nor the production of ROS were induced by cephalostatin. Thus, another mechanism should be responsible for the induction of ER stress. Proteasome inhibitors, such as bortezomib, have been described to cause accumulation of ubiquitinated proteins, leading to ER stress and apoptosis [196-199]. As a first approach, it was investigated whether proteins targeted to degradation by ubiquitin accumulated in cells treated with cephalostatin.

Interestingly, cephalostatin 1 treatment leads to a time-dependent increase of ubiquitinated proteins (Figure V.7). A slight increase in the ubiquitination of small proteins (<25 KDa) could be seen as soon as after 15 min of stimulation. A global ubiquitination of cellular proteins was clear after 1 h and increased further in the course of time. This result suggests that the primary mechanism of cephalostatin-induced ER stress could be an accumulation of ubiquitinated proteins provoked by an inhibition of proteasomal protein degradation.

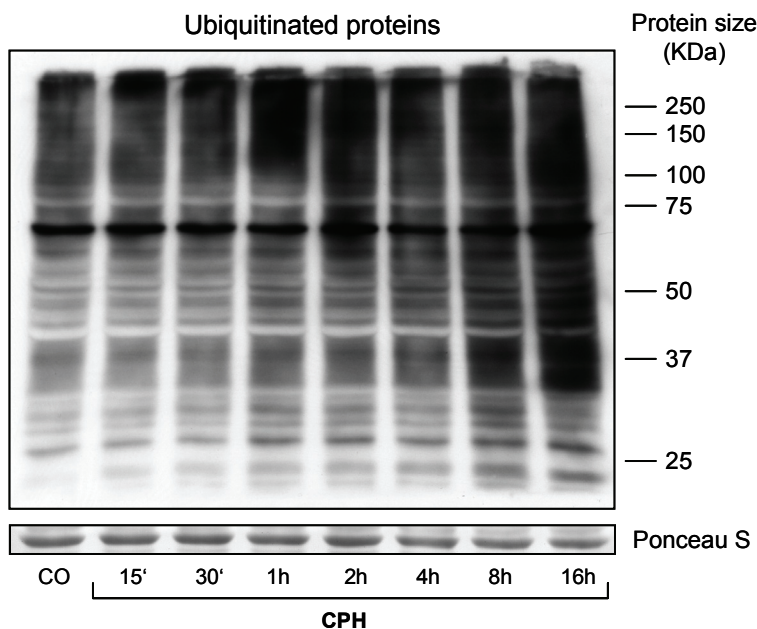


**Figure V.7: Accumulation of ubiquitin-containing proteins upon cephalostatin 1 treatment.**

Jurkat cells were either left untreated (CO) or treated with cephalostatin 1 (CPH; 1  $\mu$ M) for the indicated times. Cell lysates were analysed by Western Blot using an antibody directed against ubiquitin. One representative blot out of three is shown. Equal protein loading was controlled by staining membranes with Ponceau S (a representative fragment of the stained membrane is shown).

## 2.2 INVOLVEMENT OF THE ASK1/JNK SIGNALLING PATHWAY

### 2.2.1 Activation of ASK1 and JNK

The ASK1 and the downstream JNK cascade are known to be activated under conditions of ER stress-induced apoptosis [75]. As observed in Figure V.8, both kinases were activated very early upon cephalostatin 1 treatment. Phosphorylation of ASK1 at Thr845, which is correlated with ASK1 activity, was observed after only 15 minutes and maintained up to at least 2 h of treatment. Its downstream kinase JNK was also already phosphorylated after 15 minutes and the intensity of phosphorylation increased further in the course of time.

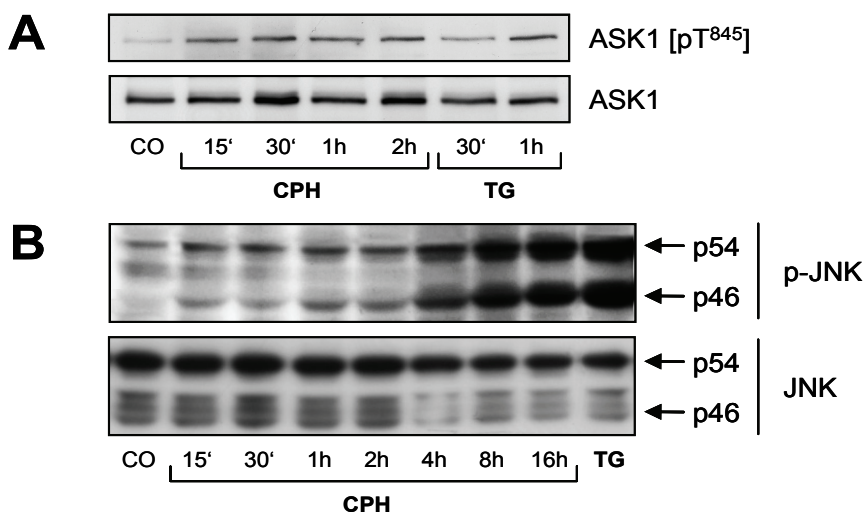


**Figure V.8: Activation of ASK1 and JNK by cephalostatin 1.**

Jurkat T cells were left untreated (CO) or stimulated with cephalostatin 1 (CPH; 1  $\mu$ M) or with thapsigargin (TG; 3  $\mu$ M) for the indicated times (p-JNK/JNK: stimulation with TG for 2 h). Western Blot experiments were performed using antibodies against the active phosphorylated forms of ASK1 (Thr845) (A) and JNK (Thr183/Tyr185) (B). Membranes were stripped and reprobed with antibodies recognising the total level of the proteins (A, B). One representative Western Blot out of three is shown.

### 2.2.2 Importance of ASK1 in cephalostatin 1-induced apoptosis

To evaluate the role of the ASK1/JNK pathway in cephalostatin 1-induced apoptosis, two Jurkat clones expressing a dominant negative ASK1 (ASK1-DN) [179] were employed. In both clones of ASK1-DN cells (A2-1, A2-3), a significant reduction of cephalostatin 1 (1  $\mu$ M, 24 h)-induced apoptosis was observed compared to control cells (Jurkat J16 clone) (Figure V.9 A). TNF- $\alpha$  (10 nM, 24 h) was used as positive control since TNF-induced apoptosis depends on the activation of ASK1 [200]. To verify the reduction of ASK1 activity of the ASK1-DN clones, Jurkat J16 and A2-3 clones were treated with cephalostatin 1 or TNF- $\alpha$  and investigated for JNK phosphorylation by Western Blot. As expected, JNK phosphorylation was impaired in A2-3 cells in both cases compared to control J16 cells (Figure V.9 B). These data show that the ASK1/JNK cascade is involved in cephalostatin 1-induced apoptosis.

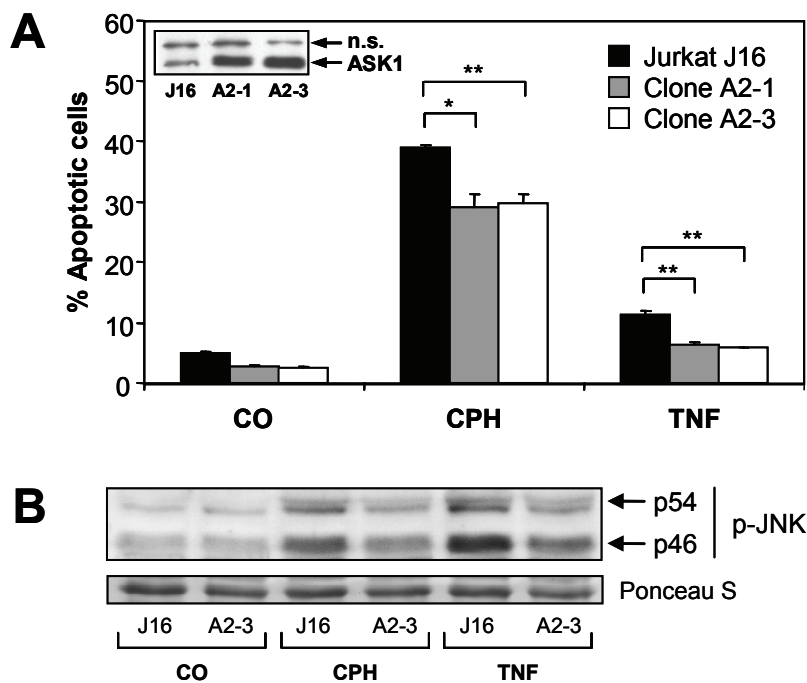


**Figure V.9: The ASK1/JNK pathway is important for cephalostatin 1-induced apoptosis.**  
**A:** Jurkat T cells (*Jurkat J16*) and Jurkat ASK1-DN cells (*clone A2-1*, *clone A2-3*) were treated for 24 hours with cephalostatin 1 (*CPH*; 1  $\mu$ M) or human tumor necrosis factor-alpha (*TNF*; 10 nM) and apoptotic cells were quantified by flow cytometry as described in “Materials and Methods”. *Insert*, the indicated cells were lysed and equal amounts of protein were separated by SDS-PAGE and further analysed by Western blot using anti-ASK1 antibodies. The lower arrow points to the endogenous and overexpressed ASK1 proteins, while the upper band detects a nonspecific (n.s.) band. **B:** Jurkat cells and ASK1-DN clone A2-3 were investigated for the activation of JNK after treatment with cephalostatin 1 (*CPH*; 1  $\mu$ M) and tumor necrosis factor-alpha (*TNF*; 10 nM). After treatment for 30 minutes, cell lysates were prepared and the phosphorylated form of JNK was detected using Western Blot analysis. Equal protein loading was controlled by staining membranes with Ponceau S. All experiments were performed three times with consistent results. Bars, the mean  $\pm$  SEM of three independent experiments performed in triplicate. \*,  $P < 0.05$ ; \*\*,  $P < 0.01$  (unpaired two-tailed *t* test).

### 2.3 ROLE OF CASPASES IN CEPHALOSTATIN 1-INDUCED ER APOPTOTIC PATHWAY

In addition to transcription factors as CHOP and kinases as ASK1/JNK, caspases are important mediators of ER stress-induced apoptosis (see III.6.3.2). It has been shown that murine caspase-12, which is capable of activating caspase-9 independently of apoptosome formation [85], is early activated by cephalostatin 1 [193]. However, functional caspase-12 is lacking in humans due to a frame shift mutation and a premature stop codon [201] and its actual role in apoptosis is controversial. Caspase-4 has been recently proposed as the human homologue of caspase-12 and seems to be activated exclusively by situations that alter ER functionality [87,110].

Caspase-2 is one of the best conserved caspase across species and has features of both initiator and effector caspases. However, assigning a distinct function to this protease has been difficult [111]. Recently evidence is given that in addition to caspase-12/-4 caspase-2 plays a role as an apical caspase in some models of ER stress-induced apoptosis [88,89].

### 2.3.1 Cephalostatin 1-induced activation of caspase-4 is necessary for apoptosis

It was hypothesised that caspase-4 might be the initiator of a cephalostatin 1-induced specific ER caspase cascade. Indeed, cephalostatin 1 as well as the well-known ER stress inducers tunicamycin and thapsigargin activate caspase-4 time-dependently (Figure V.10). Even though cleavage products of caspase-4 were difficult to detect in Jurkat cells, a strong reduction of the proform could be observed after 4 h of cephalostatin 1 treatment suggesting that caspase-4 might act as an apical caspase. Processing of procaspase-4 occurred similarly in tunicamycin- and thapsigargin-treated cells supporting the hypothesis that ER stress activates caspase-4 in Jurkat cells.

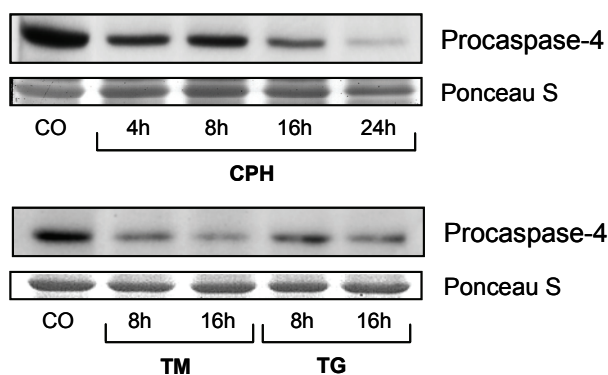


**Figure V.10: Caspase-4 activation by cephalostatin 1.**

Jurkat cells were either left untreated (CO) or treated with cephalostatin 1 (CPH; 1  $\mu$ M), tunicamycin (TM; 1  $\mu$ g/ml) or thapsigargin (TG; 3  $\mu$ M) for the indicated times. Processing of procaspase-4 was examined by Western Blot. Representative Western Blots of three independent experiments are shown.

To elucidate if caspase-4 plays a critical role in cephalostatin 1-induced apoptosis, the specific caspase-4 inhibitor zLEVD-fmk was used. Blockage of caspase-4 proteolytic activity led to a marked inhibition of cephalostatin 1-induced DNA fragmentation, demonstrating a crucial role of caspase-4 in the apoptotic pathway of cephalostatin 1 (Figure V.11 A). Caspase-4 contribution to

tunicamycin and thapsigargin-induced apoptosis was similar to that seen for cephalostatin 1 further supporting its role in ER stress-induced apoptosis.

Tetrapeptidic caspase inhibitors are not completely specific blockers of a particular caspase but usually inhibit caspases of the same subfamily [202]. Therefore, to further prove the involvement of caspase-4 in cephalostatin 1-induced apoptosis, expression of caspase-4 was inhibited by RNA interference. Two expression constructs (caspase-4a and caspase-4b, see IV.9) coding for two different siRNA sequences directed against all three caspase-4 isoforms were prepared and cells were transfected with a mixture of both constructs. As observed in Figure V.11 B, the expression of caspase-4 was strongly downregulated 24 h after transfection. Cell lines containing the empty vector or vector coding for a scramble hairpin sequence were established and employed as controls. DNA fragmentation induced by cephalostatin 1 treatment was significantly reduced ( $\sim 50\%$ ) in cells transfected with siRNA plasmids in fact being consistent with the results obtained using the caspase-4 inhibitor zLEVD-fmk.

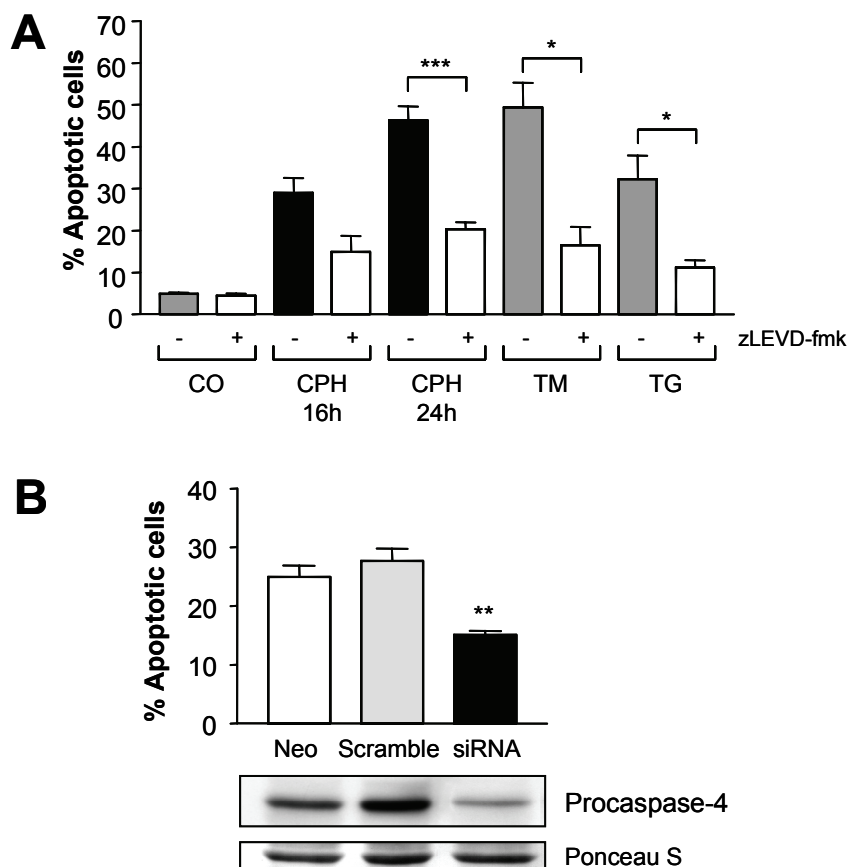
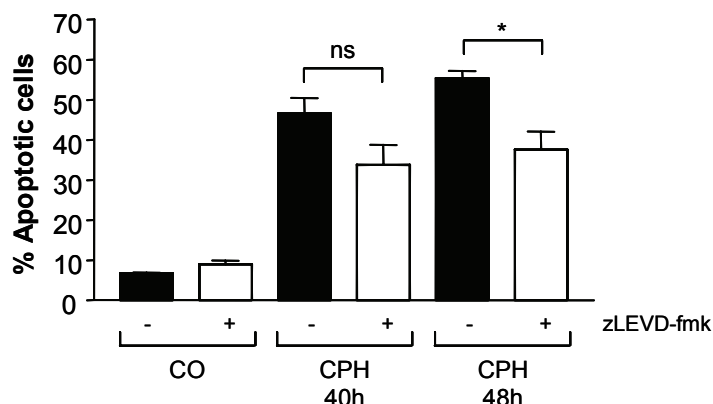


Figure V.11: Caspase-4 is necessary for apoptosis.

**A:** Jurkat cells were left untreated (CO), preincubated with the caspase-4 inhibitor zLEVD-fmk (20  $\mu$ M, 1 h) and then treated with cephalostatin 1 (CPH; 1  $\mu$ M), or stimulated with cephalostatin 1 (1  $\mu$ M) alone for the indicated times. Tunicamycin (TM; 1  $\mu$ g/ml, 24 h) or thapsigargin (TG; 3  $\mu$ M, 24 h) were used as control substances inducing ER stress. Apoptotic cells were quantified by flow cytometry. **B:** Jurkat cells were transfected with empty vector (Neo), vector containing a scramble sequence (Scramble) or a mixture of two vectors encoding respective caspase-4 siRNA sequences (siRNA) as described in "Materials and Methods" and treated with cephalostatin 1 for 16 h. Apoptotic cells were quantified by flow cytometry. A significant decrease in apoptosis compared to vector as well as scramble sequence was observed (*upper panel*). *Bottom panel* shows reduction of caspase-4 protein level in cells transfected with siRNA plasmids. All experiments were carried out three times in triplicate. Bars, the mean  $\pm$  SEM of three independent experiments performed in triplicate. \*,  $P < 0.05$ ; \*\*  $P < 0.01$ ; \*\*\*,  $P < 0.001$  (unpaired two-tailed  $t$  test).

In order to extend the knowledge about the role of caspase-4 to other cell types HeLa cells, which undergo ER stress in response to cephalostatin treatment (see Figure V.3), were pre-treated with the caspase-4 inhibitor zLEVD-fmk and subsequently with cephalostatin 2. Figure V.12 shows that apoptosis takes place in a caspase-4-dependent manner since DNA fragmentation was reduced in HeLa cells pre-treated with zLEVD-fmk. Together, these results demonstrate that caspase-4 is a central caspase in cephalostatin-induced apoptosis.



**Figure V.12 : Caspase-4 is involved in apoptosis in HeLa cells.**

HeLa cells were left untreated (CO), preincubated with the caspase-4 inhibitor zLEVD-fmk (20  $\mu$ M, 1 h) and then treated with cephalostatin 2 (CPH; 50 nM), or stimulated with cephalostatin 2 (50 nM) alone for the indicated times. Apoptotic cells were quantified by flow cytometry as described in "Materials and Methods". Bars, the mean  $\pm$  SEM of three independent experiments performed in triplicate. \*,  $P < 0.05$ ; ns, not significant (unpaired two-tailed  $t$  test).

### 2.3.2 Caspase-2 participation in apoptosis

The second point of interest was whether caspase-2 was involved in cephalostatin 1-induced apoptosis. Indeed, treatment of Jurkat cells with cephalostatin 1 leads to activation of caspase-2 as demonstrated by the appearance of the caspase-2 cleavage product p31 after 4 h of incubation (Figure V.13 A). Thapsigargin was used as positive control [89].

In order to prove whether caspase-2 is involved in apoptosis, inhibitor studies were performed. The caspase-2 inhibitor zVDVAD-fmk reduced DNA fragmentation induced by cephalostatin 1 and thapsigargin to a similar extent (Figure V.13 B), indicating that caspase-2 contributes to cephalostatin 1-mediated apoptosis.

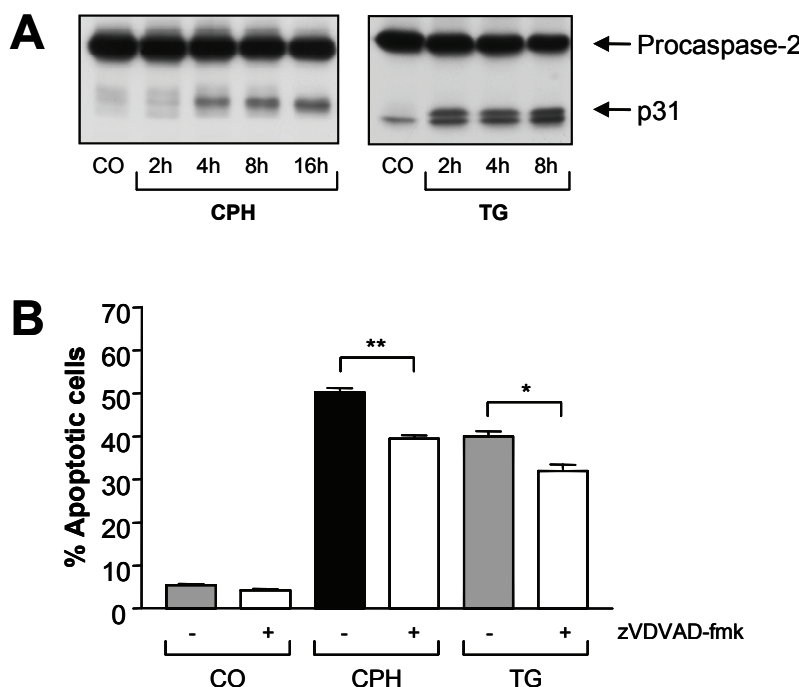


**Figure V.13 : Cephalostatin 1 activates caspase-2.**

**A:** Jurkat cells were either left untreated (CO) or treated with cephalostatin 1 (CPH; 1  $\mu$ M) or thapsigargin (TG; 3  $\mu$ M) for the indicated times. The p31 cleavage product of procaspase-2 was examined by Western Blot. **B:** Cells were left untreated (CO), preincubated with the caspase-2 inhibitor zVDVAD-fmk (20  $\mu$ M, 1 h) and then treated with cephalostatin 1 (1  $\mu$ M), or stimulated with thapsigargin (3  $\mu$ M, 24 h) was used as a positive control. All experiments were carried out three times with consistent results. Bars, the mean  $\pm$  SEM of three independent experiments performed in triplicate. \*, P < 0.05; \*\*, P < 0.01 (unpaired two-tailed t test).

### 2.3.3 Caspase-4 and caspase-2 are activated upstream of caspase-9

The strong processing of caspase-4 as early as 4 h after stimulation supported the notion that caspase-4 could function as an initiator caspase in the apoptotic pathway of cephalostatin 1. Caspase-2 has been reported to act as an initial caspase [64,203], but also to be activated downstream of caspase-9 [204]. To investigate whether caspase-4 and/or caspase-2 act as initiator caspases in cephalostatin-induced apoptosis, it was taken advantage of the caspase-9-deficient (Casp.9-/-) Jurkat cell line.

First, it was examined whether caspase-4 and caspase-2 are processed in caspase-9-deficient cells or if, on the contrary, activation of these proteases is an event occurring downstream of activated caspase-9. The results depicted in Figure V. 14 deliver evidence supporting the first hypothesis. Procaspsase-4 was cleaved strongly and time-dependently in caspase-9 deficient cells upon cephalostatin 1 treatment (Figure 14 A) but not by thapsigargin or tunicamycin, substances that in contrast to cephalostatin 1 induce cytochrome c release and apoptosome formation. Processing of the caspase-2 proform was observed upon cephalostatin 1 as well as thapsigargin but not after tunicamycin treatment (Figure V.14 B), supporting the notion that caspase-2 activation is dependent on the apoptotic stimulus [111].

In addition, pre-treatment of Casp.9-/- cells with the specific caspase-4 inhibitor zLEVD-fmk or the caspase-2 inhibitor zVDVAD-fmk was not able to reduce the residual DNA fragmentation induced by cephalostatin 1 (Figure V.14 C). This fact supports the hypothesis that caspase-4 and -2 are activated upstream of caspase-9 and require the presence of caspase-9 to induce apoptosis.

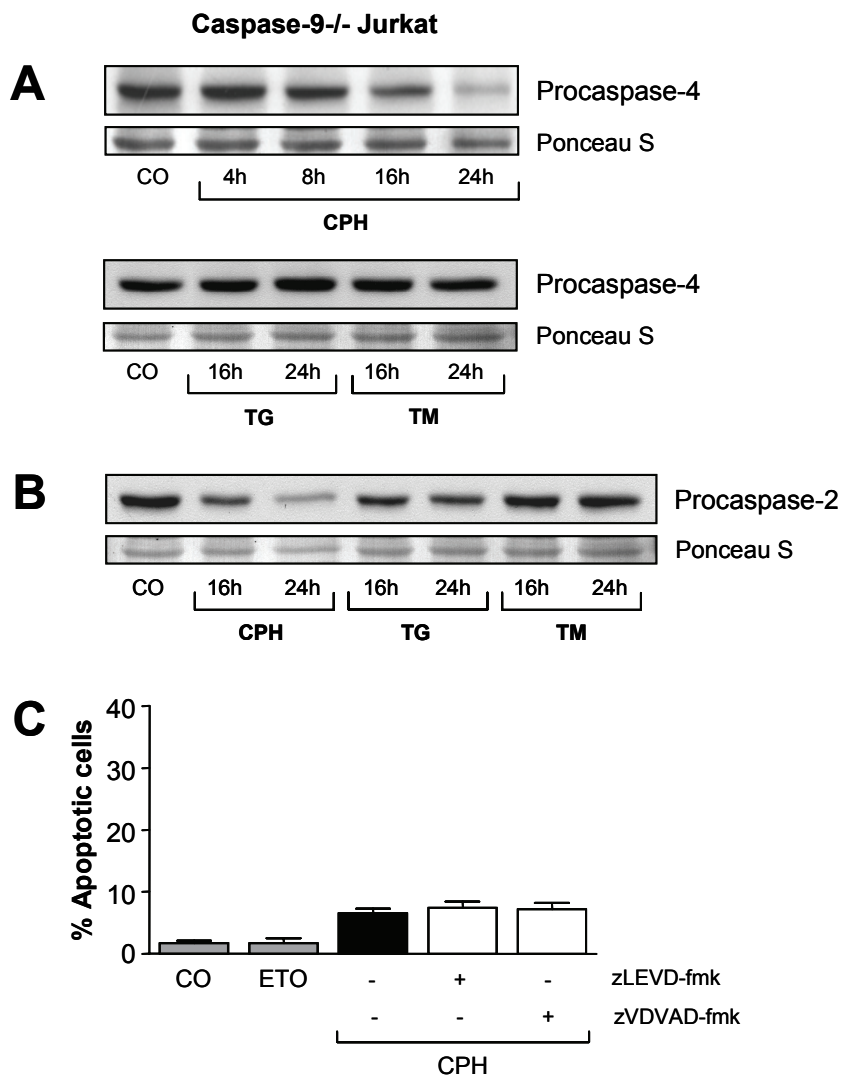


**Figure V.14: Caspase-4 and caspase-2 are activated upstream of caspase-9 in cephalostatin 1-induced apoptosis.**

**A:** Jurkat cells lacking caspase-9 were either left untreated (CO) or treated with cephalostatin 1 (CPH; 1  $\mu$ M), thapsigargin (TG; 3  $\mu$ M) or tunicamycin (TM; 1  $\mu$ g/ml) for the indicated times. Cell lysates were prepared and processing of procaspase-4 was examined by Western Blot. **B:** Caspase-9<sup>-/-</sup> Jurkats were incubated for the indicated times with cephalostatin 1 (CPH; 1  $\mu$ M) or with the known ER stress inducers thapsigargin (TG; 3  $\mu$ M) or tunicamycin (TM; 1  $\mu$ g/ml) and caspase-2 activation was investigated by Western Blot. **C:** Caspase-9<sup>-/-</sup> cells were left untreated (CO) or treated for 24 hours with etoposide (ETO; 2  $\mu$ M) or cephalostatin 1 (CPH; 1  $\mu$ M) with or without preincubation with the caspase-4 inhibitor zLEVD-fmk or the caspase-2 inhibitor zVDVAD-fmk (20  $\mu$ M, 1 h). Apoptotic cells were quantified by flow cytometry. All experiments were carried out three times with consistent results. Bars, the mean  $\pm$  SEM of three independent experiments performed in triplicate.

### 2.3.4 Caspase-4 and caspase-2 are required for caspase-9 activation and apoptosis

To verify the notion that caspase-4 and caspase-2 act as initiator caspases in cephalostatin 1-induced apoptosis the impact of the inhibition of these caspases on caspase-9 activation and apoptosis was investigated.

Biochemical and genetic inhibition experiments were used to study possible consequences of the inhibition of these caspases in the initial as well as late activation of caspase-9. As represented in Figure V.15 A, activation of caspase-9 was measured already 4 h following treatment with cephalostatin 1 and employment of specific caspase-4 and -2 inhibitors (zLEVD-fmk and zVDVAD-fmk, respectively, or a combination of both) completely inhibited the catalytic activity of caspase-9.

To confirm these data, activation of caspase-9 in the execution phase of apoptosis (16-24 h) was studied by Western Blot. Inhibition of active caspase-4 resulted in a marked reduction in the cleavage of caspase-9 whereas employment of the caspase-2 inhibitor led to a less pronounced inhibition of the appearance of caspase-9 active fragments (Figure V.15 B). These results correlate with the individual contribution of each caspase to apoptosis (Figure V.11 and V.13 B).

Additional evidence for the upstream role of caspase-4 is shown in Figure V.15 C. Jurkat cells with a completely reduced caspase-4 expression were generated by siRNA techniques, stimulated with cephalostatin 1 for 16 and 24 h and caspase-9 activation was analysed by Western Blot and compared to cell lines expressing the empty vector or vector containing a scramble sequence. Caspase-4 siRNA treated cells showed a marked inhibition of the activation of caspase-9 in response to cephalostatin 1. Reduction of caspase-4 expression also inhibited the activation of caspase-9 by thapsigargin and tunicamycin, pointing to a general involvement of caspase-4 in caspase-9 activation upon induction of ER stress.

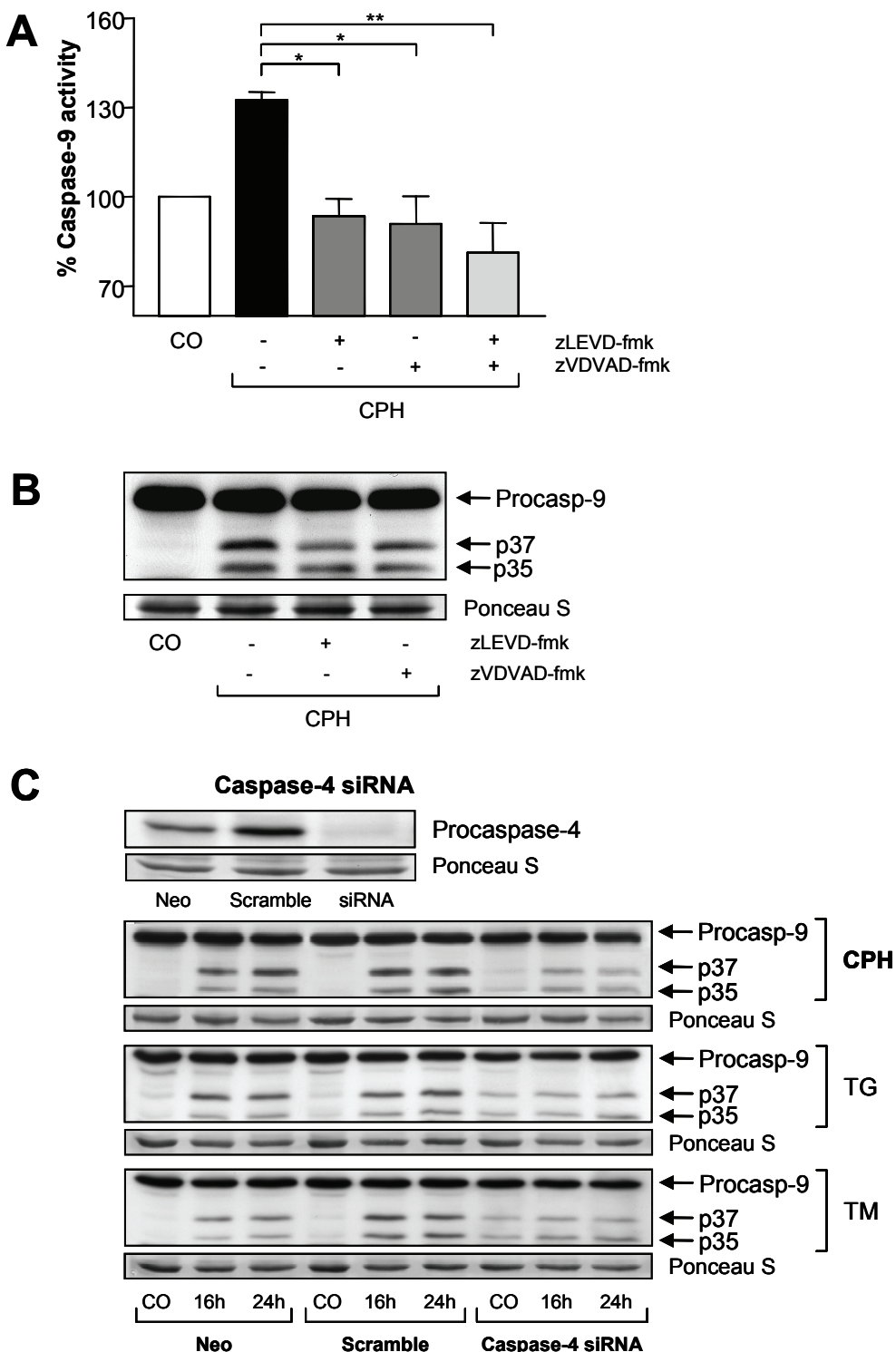


**Figure V.15: Caspase-4 and caspase-2 are required for cephalostatin 1-induced caspase-9 activation.**

**A:** Jurkat T cells were either left untreated (CO), treated with cephalostatin 1 (CPH; 1  $\mu$ M) or preincubated with the caspase-4 inhibitor zLEVD-fmk (20  $\mu$ M, 1 h), the caspase-2 inhibitor zVDVAD-fmk (20  $\mu$ M, 1 h) or a combination of both and then treated with cephalostatin 1 for 4 h. Caspase-9 activity was measured by luminescence using the Caspase-Glo™ 9 Assay. **B:** Representative Western Blot showing the reduced processing of pro-caspase-9 into its

intermediates in response to cephalostatin 1 (CPH; 1  $\mu$ M) treatment for 16 h when cells were pre-treated with specific caspase-4 or caspase-2 inhibitors. **C**: Decrease in caspase-9 activation by cephalostatin 1 after inhibition of caspase-4 expression by siRNA. Jurkat cells were transfected with a mixture of plasmids encoding siRNA sequences and selected with G418 for 48 h as described in "Materials and Methods". Empty vector (*neo*), scramble and caspase-4 siRNA cells were seeded in G418-free medium and stimulated with cephalostatin 1 (CPH; 1  $\mu$ M) for 16 and 24 h. Cell lysates were prepared and caspase-9 activation was analysed by Western Blot. Activation of caspase-9 by thapsigargin (TG; 3  $\mu$ M) and tunicamycin (TM; 1  $\mu$ g/ml) was also investigated. As a control, caspase-4 protein level in cell lysates from *neo*, scramble and caspase-4 siRNA cells was analysed by Western Blot. One Western Blot representative out of three is shown. Equal protein loading was controlled by staining membranes with Ponceau S (a representative fragment of the stained membrane is shown). Bars, the mean  $\pm$  SEM of three independent experiments performed in triplicate. \*,  $P < 0.05$ ; \*\*,  $P < 0.01$  (ANOVA/Bonferroni's test).

Finally, the effect of the simultaneous inhibition of both initiator caspases was investigated. Figure V.16 shows that the reduction in DNA fragmentation after blockage of both caspases was additive and in fact, very similarly to the absence of caspase-9 (see Figure V.1).

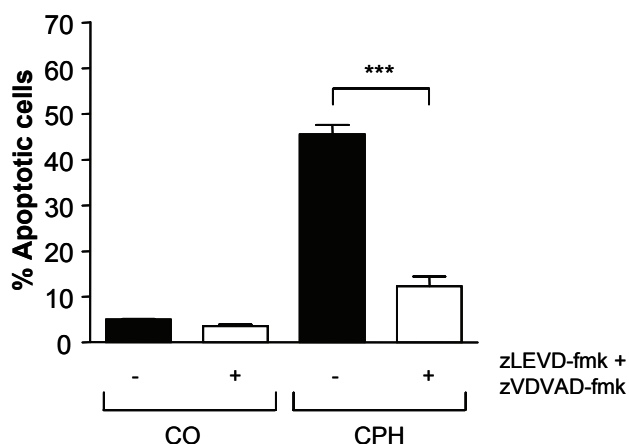


**Figure V.16: Caspase-4 and -2 activation are essential for cephalostatin 1-induced apoptosis.**

Cells were left untreated (CO), preincubated with a combination of zLEVD-fmk (20  $\mu$ M, 1 h) and zVDVAD-fmk (20  $\mu$ M, 1 h) and then treated with cephalostatin 1 (1  $\mu$ M), or stimulated with cephalostatin 1 alone for 24 h. Apoptotic cells were quantified by flow cytometry. Bars, the mean  $\pm$  SEM of three independent experiments performed in triplicate. \*\*\*,  $P < 0.001$  (unpaired two-tailed *t* test).

In summary, these data demonstrate an initial and essential role of caspase-4 and caspase -2 in cephalostatin 1-induced apoptotic signalling. Engagement of these caspases is followed by an activation of caspase-9 that leads to apoptosis.

## 2.4 ASK1/JNK AND CASPASE-4 PATHWAYS ACT INDEPENDENTLY

The ASK1 kinase has been described to be activated in case of ER stress and induce a sustained activation of JNK that leads to apoptosis [79,200,205]. Activation occurs via TRAF2, an adaptor protein that couples IRE1 activation in ER stress to cytosolic signalling. On the other hand caspase-12, the murine homologue of caspase-4, has been proposed to be activated *via* a similar mechanism. Caspase-12 forms a complex with IRE1 and TRAF2 and is activated, as other initiator caspases, by an autocatalytic mechanism [206]. Interestingly, a cross-talk between these two pathways has been very recently described [197]. The authors show that the proteasome inhibitor bortezomib induces ER stress and apoptosis by mechanisms involving JNK and caspase-4 activation. Herein, JNK seemed to be responsible for caspase-4 activation since inhibition of JNK completely inhibited caspase-4 processing.

However, cephalostatin 1-induced caspase-4 activation was neither affected by overexpression of ASK1-DN nor inhibition of JNK (Figure V.17). Examination of the processing of caspase-4 in ASK1-DN cells revealed a similar activation as compared to control cells. Furthermore, the JNK inhibitor SP600125 did not impair but even increased activation of caspase-4 upon cephalostatin 1 treatment in Jurkat cells. Therefore, we assume that caspase-4 activation occurs at the ER membrane independently of the ASK1/JNK kinase pathway.

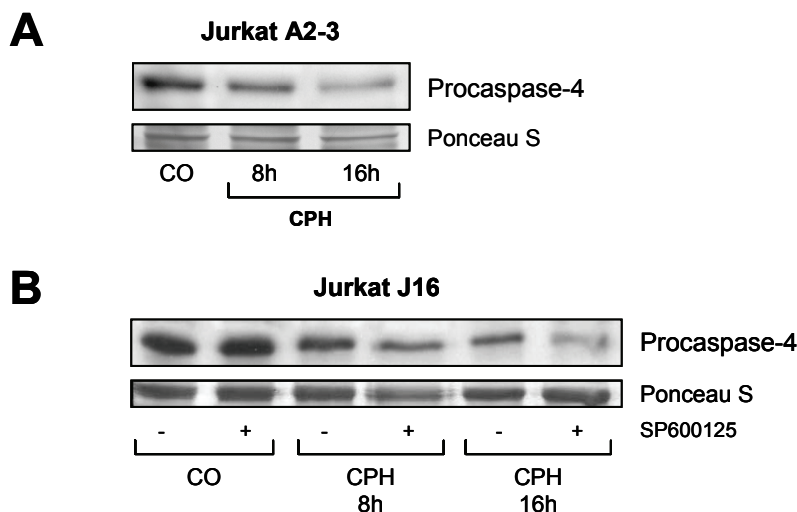


**Figure V.17: Neither ASK1 nor JNK are involved in caspase-4 activation.**

ASK1-DN cells (Jurkat A2-3) were treated with cephalostatin 1 (CPH; 1  $\mu$ M) for the indicated times (**A**) and Jurkat cells (Jurkat J16) were left untreated or pretreated with the JNK inhibitor SP600125 (SP; 10  $\mu$ M, 30 min preincubation) before stimulation with cephalostatin 1 (CPH; 1  $\mu$ M) as indicated (**B**). Cell lysates were prepared and processing of procaspase-4 was studied by Western Blot. One Western Blot representative out of three is shown. Protein loading was controlled by staining membranes with Ponceau S.

## B. SESQUITERPENE LACTONES (SQTL)

First, the morphological and biochemical features of programmed cell death (PCD) induced by SQTL bearing only one of the biologically active groups ( $\alpha$ -methylene- $\gamma$ -lactone *versus* an  $\alpha,\beta$ -unsaturated cyclopentenone) were characterised in order to examine the impact of these chemical moieties on cell death. The experiments displayed in V.B.1 (except V.B.1.3.1 and V.B.1.3.3) were performed by Prof. Verena M. Dirsch and Dulce Ferreira but are exhibited here for a proper understanding of the results presented in V.B.2.

The objective of the second part was to investigate whether the mode of cell death induced by SQTL can be related to the response of human macrophages (phagocytosis and cytokine response).

### 1 CHARACTERISTICS OF SQTL-INDUCED CELL DEATH

#### 1.1 CYTOTOXIC ACTIVITY

Overall cytotoxicity of all three SQTL was assessed. For this purpose, Jurkat T cells were exposed to increasing concentrations of SQTL for 24 h and cell viability was determined by the MTT assay. Dose-response curves were created and the IC<sub>50</sub> values calculated (Figure V.18). The values obtained are for DHA IC<sub>50</sub>: 45.8  $\mu$ M (95% CI: 36.2–57.9  $\mu$ M, n = 3), for HC IC<sub>50</sub>: 26.5  $\mu$ M (95% CI: 21.6–32.4  $\mu$ M, n = 3) and for EM IC<sub>50</sub>: 5  $\mu$ M (95% CI: 3.5–7.1  $\mu$ M, n = 3). Thus, as expected, the cytotoxicity of compounds with one  $\alpha,\beta$ -unsaturated carbonyl group such as DHA ( $\alpha,\beta$ -unsubstituted cyclopentenone group) and HC ( $\alpha$ -methylene- $\gamma$ -lactone group) is lower than that of EM bearing in addition to an  $\alpha$ -methylene- $\gamma$ -lactone group further reactive centers. The  $\alpha$ -methylene- $\gamma$ -lactone group seems to be more effective than the cyclopentenone group.

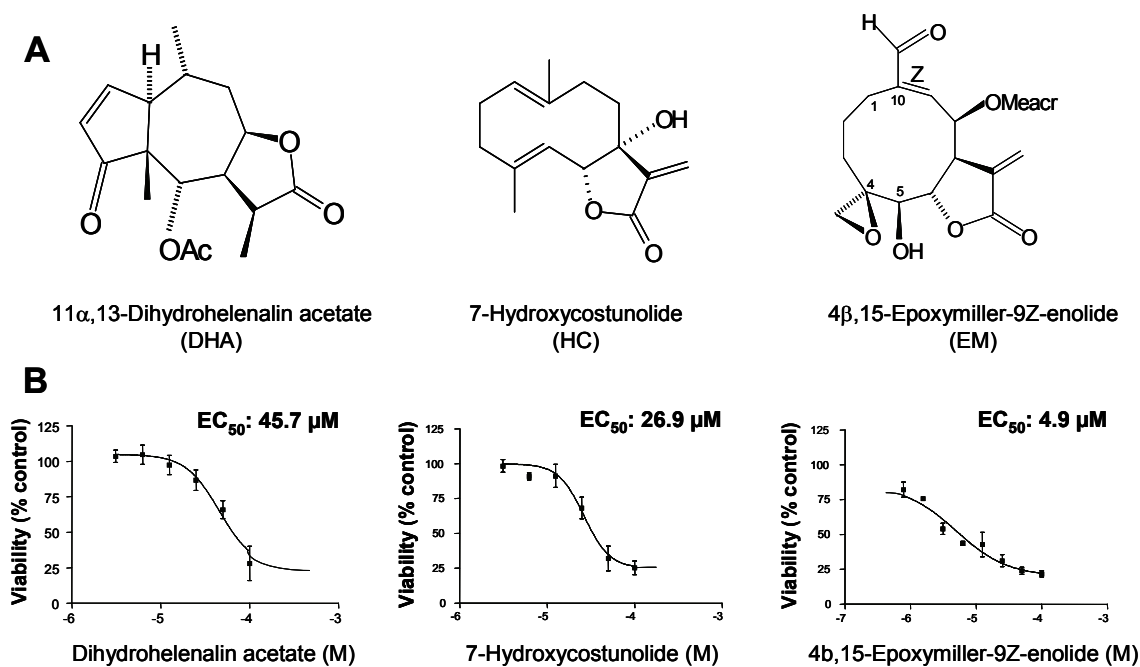


**Figure V.18: Chemical structure and cytotoxic activity of the SQTL in study.**

**A:** Chemical structure of DHA ( $\alpha,\beta$ -unsaturated cyclopentenone), HC ( $\alpha$ -methylene- $\gamma$ -lactone) and EM ( $\alpha$ -methylene- $\gamma$ -lactone and other reactive centers). **B:** Jurkat cells were stimulated with SQTL (concentrations as indicated) for 24 h. Impairment of cell viability was analysed by an MTT assay. Represented are the mean  $\pm$  SEM of three independent experiments performed in triplicate.

## 1.2 MORPHOLOGIC CHANGES OF THE NUCLEUS (DNA CONDENSATION AND FRAGMENTATION)

One typical feature of classical apoptotic cell death is the fragmentation of DNA. Thus, an easy and widely used assay to quantify apoptotic cell death is the counting of nuclei with a subdiploid DNA content after staining with PI [182]. In order to examine whether the observed cytotoxicity is due to apoptosis dose-response studies within the concentration ranges proven to be cytotoxic were performed using this method (Figure V.19 A). Surprisingly, only DHA treatment induced significant DNA fragmentation. HC and EM employed at concentrations even four times higher than the determined IC<sub>50</sub> value for cytotoxicity did not lead to fragmented DNA. This observation was confirmed by staining nuclei with the fluorescent dye Hoechst 33342 (Figure V.19 B). HC (20 μM) and EM (5 μM), however, led to a more condensed chromatin since Hoechst 33342-stained nuclei of HC and EM-treated cells appeared much brighter than control nuclei. This chromatin condensation was apparent also after staining nuclei with PI followed by FACS analysis: although no typical “sub-G<sub>1</sub> peak” was observed the G<sub>1</sub>, S and G<sub>2</sub>/M peak was shifted slightly to the left, possibly reflecting a

lower degree of PI staining due to changes in chromatin density (Figure V.19 A, *inserts*).

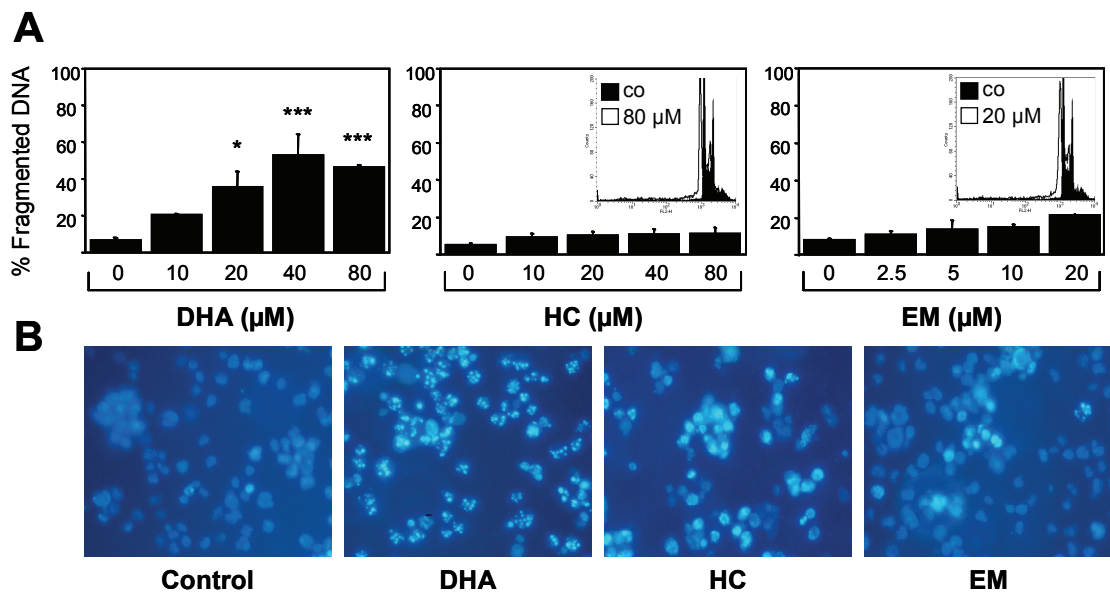


**Figure V.19: Induction of DNA fragmentation and condensation, respectively, by SQTL.**

**A:** Jurkat T cells were treated with the indicated compounds, 11 $\alpha$ ,13-dihydrohelenalin acetate (DHA), 7-hydroxycostunolide (HC) and 4 $\beta$ ,15-epoxymiller-9Z-enolide (EM) at the indicated concentrations for 24 h. Cells were harvested and nuclei stained with PI as described under "Materials and Methods". DNA fragmentation was quantified by counting nuclei with a sub-diploid DNA content by flow cytometry. The inserts show an overlay of the G<sub>1</sub>,S and G<sub>2</sub>/M peaks obtained without treatment (CO; control) and after treatment with the highest concentration of HC (80  $\mu\text{M}$ ) and EM (20  $\mu\text{M}$ ), respectively. **B:** Jurkat T cells were left untreated (*control*) or treated with the SQTL DHA (40  $\mu\text{M}$ ), HC (20  $\mu\text{M}$ ) and EM (5  $\mu\text{M}$ ) for 24 h. Nuclei were stained with Hoechst 33342 and analysed by fluorescence microscopy. A representative picture out of three experiments is shown. Bars, the mean  $\pm$  SEM of three independent experiments performed in duplicate. \*, P < 0.05; \*\*\*, P < 0.001 (ANOVA/Dunnett's test).

These results show that only DHA, the SQTL with an  $\alpha,\beta$ -unsaturated cyclopentenone group, was able to induce DNA fragmentation, but not those SQTL with an  $\alpha$ -methylene- $\gamma$ -lactone moiety or an  $\alpha,\beta$ -unsaturated aldehyde group nearby of an unsaturated acyl moiety. An epoxide group as in the case of EM does not influence this outcome.

## 1.3 CHANGES IN CELL MORPHOLOGY, PHOSPHATIDYL SERINE EXPOSURE AND MEMBRANE INTEGRITY

### 1.3.1 Light microscopic analysis of SQTL-treated cells

During classical apoptosis cells undergo morphologic changes such as cell shrinkage and formation of apoptotic bodies, easy to detect performing a light microscopic analysis.

SQTL treatment leads to prominent morphologic changes (Figure V.20). Cells treated with DHA showed classical apoptotic morphology, consisting of cell shrinkage and formation of apoptotic bodies. Interestingly, HC- and EM-treated cell populations contained cells of apoptotic morphology but also cells showing unusual morphologies. In some cells the cytoplasm was condensed at one region of the cell whereas plasma membrane was dilated but still closed. Moreover in samples stimulated with EM some cells were swollen, consistent with an atypical death style.

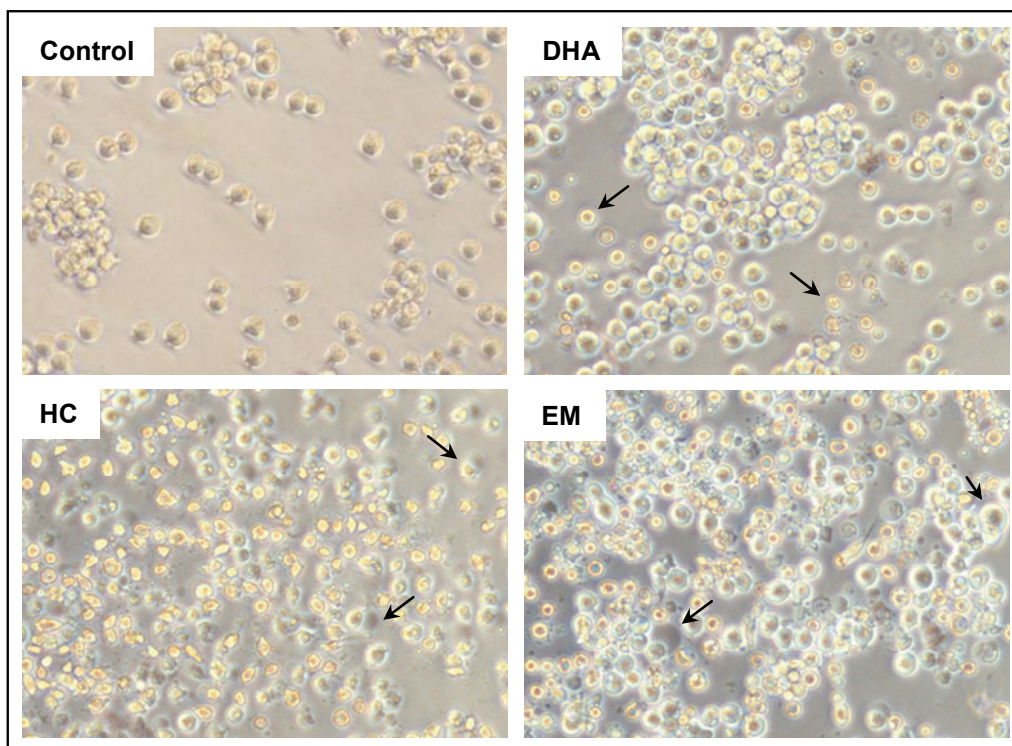


**Figure V.20: Light microscopic pictures of SQTL-treated Jurkat T cells.**

Pictures taken from untreated Jurkat T cells (*Control*) or cells treated for 24 h with 11 $\alpha$ ,13-dihydrohealenalin acetate (*DHA*; 40  $\mu$ M), 7-hydroxycostunolide (*HC*; 20  $\mu$ M) or 4 $\beta$ ,15-epoxymiller-9Z-enolide (*EM*; 5  $\mu$ M). Arrows show apoptotic cells (*DHA*) and “atypical” morphologies of programmed cell death (*HC, EM*).

### 1.3.2 Flow cytometric analysis of cell morphology, membrane permeability and translocation of phosphatidylserine

Due to the conspicuous differences in nuclear morphology induced by DHA (DNA fragmentation) versus HC and EM (no DNA fragmentation) and the observation of atypical cell shapes, the morphological changes as well as the induction of apoptotic biochemical features by these compounds were further investigated by flow cytometry.

Quantifying the appearance of small (shrunken) cells with a high granularity (typical apoptotic morphology) it was determined that all three compounds applied at the same concentration as used for Hoechst staining (Figure V.19 B) led to a comparable amount of cells with apoptotic morphology. The kinetic by which these compounds induce apoptotic morphology, however, was different (Figure V.21 A). Interestingly, HC inducing no DNA fragmentation, led very rapidly to small and granular cell morphology. However, cells treated with HC lost cell membrane integrity with a similar kinetic as after treatment with the other SQTL (Figure V.21 B).

Externalization of phosphatidylserine (PS) represents the most important “eat me” signal to surrounding phagocytosing cells [140]. Comparing the extent and kinetic of PS translocation again it was found a striking behaviour for HC (Figure V.21 C). It induced a very rapid and strong PS translocation. In contrast, PS externalization induced by DHA occurred late (8 h) compared to the other compounds (4 h) and was weak. All compounds clearly induced PS translocation before cells lost membrane integrity.

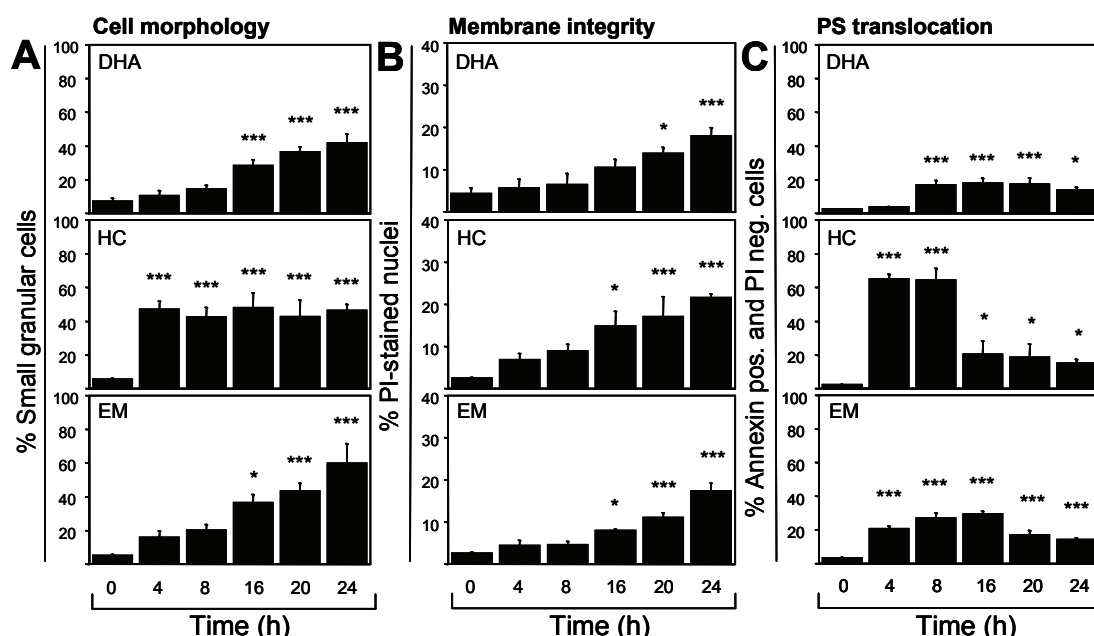


**Figure V.21: Temporal changes in cell morphology, membrane permeability and translocation of PS due to SQTL treatment.**

**A:** Jurkat T cells were treated with 11 $\alpha$ ,13-dihydrohelenalin acetate (*DHA*; 40  $\mu$ M), 7-hydroxycostunolide (*HC*; 20  $\mu$ M) or 4 $\beta$ ,15-epoxymiller-9Z-enolide (*EM*; 5  $\mu$ M). The appearance of small granular cells was quantified by flow cytometry counting cells with a low FSC and high SSC. **B:** Cells were treated as in **A** and incubated with PI (1  $\mu$ g/ml). Only cells staining positively with PI were counted by flow cytometry. **C:** Cells treated with SQTL as in **A** and **B** were labeled with Annexin V-FITC (0.5  $\mu$ g/ml) and PI (1  $\mu$ g/ml). Only Annexin V-FITC positive and PI negative cells were counted by flow cytometry. All data represent mean  $\pm$  SEM of three independent experiments performed in duplicate. \*,  $P < 0.05$ ; \*\*\*,  $P < 0.001$  (ANOVA/Dunnett's test).

### 1.3.3 Analysis of membrane integrity by measure of LDH activity

In late phases of apoptotic and in necrotic cell death plasma membrane integrity is lost and intracellular constituents are released into the extracellular space. Membrane integrity can be also investigated by quantifying the LDH present in culture medium of treated cells compared to untreated cells.

Measurement of LDH in Jurkat cell culture supernatants 24 h after addition of SQTL (Figure V.22) indicated that LDH levels in culture medium of HC-treated Jurkat cells were almost 5-fold higher than control whereas 2-fold in case of EM and only slightly increased in DHA-treated cells. This result suggests that HC-treated cells undergo cell death very fast and are not able to maintain membrane integrity as long as DHA- or EM-treated cells.

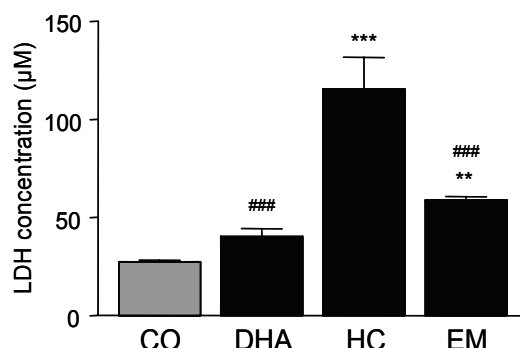


**Figure V.22: LDH levels in culture medium of SQTL-treated Jurkat cells.**

Jurkat cells were either left untreated (CO) or incubated with SQTL for 24 h. Culture supernatants were recovered by centrifugation and LDH concentration was determined using a Lambda Bio 20 photometer as described in "Materials and Methods". Bars represent the mean  $\pm$  SEM of three independent experiments performed in triplicate. \*\*,  $P < 0.01$ ; \*\*\*,  $P < 0.001$  (ANOVA/Bonferroni's test) vs. control. #,  $P < 0.001$  (ANOVA/Bonferroni's test) vs. HC.

## 1.4 CASPASE ACTIVATION

Caspases are pivotal executioners of apoptosis responsible for the induction of classic apoptotic morphological features (see III.6.1). Since HC and EM induced no classic form of apoptosis it was examined whether the three SQTL differ in their ability to activate caspases as the observed morphology (DNA fragmentation or changes in chromatin density) is dependent on active caspases.

Total caspase activity was detected using the fluorescent *in situ* marker FITC-VAD-fmk. According to the temporal onset of cell death (Figure V.21) cells were incubated for either 16 h (DHA, HC, EM) or 5 h for the positive control etoposide before addition of FITC-VAD-fmk and flow cytometric analysis. As shown in Figure V.23 A, all SQTL at effective cytotoxic concentrations led to caspase activation. Surprisingly, DHA induced only moderate caspase activity compared to HC and EM. This observation was not due to kinetic differences since DHA-induced caspase activity did not further increase up to 20 and 24 h (data not shown).

To examine whether cell death morphology is dependent on caspase activation Jurkat T cells were preincubated with the pan-caspase inhibitor zVAD-fmk and subsequently treated with SQTL for 24 h. Quantification of changes in nuclear morphology was performed by flow cytometry after PI staining. All nuclei appearing left of the G<sub>1</sub> peak of control cells were counted. As shown in Figure V.23 B, changes in nuclear morphology induced by all three SQTL were significantly reduced by zVAD-fmk.

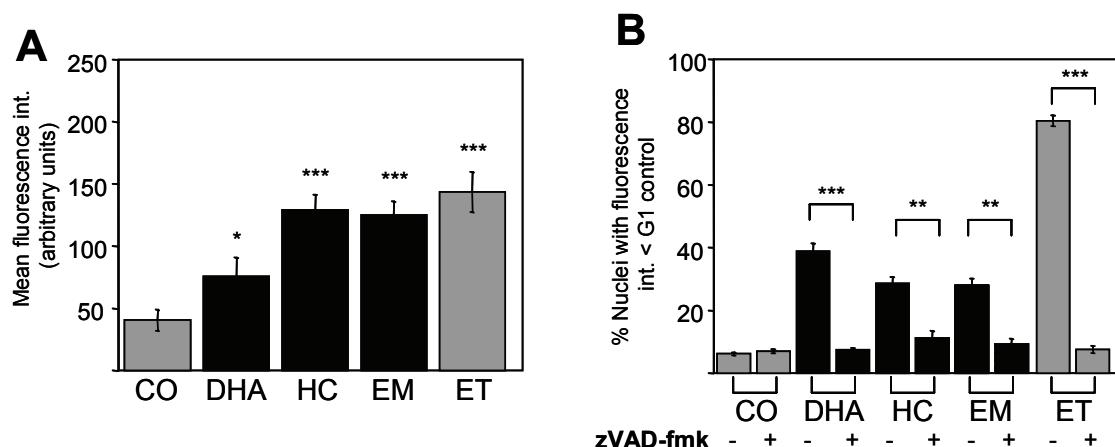


**Figure V.23: Caspases are activated and responsible for changes in nuclear morphology in response to SQTL treatment.**

**A:** Jurkat T cells were either left untreated (CO) or treated with 11 $\alpha$ ,13-dihydrohelenalin acetate (DHA; 40  $\mu$ M), 7-hydroxycostunolide (HC; 20  $\mu$ M) or 4 $\beta$ ,15-epoxymiller-9Z-enolide (EM, 5  $\mu$ M) for 16 h. As a positive control etoposide (ET, 25  $\mu$ g/ml, 5 h) was applied. Then FITC-VAD-fmk (5  $\mu$ M) was added, incubated for 20 min (37°C) and cells were analysed by flow cytometry. **B:** Jurkat cells were pretreated (+) or not (-) with the pan-caspase inhibitor zVAD-fmk (50  $\mu$ M, 1 h), then exposed to SQTL and analysed by flow cytometry. Depicted are the mean  $\pm$  SEM of the mean fluorescence intensity ( $n = 3$ , in duplicate). \*,  $P < 0.05$ ; \*\*\*,  $P < 0.001$  (Anova/Dunnett's test) (A); \*\*,  $P < 0.01$ , \*\*\*,  $P < 0.001$  (two-tailed unpaired student's  $t$  test) (B).

## 2 MACROPHAGE RESPONSE

### 2.1 ANALYSIS OF PHAGOCYTOSIS BY FLOW CYTOMETRY

The exposure of PS is the all-important and best studied cell surface marker involved in the removal of dying cells by macrophages [138,141,167,207]. The SQTL in study showed great differences in the extent and kinetic of PS translocation. Thus, the next objective was to investigate whether SQTL-treated Jurkat cells were differently phagocytosed by employing THP-1-derived macrophages.

Several methods can be used for the investigation of phagocytosis: measure of LDH concentration in co-culture supernatants after the phagocytic process [174], counting by microscopy of the number of macrophages that have ingested stained target cells [138,145,155] or quantification of the increase in macrophages size [162] or fluorescence [149,162,208,209] by flow cytometry.

#### 2.1.1 Increase in macrophages cell size

The first approach employed consisted of the analysis of the increase in THP-1 cell size after co-culture with Jurkat cells. Target cells were stimulated with SQTL for 4 h before feeding because differences in the percentage of PS positive/PI negative cells were maximal for all three substances, whereas the percentage of PI positive cells was very similar at that time point (see Figure V.21).

Time-course studies had shown that 3.5 h of co-culture delivered the higher increase in macrophages cell size (data not shown) and this was the incubation time used for all experiments. Interestingly, macrophages fed with HC-treated Jurkat cells experienced the higher increase in cell size (Figure V.24). This fact points to a correlation between the degree of PS exposed in the apoptotic cells and the efficiency of their removal by phagocytes.

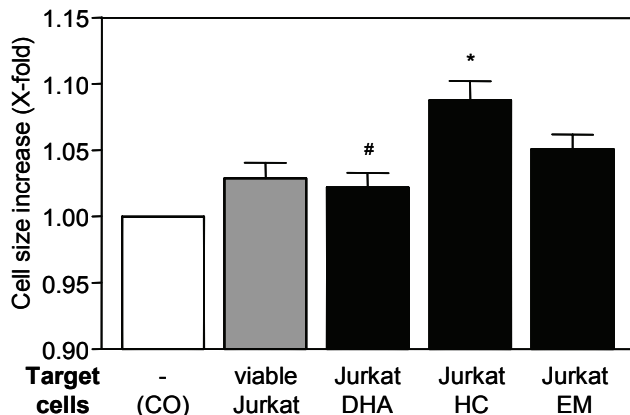


**Figure V.24: Quantification of the increase in THP-1-derived macrophages cell size after phagocytosis of Jurkat cells.**

Macrophages were cultured in medium alone (CO) or co-cultured with untreated (*viable*) or SQTL-treated (4 h) Jurkat cells for 3.5 h as described in “Materials and Methods”, followed by evaluation of cell size by flow cytometry. Bars represent the mean  $\pm$  SEM of three independent experiments performed in triplicate. \*,  $P < 0.05$  (ANOVA/Bonferroni’s test) vs. *viable* Jurkat. #,  $P < 0.05$  (ANOVA/Bonferroni’s test) vs. Jurkat HC.

### 2.1.2 Quantification of phagocytosis by analysis of cell fluorescence (FL1)

To confirm this result and exclude differences due to different kinetics in the phagocytosis of target cells, an additional procedure consisting of a fluorescent staining of Jurkat cells was developed.

Target Jurkat cells were stained with the fluorescent marker CCFSE and then cell death was induced. At the concentrations used, the dye showed no toxicity and was retained by cells throughout the whole experiment (data not shown). Jurkat cells were left untreated, treated with SQTL (DHA, HC, EM) or etoposide (1.5  $\mu$ M) for 4 h, or killed with heat (55°C, 15 min) to generate pathological cell death (necrosis). The efficient induction of cell death was checked for each experiment by PI exclusion assay after 24 h of treatment with SQTL/etoposide (data not shown). After co-culture for 3.5 h, macrophages were recovered and analysed by flow cytometry. As shown in Figure V.25, the mean green fluorescence of THP-1-derived macrophages as well as the number of green positive macrophages increased after co-culture, indicating uptake of target cells.

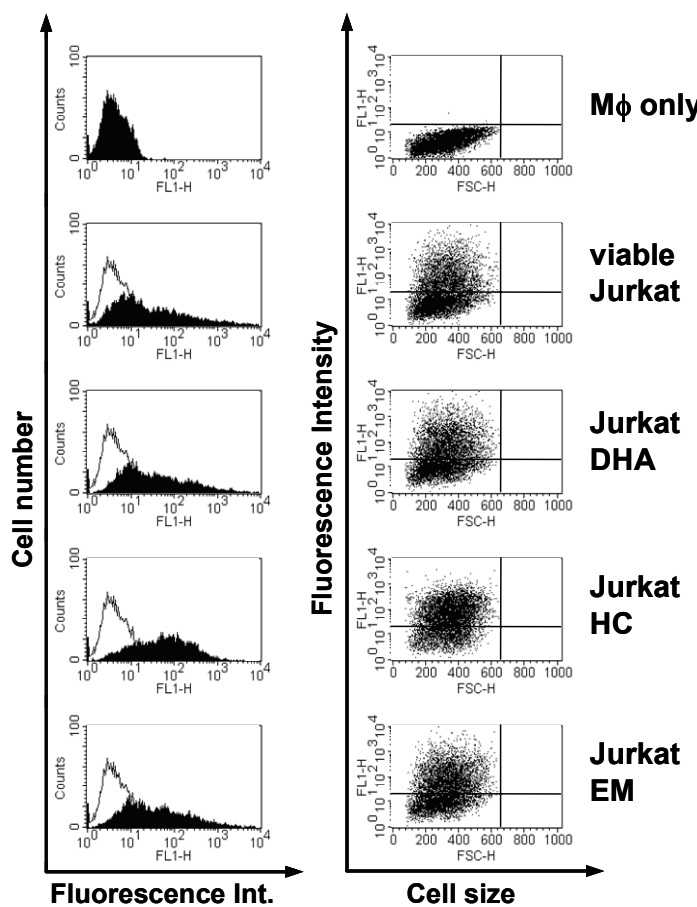


**Figure V.25: Phagocytotic activity of differentiated THP-1 cells fed with SQTL-treated Jurkat cells.**

Jurkat T cells labeled covalently with the green fluorescent marker CCFSE were left untreated (*viable*) or treated with SQTL for 4 h and co-cultured with PMA-treated THP-1 cells (macrophages;  $M\phi$ ) at a ratio 2:1 during 3.5 h. Adherent cells were recovered and analysed by flow cytometry. Representative histogram plots show the green fluorescence intensity (FL1-H) of macrophages. The experimental histograms are shaded in black, while the control profile is outlined. Dot plots show that the number of macrophages FL1 positive (upper quadrants) increased after co-culture with Jurkat cells.

Phagocytosis was quantified on the basis of the increase in mean green fluorescence intensity of macrophages co-cultured with target cells referred to unfed macrophages (extent of phagocytosis, Figure V.26 A) or as the percentage of FL-1 positive macrophages (percent of phagocytosing macrophages, Figure V.26 B). Jurkat cells that had been treated with HC were phagocytosed, again, more efficiently than DHA- or EM-treated Jurkats (“classical” apoptosis) or heat-killed cells (necrosis) (Figure V.26 A). In accordance, HC-treated Jurkat stimulated most macrophages to phagocytose (Figure V.26 B). In fact, the results obtained with both approaches were very similar.

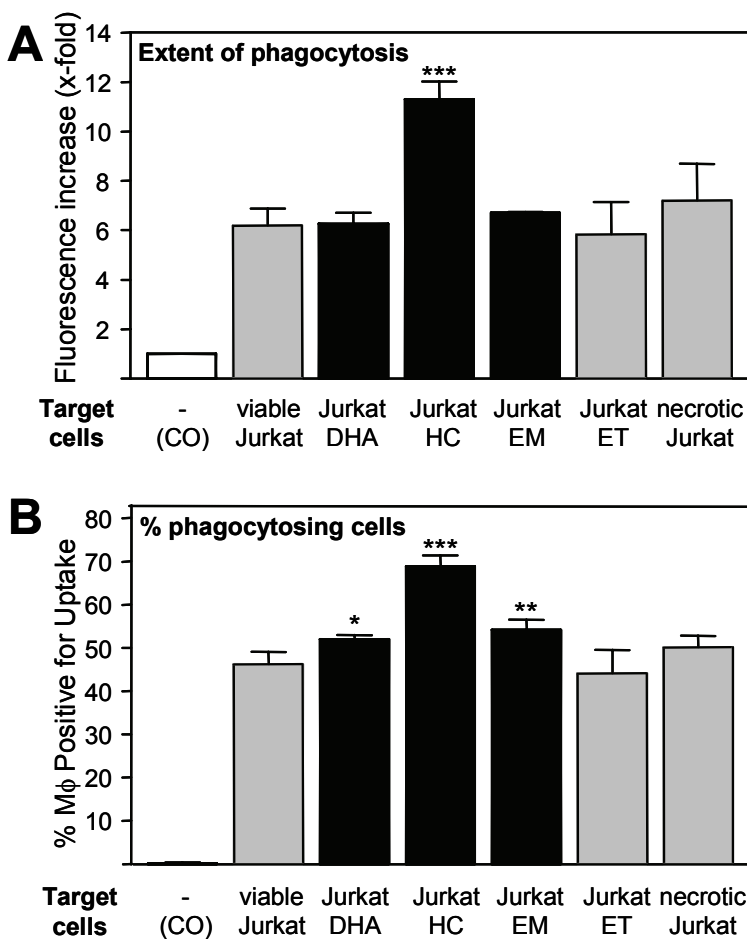


**Figure V.26: Quantification of phagocytosis by differentiated THP-1 cells fed with SQTL-treated Jurkat cells by flow cytometry.**

Experiments were performed as described in Figure V.25 and in “Materials and Methods”. Phagocytosis was quantified on the basis of the increase in mean green fluorescence intensity (FL1) of engulfing macrophages referred to macrophages alone (CO, control) (A), or as the percentage of FL1-positive macrophages (B). As control, phagocytosis of etoposide-treated Jurkat cells, (ET; 1.5 µM, 4 h) and heat-killed Jurkats (necrotic; 15 min at 55°C), was also quantified. Bars represent the mean ± SEM of three independent experiments performed in triplicate. \*, P < 0.05; \*\*, P < 0.01; \*\*\*, P < 0.001 (Anova/Bonferroni’s test) vs. viable Jurkat.

### 3 CONFOCAL MICROSCOPY

The phagocytosis of apoptotic (etoposide-treated), necrotic, SQTL-treated and untreated Jurkat cells was confirmed by confocal laser scanning microscopy. For this purpose, macrophages were stained with the red fluorescent substance PKH26 before co-culture with CCFSE-stained Jurkat cells. Fluorescence images were taken to detect target cells (green, 505-530 nm) and macrophages (red, >560 nm) as well as transmitted light images to show cell shapes. Figure V.27 shows the co-localisation of red and green fluorescence, displayed as yellow colour, in macrophages that have phagocytosed Jurkat cells.

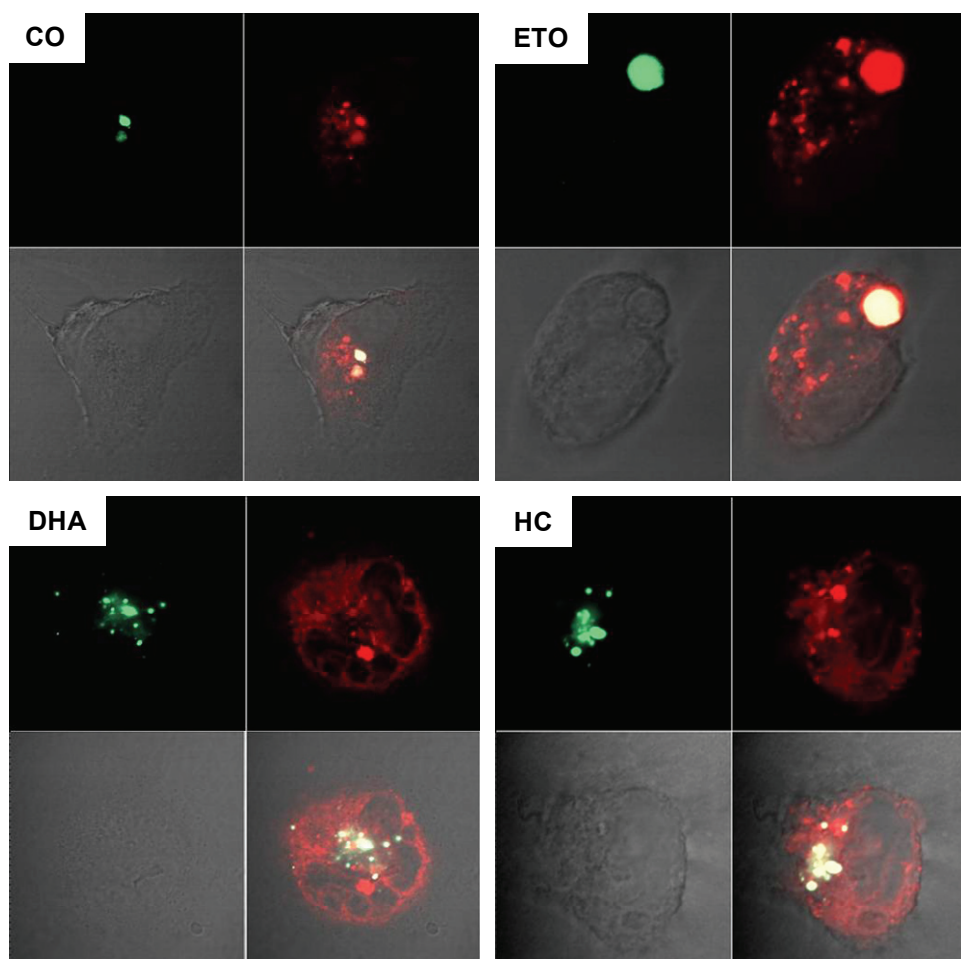


**Figure V.27: Representative pictures showing co-localisation of macrophages and target cells fluorescence.**

PKH26-stained macrophages (red) and CCFSE-stained Jurkat cells (green) were co-cultured for 3.5 h and macrophages were fixed with formaldehyde. Preparations were analysed by confocal microscopy as described in “Materials and Methods” to obtain target cells (upper left), macrophages (upper right) or transmission (lower left) images. Lower right, merged confocal images of the three channels.

To confirm that Jurkat cells were located inside macrophages and not just adhered to the surface of the cells, a stack of fluorescence images that traversed the z dimension of the samples were collected. Stacks of serial sections were projected and visualised in three dimensions (Figure V.28). These results clearly demonstrate that CCFSE-stained Jurkat cells are engulfed by THP-1-derived macrophages.

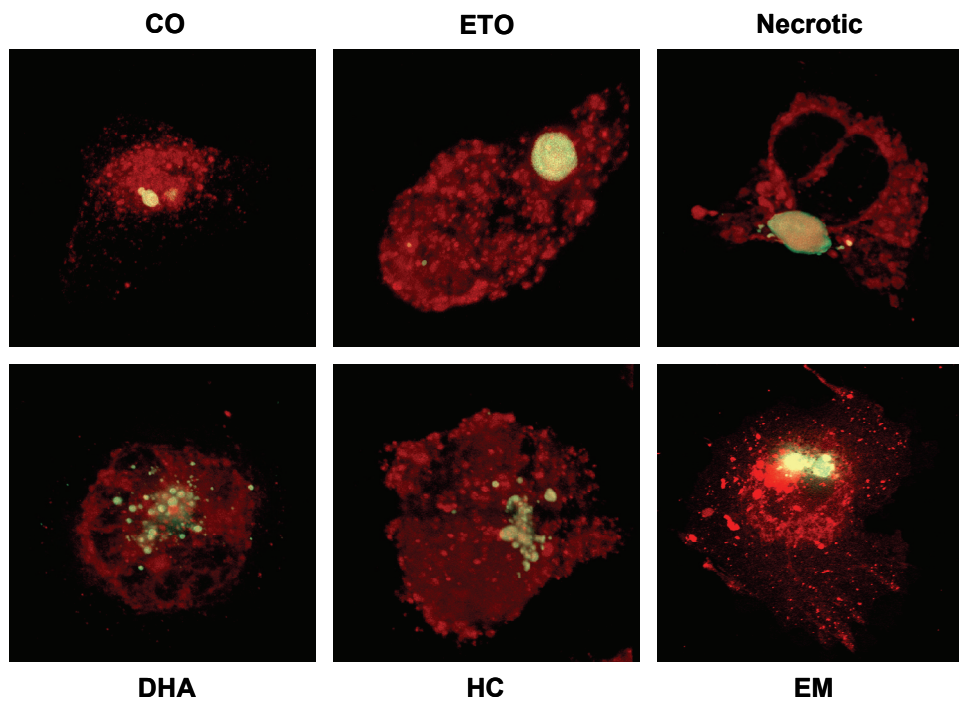


**Figure V.28: 3D projections of macrophages that have engulfed Jurkat cells.**

After co-culture with Jurkat cells and sample preparation as described in “Materials and Methods”, macrophages were analysed by confocal microscopy. Z-stacks of the macrophages that showed a co-localisation with Jurkat cells were obtained and 3D projections were created.

#### 4 CYTOKINE RELEASE

The removal of apoptotic cells by macrophages has been mostly related to anti-inflammatory and immunosuppressive responses, associated with a reduction in the levels of pro-inflammatory cytokines such as TNF- $\alpha$ , IL-1 $\beta$  or IL-12 and/or the release of anti-inflammatory mediators as TGF- $\beta$  or IL-10 [153-156] and indeed attributed to the interaction of macrophage and target cell through the phosphatidylserine receptor (PSR) [138,140,141]. Given that HC-treated Jurkat cells strongly exposed PS and were efficiently taken up by macrophages, it was hypothesised that phagocytosis of SQTLC-treated cells, at least in case of HC, could be mediated by the PSR and followed by a modulation of cytokine production by macrophages leading to an anti-inflammatory effect.

To investigate this notion, an experiment analogue to the phagocytosis assay was performed. Culture supernatants were collected after 3.5 and 18 h of co-culture and analysed for TNF- $\alpha$  and TGF- $\beta$  concentration by ELISA (Figure V.29). To our surprise, HC-treated cells significantly increased TNF- $\alpha$  levels, but to a lesser extent than necrotic cells (Figure V.29 A). A similar tendency was observed for DHA and EM although differences were not significant. On the

other hand, TGF- $\beta$  levels after 18 h of co-culture were nearly unaffected by the presence of SQTL- or etoposide-treated cells, but strongly reduced by necrotic cells (Figure V.29 B). Viable, necrotic or stimulated Jurkat cells did not release any detectable levels of cytokines (data not shown). Induction of cell death was verified for each experiment by PI exclusion assay of Jurkat cells after 24 h of treatment with SQTL/etoposide (data not shown).

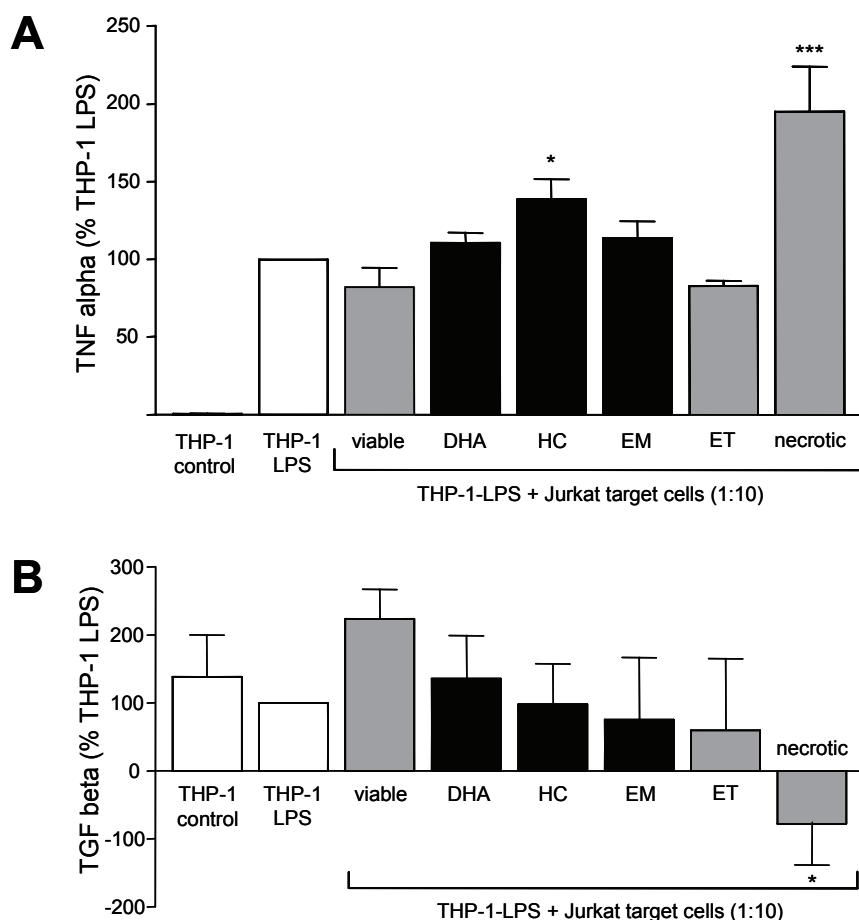


**Figure V.29: Concentration of TNF- $\alpha$  and TGF- $\beta$  in culture supernatants of THP-1 cells fed with SQTL-treated Jurkat cells.**

THP-1-derived macrophages were stimulated with 0.1  $\mu$ g/ml LPS for 3 h before addition of Jurkat cells at a ratio of 10:1 followed by incubation for 3.5 and 18 h. For comparison, THP-1 received untreated (*viable*), etoposide-treated (*ET*; 1.5  $\mu$ M, 4 h) or heat-killed (*necrotic*) (30 min at 55°C) Jurkat cells. **A:** TNF- $\alpha$  was quantified by means of specific ELISA after 3.5 h of co-culture. TNF- $\alpha$  was not detectable in supernatants of unstimulated macrophages (*THP-1 control*). Data are expressed as TNF- $\alpha$  concentration ( $\pm$  SEM) relative to LPS-stimulated macrophages which are indicated as 100% (n = 3, in triplicate). The 100% TNF- $\alpha$  production of LPS-stimulated macrophages corresponds to a mean value of 146 pg/ml. **B:** Supernatants were recovered after 18 h of co-culture and TGF- $\beta$  concentration was quantified by ELISA. Bars represent the TGF- $\beta$  concentration ( $\pm$  SEM) relative to LPS-stimulated macrophages which are indicated as 100% (n = 3, in triplicate). TGF- $\beta$  contained in culture medium was subtracted from the experimental values. \*, P < 0.05; \*\*\*, P, < 0.001 (Anova/Bonferroni's test) vs. viable Jurkat (A); \* P < 0.05 (two-tailed unpaired t test) vs. viable Jurkat (B).



## **VI. DISCUSSION**

## VI. DISCUSSION

### A. CEPHALOSTATIN 1

A wide range of chemotherapeutic drugs employed in cancer therapy induce apoptosis, most of them by mechanisms involving death receptors and mitochondrial pathways [3,4]. Unfortunately, tumour cells often develop chemoresistances due to defects or mutations in these pathways [6], leading to therapy failure. Hence, novel mechanisms of action are required to resensitise cancer cells to chemotherapy. In this respect, cephalostatins are promising substances. It had been previously described that cephalostatin 1 induces apoptosis in a CD95-, caspase-8- and apoptosome-independent manner [20]. It was sought to further characterise the apoptotic pathways employed by cephalostatin 1, since they could represent novel targets for the development of new cancer chemotherapeutic strategies.

#### 1 REQUIREMENT OF CASPASE-9

Intriguingly, caspase-9 was activated and found essential for cephalostatin 1-induced apoptosis despite the absence of an apoptosome. Thus, caspase-9 can be the central caspase in apoptosome-independent apoptosis. Up to now apoptosome-independent apoptotic cell death has been described in the literature before [210,211], but in these cases apoptosis occurred also independently of caspase-9 activation.

In search of the mechanism(s) responsible for apoptosome-independent caspase-9 activation and apoptosis, it was hypothesised that cephalostatin 1 may target the endoplasmic reticulum (ER) and induce apoptosis by triggering ER-specific pathways.

#### 2 INDUCTION OF ER STRESS

The role of ER stress in tumour development and therapy is unclear at present, although supposedly ER stress response is important for regulating the balance between tumour cell death and its growth as well as for the sensitivity to chemotherapeutic agents [212]. Up to now only a few chemotherapeutic drugs including cisplatin [197,213] and proteasome inhibitors [196-198] have been reported to induce ER stress and ER-related apoptotic pathways. ER stress

pathways linked to apoptosis have been reported in pathological states such as ischemia-reperfusion injury and diabetes as well as in neurodegenerative diseases such as Alzheimer's and Parkinson's disease [76,78,194,214].

The induction of ER stress by cephalostatin 1 was investigated and demonstrated by the influence on several classical ER stress markers. The chaperone protein BiP is a sensor of ER stress as well as a target gene of the unfolded protein response (see III.6.3.2). The increase in BiP levels observed the first hour after stimulation with cephalostatin and later in the apoptotic process (16 h) probably represents an attempt of the cells to survive ER stress. The fast and strong up-regulation of the transcription factor CHOP was a further sign of ER stress and, most importantly, could initiate or potentiate apoptotic pathways through modulation of its target genes. Overexpression of CHOP has clearly shown to lead to cell cycle arrest and/or apoptosis [82,215] and therefore an increase of its expression may represent a new anticancer strategy. Phosphorylation of the translation initiator factor eIF2 $\alpha$ , which leads to an attenuation of general protein synthesis, was particularly strong and sustained upon cephalostatin 1 treatment.

All these ER stress parameters were also modulated by cephalostatin in the carcinoma HeLa cell line and have been described for agents known to induce ER stress such as tunicamycin or thapsigargin [83,215,216], supporting the assumption that cephalostatin 1 induces ER stress.

The next point of interest was to investigate how cephalostatin induces ER stress. Calcium ion ( $\text{Ca}^{2+}$ ) is an intracellular signal playing a dual role in living organisms: necessary for cell survival but also trigger of cell death [90-92,217,218]. It is largely known that disruption in  $\text{Ca}^{2+}$  cellular distribution, normally provoked by the release of  $\text{Ca}^{2+}$  from ER stores, leads to ER stress and apoptosis. Cephalostatin did not induce a noticeable increase in global cytosolic  $\text{Ca}^{2+}$  concentration whereas the positive control thapsigargin did so. It was a surprising result in disaccord with the observed calpain activation by cephalostatin [193]. A possible explanation is that cephalostatin may disrupt the subcellular distribution of  $\text{Ca}^{2+}$ , leading to calpain activation at the ER or Golgi complex membranes. Accordingly, a recent report has proposed that the disregulation of intracellular  $\text{Ca}^{2+}$  linked to an activation of the mitochondrial  $\text{Ca}^{2+}$  uniporter is a critical determinant of bortezomib (a proteasome inhibitor) cytotoxicity [199]. Treatment with cephalostatin 1 neither increased the intracellular production of ROS, which has also been associated with induction of ER stress [195,196].

Proteasome inhibitors constitute a group of promising anticancer agents, able to sensitise malignant cells and tumours to conventional chemotherapy [219,220]. They block the degradation of ubiquitin-targeted proteins, a physiological process required for normal protein turnover. Interestingly, proteasome inhibitors can induce ER stress and initiate ER-specific apoptotic pathways [196-198], probably due to an excessive accumulation of ubiquitinated proteins that leads to protein aggregation and proteotoxicity. Importantly, treatment of Jurkat cells with cephalostatin 1 induced a progressive increase in the number of ubiquitinated proteins with similar kinetics to the induction of ER stress markers. According to this observation, it can be hypothesised that cephalostatin 1 either promotes the ubiquitination of certain target proteins by inducing an ubiquitin ligase or inhibits proteasomal activity leading to an unspecific ubiquitination of cellular proteins.

### **3 ASK1/JNK PATHWAY**

Besides the induction of the pro-apoptotic transcription factor CHOP, other apoptotic pathways can be initiated at the endoplasmic reticulum. ER stress activates JNKs through activation of IRE1 that bind TRAF2, an adaptor protein that couples plasma membrane receptors to JNK activation [80]. JNK activation can promote cell survival as well as death. However, sustained activation of JNK is known to lead to apoptosis and requires activation of ASK1. It is well known that ASK1 is activated in cells treated with death receptor ligands and oxidative stress [200], but also required for ER stress-induced apoptosis [221]. Cephalostatin 1 activates ASK1 very early and induces a strong and sustained activation of JNK. The reduction of DNA fragmentation in Jurkat cells overexpressing a dominant negative form of ASK1 (ASK1-DN) identifies this pathway as an important element in the apoptotic pathway employed by cephalostatin 1.

### **4 INITIATOR CASPASES**

The group of caspases activated under conditions of ER stress has not been completely defined. Only caspase-12 has been characterised as ER-specific initiator caspase [80]. However, functional caspase-12 is lacking in most humans [201] due to a frame shift mutation and a premature stop codon. Human caspase-4 has been recently identified as a gene homologous to caspase-12 and suggested to mediate apoptosis induced by ER stress stimuli as thapsigargin or tunicamycin [80,87] and to be involved in neuronal cell death

in Alzheimer's disease [214]. Caspase-2 is an interesting initiator caspase with still unclear functions. Some reports have linked it to ER stress-induced apoptosis [88,89] and was therefore investigated as a possible mediator of cephalostatin 1-induced cell death.

Caspase-4 was processed and participated in apoptosis upon cephalostatin 1 treatment similarly to the ER stress inducing substances thapsigargin and tunicamycin. In addition, caspase-2 was activated by cephalostatin 1 and thapsigargin and contributed to apoptosis. These results confirmed the importance of ER apoptotic pathways, including members of the caspase family, in cephalostatin 1-induced apoptosis.

#### 4.1 CASPASE-4

Caspase-4 was characterised as an apical caspase in cephalostatin 1 apoptotic pathway. Given that caspase-9 is essential in cephalostatin-induced apoptosis and can be activated by the caspase-4 homologue caspase-12, it was hypothesised that caspase-4 may act upstream of caspase-9. Multiple experiments confirmed this assumption. Caspase-4 was clearly activated in caspase-9-deficient cells but employment of a caspase-4 inhibitor did not reduce DNA fragmentation, suggesting that the apoptotic efficacy of caspase-4 lies on caspase-9. Furthermore, inhibition of caspase-4 inhibited early caspase-9 activity (4 h) as well as the appearance of caspase-9 active fragments (16 and 24 h). In contrast, caspase-4 did not seem to be activated the same modus by thapsigargin and tunicamycin. Caspase-4 was not processed in caspase-9-deficient cells, suggesting that caspase-4 activation may be a downstream event. However, inhibition of caspase-4 by siRNA dramatically inhibited caspase-9 activation. Thus, caspase-4 and caspase-9 may be part of a self-activating caspase cascade, involving a simultaneous activation of caspase-9 at the apoptosome and downstream of previously activated caspase-4.

Two very recent reports argued against the role of caspase-12 and caspase-4 in ER stress-induced apoptosis [222,223]. Certain cell lines (a murine pro-B cell line and a human myeloma cell line) which do not express caspase-12 and caspase-4, respectively, were shown to respond to ER stress agents via apoptotic cell death, which did not differ from cells retransfected with caspase-12 [222]. Furthermore, a neural cell line which has been depleted of caspase-12 by RNA interference was reported to undergo apoptosis upon tunicamycin-induced ER stress [223]. The data presented in this work certainly support the role of caspase-4 in ER stress-induced apoptosis, since it was necessary for caspase-9 activation and apoptosis. However, only upon cephalostatin 1

treatment caspase-4 was activated upstream of caspase-9. Thus, the role of caspase-4 may depend on the cell type and on the mechanism of action of the ER stressor. Importantly, the exceptional mechanism employed by cephalostatin 1 demonstrates that caspase-4 can be activated independently of cytochrome c release and apoptosome formation.

Several mechanisms for the activation of caspase-12 and possibly caspase-4 have been proposed. For example, calpain, a protease that can be activated by calcium released from ER upon ER stress starts cleavage of caspase-12 [99]. Caspase-7 for instance is reported to cleave caspase-12 [224], but is not able to cleave caspase-4 upon sustained ER stress [87]. Caspase-12 and possibly caspase-4 could also be activated via TRAF2 [206] or through the recently described “ERaptosome” [75,225], a putative caspase-activating complex including caspase-12 and caspase-9. A possible role of JNK in caspase-4 activation has also been described [197]. The proteasome inhibitor bortezomib induces ER stress and leads to apoptosis via a mechanism where JNK seems to be responsible for caspase-4 activation. However, cephalostatin 1-induced caspase-4 activation was neither affected by overexpression of ASK1-DN nor inhibition of JNK.

#### **4.2 CASPASE-2**

Caspase-2 activation may be a downstream event [204], but it is accepted that it can be also activated upstream of mitochondrial damage [226]. Indeed, caspase-2 was activated upstream of caspase-9 when cephalostatin 1 or thapsigargin were used. In addition, a caspase-2 specific inhibitor blocked early caspase-9 activation by cephalostatin 1 and reduced the processing of caspase-9 to its active fragments at a later time point. On the contrary, treatment with tunicamycin, which also activates caspase-2 in parental Jurkat cells (data not shown), did not lead to processing of caspase-2 in caspase-9-deficient Jurkat cells, pointing to a downstream activation by caspase-9.

Caspase-2 can be activated by recruitment into a large multiprotein complex independently of Apaf-1 and cytochrome c [203]. This putative complex has been proposed to be the PIDDosome [64], formed by association of the protein PIDD (p53-induced protein with a DD), RAIDD (RIP associated ICH-1/CED-3-homologous protein with DD) and procaspase-2. The PIDDosome was proposed to regulate caspase-2 activation and apoptosis induced by genotoxic agents. Upon recruitment to the complex, caspase-2 was activated and autoprocessed, but it was not clear whether activated caspase-2 was involved in cell death. RAIDD together with caspase-2 has been recently demonstrated

to participate in the induction of apoptosis under conditions of trophic factor withdrawal but not DNA damage [112], arguing against the exclusive formation of the caspase-2 activation complexes by genotoxic stress [64]. Since caspase-2 is able to bind to a range of adaptor proteins [111], different protein complexes may be formed depending on the stimulus and cell type and result in caspase-2 activation. In fact, caspase-2 can form another large complex with TRAF2 and RIP1, leading to a CARD-dependent activation of NF- $\kappa$ B and p38 MAPK [227]. Hence, cephalostatin 1 treatment may induce recruitment of caspase-2 to a multiprotein complex, where it would be activated and subsequently participate in activation of caspase-9.

## 5 CONCLUDING REMARKS AND FUTURE DIRECTIONS

The present work has demonstrated that the ER stress response evoked by cephalostatin 1 activates several apoptotic pathways that, in turn, are able to induce apoptosis efficiently independently from cytochrome c release and apoptosome formation. The ASK1/JNK cascade and ER-associated caspases as caspase-4 were identified as the primary molecular players being involved in apoptosome-independent execution of cell death.

Notably, the identification of caspase-2 and caspase-4 as initiator caspases provided an explanation of how caspase-9 can be activated independently from apoptosome. The dramatic reduction in apoptosis observed upon caspase-9-deficiency was comparable to that observed through the concomitant inhibition of caspase-4 and -2. The mitochondrial protein Smac, which is released selectively upon cephalostatin 1 treatment [193], could act as a stabiliser of active caspase-9 by avoiding its sequestration by XIAP.

Three major questions remain to be answered and require further studies: i) which is the primary target of cephalostatin?, ii) how is ER stress induced? and iii) how is caspase-4 activated by cephalostatin 1? The proteasome complex appears a plausible candidate target for cephalostatin 1. The accumulation of ubiquitinated proteins and the necessity of JNK and caspase-4 for apoptosis are features common to the proteasome inhibitor bortezomib [197].

The novel mechanism of action of cephalostatin 1 makes it a good candidate for the sensitisation of chemotherapy-resistant tumour cells. Engagement of the ER apoptotic pathway by cephalostatin provides a range of promising targets. Caspase-4 is one of the genes stimulated by interferon (INF) treatment and seems to be involved in the sensitisation of tumour cells to apoptosis mediated

by death ligands as TRAIL or FasL [107,109]. The transcription factor CHOP could contribute to cell death by promoting the transcription of the TRAIL receptor DR5 and other target genes.

## B. SESQUITERPENE LACTONES

To understand the cytotoxicity as well as the anti-inflammatory potential of sesquiterpene lactones (SQTL) is an ongoing challenge since decades. Starting with the pioneering work of Kupchan and co-workers [24], numerous studies have been performed that led to the current view that the biological activity of SQTL is dependent on the presence of a cyclopentenone group or other  $\alpha,\beta$ -unsaturated carbonyl functions in addition to an  $\alpha$ -methylene- $\gamma$ -lactone, increasing lipophilicity as well as the number of hydrogen-bond acceptors. The objective of this work was to try to link both activities and find differences in the biological activity depending on the reactive groups.

### 1 INDUCTION OF PCD BY SESQUITERPENE LACTONES

Early structure-activity relationships reported that the presence of the  $\alpha$ -methylene- $\gamma$ -lactone group was essential for the cytotoxic activity of SQTL and an  $\alpha,\beta$ -unsaturated ester or cyclopentenone strengthened this property [24,25]. On the contrary, studies on helenalin derivatives showed that the most active compounds possess both reactive structural elements, but the contribution of a cyclopentenone group to cytotoxicity is considerably higher than that of the methylene lactone group (summarized in [23]). Interestingly, the present study shows that treatment of Jurkat T cells with the  $\alpha$ -methylene- $\gamma$ -lactone 7-hydroxycostunolide (HC) results in a lower IC<sub>50</sub> value (26.5  $\mu$ M) than treatment with the  $\alpha,\beta$ -unsaturated cyclopentenone 11 $\alpha$ ,13-dihydrohelenalin acetate (DHA) (45.8  $\mu$ M), in agreement with the first studies comparing different SQTL. This may be partly due to the freely accessible hydroxyl group in the vicinity of the lactone moiety of HC, which may facilitate anchoring the molecule to the respective proteins [33]. In accordance with all studies, a higher number of reactive centers as in 4 $\beta$ ,15-epoxymiller-9Z-enolide (EM) increases cytotoxicity.

But the most striking differences were observed in the characteristics of cell death induced by SQTL, especially when comparing the monofunctional DHA and HC. The morphology of DHA (cyclopentenone)-induced cell death meets the classical characteristics of apoptosis. In contrast, the  $\alpha$ -methylene- $\gamma$ -lactone SQTL, HC induces an “atypical” form of PCD. The induction of apoptotic

morphology was incredibly rapid (<4 h), accompanied with a strong phosphatidylserine (PS) externalisation and caspase activation, hallmarks of classical apoptosis. In contrast, DNA fragmentation, maybe the parameter mostly used to differentiate apoptosis from other forms of PCD, was not observed upon HC treatment. After long incubation periods (24 h) with HC and EM, both containing an  $\alpha$ -methylene- $\gamma$ -lactone, non-apoptotic cellular morphologies were observed, including swollen cells with a dilated plasma membrane and condensed cytoplasm. At that time point and when compared to DHA, the plasma membrane of HC-treated cells was more permeable to the intracellular enzyme LDH whereas the permeability to PI was very similar, indicating that late apoptotic cells treated with HC may release some intracellular components but membrane integrity is generally maintained.

Whereas the  $\alpha,\beta$ -unsaturated cyclopentenone group of cytotoxic SQTL induces classical apoptosis, the  $\alpha$ -methylene- $\gamma$ -lactone group is responsible for the induction of an atypical form of “apoptosis-like” PCD characterised by caspase activation, strong PS externalisation but absence of DNA fragmentation.

## 2 ANTI-INFLAMMATORY EFFECT

The anti-inflammatory activity of SQTL has been linked mainly to an inhibition of the activity of the transcription factor NF- $\kappa$ B, although there is no agreement in whether the primary target is the transcription factor itself [28,39] or the kinase complex involved in NF- $\kappa$ B activation [38]. Since SQTL are known not only to alleviate inflammation locally but also to exert cytotoxicity, it was hypothesised that in addition to the NF- $\kappa$ B-inhibitory effect, SQTL may contribute to local inflammation/immune resolution by induction of apoptosis in immune cells and subsequent phagocyte removal of dying cells, accompanied by a shift from pro- to anti-inflammatory cytokine release. Several studies had suggested that the  $\alpha$ -methylene- $\gamma$ -lactone moiety was the most important for the anti-inflammatory activity [31,33]. The results obtained in the study of PCD agreed with this hypothesis, since the  $\alpha$ -methylene- $\gamma$ -lactone SQTL induced a stronger PS translocation, the most prominent “eat-me” and immunomodulatory signal on the surface of apoptotic cells.

## 2.1 EFFICIENT REMOVAL OF DYING CELLS

Indeed, the levels of PS in SQTL-treated Jurkat cells were in accordance with the observation that macrophages showed a significant better phagocytic response to HC-treated compared to DHA-, EM-, etoposide-treated or heat-killed (necrotic) Jurkat cells. Phagocytosis of Jurkat cells was investigated by flow cytometry studying different parameters. The increase in cell size of macrophages which had been fed with Jurkat cells correlated perfectly with the levels of PS induced by SQTL treatment. Staining of target cells and measure of the fluorescence of macrophages after co-culture ruled out differences due to a different kinetic in the phagocytosis. It could be questioned whether PS induced a gain of function in the phagocytic activity of macrophages or more macrophages were mobilised to engulf dying cells. Comparing the results obtained when measuring the fluorescence intensity or the percentage of fluorescent macrophages, it seems that PS recruits more macrophages to phagocytose but specially increases their engulfing capacity. Confocal microscopy experiments demonstrated that all the target cells had been efficiently engulfed and not only recognised by macrophages.

The mechanisms of phagocytosis depend on the apoptotic cell type, the means of induction of cell death, the stage of apoptosis, the type and state of differentiation of the phagocyte, and the surrounding microenvironment [120]. THP-1 cells have been reported to express several receptors including the PS receptor [138],  $\alpha\beta_3$  (vitronectin receptor), CD36 [228], CD14 and scavenger receptors (acetylated/oxidized LDL receptors, [229]). They also contain lectin-like proteins on their surface that recognise sugar chains on the target cell [230]. Factors present in serum as protein S [231] or C-reactive protein [148] could bind to PS and enhance phagocytosis. Thus, the “phagocytic synapse” of THP-1 and Jurkat cells appears a complex system. Viable Jurkats are phagocytosed probably due to the inherent activation of THP-1-derived macrophages and the binding to Jurkat cells of molecules present in serum that increase their immunogenicity and make them attractive to macrophages. SQTL-treated Jurkat cells are probably engulfed through the ligation of PS by the PSR and the vitronectin receptor, and the binding of oxidised membrane structures (favoured by the depletion of glutathione that SQTL produce) by scavenger receptors, among others. Cell debris of late apoptotic cells may be recognised by opsonins and receptors of the innate immune system. Etoposide (classical chemotherapeutic drug)-treated Jurkats were phagocytosed similarly to viable Jurkat cells, which could be explained by a very low or absent PS exposure [232]. Heat-killed cells (necrotic) should be basically removed through mechanisms of the innate immune system.

## 2.2 RELEASE OF CYTOKINES BY MACROPHAGES

After confirming the importance of PS in the phagocytosis of SQTL-treated Jurkat cells, a possible modulation of the cytokine profile of engulfing macrophages was studied. This hypothesis was based on *in vitro* observations that apoptotic cells increase release of anti-inflammatory cytokines as IL-10, TGF- $\beta_1$ , PAF and reduce release of TNF- $\alpha$ , IL-1 $\beta$ , IL-12, IL-8, GM-CSF from phagocytating cells [153-156]. *In vivo* models of inflammation had shown that clearance of apoptotic cells in inflammatory lesions leads to accelerated resolution of inflammation, mediated by the increased production of TGF- $\beta_1$  [136,153,154,166,170], cytokine which would also explain the wound healing effect of SQTL.

To check this notion, the concentration of the pro-inflammatory cytokine TNF- $\alpha$  and the anti-inflammatory TGF- $\beta_1$  were measured in culture supernatants. These cytokines and the time points of analysis were chosen according to the literature. Surprisingly, a moderate increase but not a reduction in TNF- $\alpha$  level in the supernatants of macrophages incubated with SQTL was observed. Viable and etoposide-treated Jurkats slightly reduced TNF- $\alpha$  concentration. Interestingly, the ability of SQTL-mediated cell death to increase the number of phagocytating macrophages tended to correlate with the early TNF- $\alpha$  production by macrophages, although only HC-treated Jurkat cells significantly increased TNF- $\alpha$  level in macrophage supernatants. The most pronounced increase in TNF- $\alpha$  production was observed in response to phagocytosis of heat-killed necrotic cells, suggesting that HC-mediated Jurkat cell death shares some features with necrosis. In accordance with this, a recent study [233] reported a necrosis-like cell death induced by some *ent*-kaurene diterpenes possessing also an exocyclic  $\alpha,\beta$ -unsaturated carbonyl group. However, in this study, “necrotic” cell death seemed to be caspase-independent and apoptotic cell death was exclusively evaluated by DNA parameters and permeability to trypan blue [234].

The analysis of TGF- $\beta$  production did not help to establish differences between the SQTL in study but to confirm that SQTL-treated Jurkat cells do not behave as necrotic cells. In fact, they affected TGF- $\beta$  levels similarly to apoptotic cells (etoposide-treated). Only necrotic cells reduced TGF- $\beta$  concentration significantly after 18 h of co-culture when compared to viable cell feeding.

The relative dominance of the receptors engaged in the interaction macrophage-target cell determines the final outcome. For instance, signalling through the immunoglobulin Fc receptor in macrophages can override signalling through the PSR, which in turn appears to override that derived from the Toll-

like receptor 4 [155,235]. Since HC-treated Jurkat cells exposed high levels of PS, a pro-inflammatory stimulus must accompany and temporally override the anti-inflammatory effect of PS but disappear later, because after 18 h of co-culture these cells behaved as classic apoptotic cells. This could be explained by the participation of innate immune stimuli, which normally stimulate pro-inflammatory cytokine production to efficiently eliminate the invading agent. Supporting this hypothesis, an interesting study has shown that the combination of apoptotic cells and ligands for Toll-like receptors (members of the innate immunity) induced an early and sustained secretion of TNF- $\alpha$  by macrophages which was followed, however, by increased late TGF- $\beta_1$  release [236].

In summary, phagocytosis of SQTL-treated immune cells induces an unusual profile of cytokine secretion in macrophages characterised by a transient TNF- $\alpha$  release proposed to stimulate the immune response and a later unmodified or slightly increased level of TGF- $\beta_1$  that ensures the proper resolution of inflammation.

### **3 CONCLUDING REMARKS**

Phagocytosis and subsequent physiological consequences of cells dispatched by PCD other than classical apoptosis have yet been poorly studied. In some forms of necrotic-like PCD, where subsequent phagocytosis was PS-dependent, macrophages were found to react very similarly (if not equally) as to apoptotic cells reducing TNF- $\alpha$  levels [167]. Moreover, the ligation of PS receptor has been proposed as the primary mechanism to block the release of pro-inflammatory cytokines *in vitro* and *in vivo* [170]. This contrasts to this study, which shows that a rapid and strong PS externalization and subsequent phagocytosis may be also accompanied by a transient increase in TNF- $\alpha$  release.

Besides the intriguing concept that cytokine modulation in response to apoptotic cell clearance by macrophages may contribute to resolution of inflammation, phagocytosis *per se* is an essential anti-inflammatory process by protecting tissues from harmful exposure to the inflammatory or immunogenic contents of dying cells. The extremely fast and strong exposure of PS in HC-treated cells ensures that they are properly engulfed by phagocytes, avoiding secondary necrosis and long-term negative consequences for the organism. The ability of HC to stimulate the immune system by increasing the phagocytic activity of macrophages and TNF- $\alpha$  levels transiently would agree with prior structure-activity investigation of the anti-inflammatory activity.

It is highly unlikely to separate the normally wanted anti-inflammatory activity of SQTL from side effects such as toxicity due to unspecific alkylation of biological structures. Preparations from Arnica should be used only externally because of the reported gastrointestinal and cardiac toxicities [237]. Even though the anticancer potential of SQTL is attracting increasing interest [26], structures with lower systemic toxicity should be found before their chemotherapeutic use.



## **VII. SUMMARY**

## VII. SUMMARY

### A. CEPHALOSTATIN 1

The present study demonstrates that the ER stress response evoked by cephalostatin 1 induces specific signalling pathways that lead to apoptosis (represented in Figure VII.1). Interestingly, caspase-9 was found to be necessary for cephalostatin 1-induced apoptosis despite the absence of an apoptosome. Cephalostatin 1 initiates a rapid endoplasmic reticulum (ER) stress response characterised by phosphorylation of the translation initiator factor eIF2 $\alpha$  and increased expression of the chaperone BiP/GRP78 as well as the transcription factor CHOP/GADD153. Activation of apoptosis signal-regulating kinase 1 (ASK1) and c-Jun N-terminal kinase (JNK), presumably activated at the ER membrane through TRAF2, are involved in cephalostatin 1-induced apoptosis, as assessed by stable expression of a dominant negative ASK1. The ER-associated caspase-4 is required and acts upstream of caspase-9 in cephalostatin 1-induced apoptosis. Caspase-2 is activated upstream of caspase-9, probably in a specific complex at the ER nearby, and participates in caspase-9 activation and apoptosis.

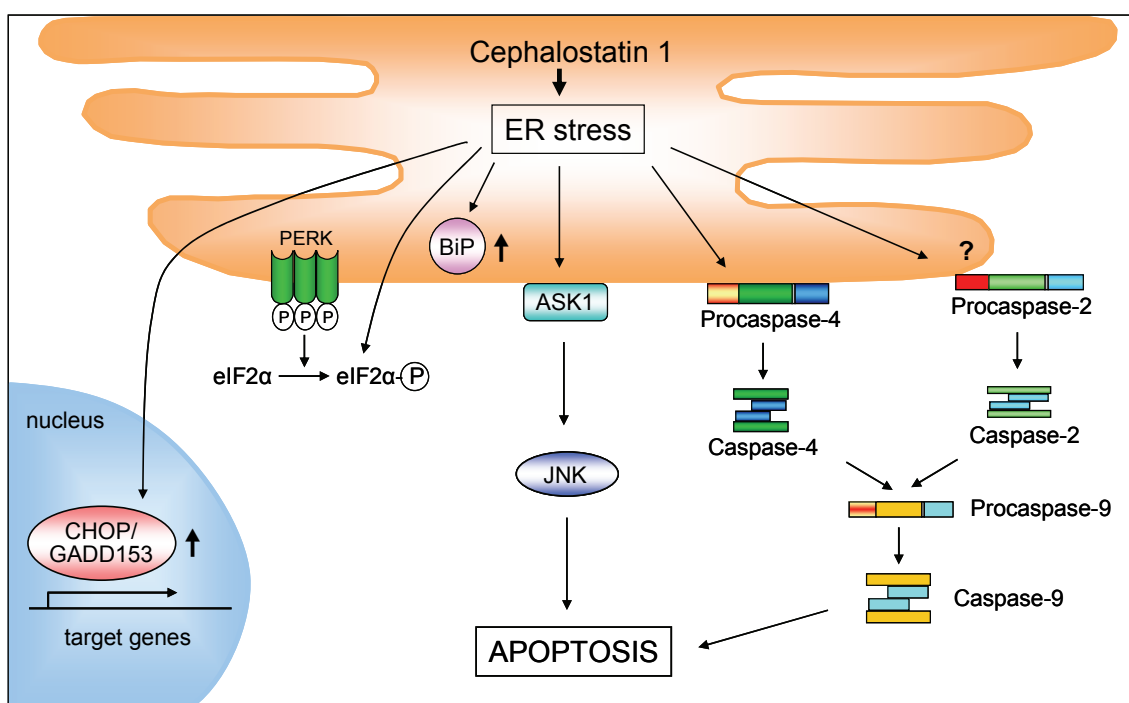


Figure VII.1: Schematic illustration of cephalostatin 1-induced ER stress markers and apoptotic pathways.

Thus, cephalostatin 1 uses the ER stress pathway rather than the classical intrinsic mitochondrial pathway, which might be of advantage in the treatment of tumours chemoresistant due to defects in the mitochondrial pathway.

## B. SESQUITERPENE LACTONES

This work sought to characterise the mode of cell death induced by distinct sesquiterpene lactones (SQTL) and investigate its consequence on macrophage function as a putative anti-inflammatory mechanism. It was found that the  $\alpha,\beta$ -unsaturated cyclopentenone SQTL, DHA, induces classical apoptosis whereas HC, bearing an  $\alpha$ -methylene- $\gamma$ -lactone group, induces a form of “apoptosis-like” programmed cell death that features the following striking characteristics: i) caspase activation, DNA condensation and a rapid and strong induction of apoptotic morphology and translocation of phosphatidylserine (PS); ii) strong induction of the phagocytic response of macrophages that correlates with PS exposure on target cells; iii) a transient increase in TNF- $\alpha$  levels in supernatants after co-culture.

**Table VII.1: Cell death characteristics of 11 $\alpha$ ,13-dihydrohelenalin acetate (DHA) and 7-hydroxycostunolide (HC).**

	$\alpha,\beta$ -unsaturated cyclopentenone (DHA)	$\alpha$ -methylene- $\gamma$ -lactone (HC)
<b>Nuclear morphology</b>	DNA fragmentation	DNA condensation
<b>Apoptotic cell morphology</b>	Progressive	Very rapid (<4h)
<b>Phosphatidylserine exposure</b>	Late and weak	Rapid and strong
<b>Caspase activity</b>	$\approx$ 2 fold (1.86)	$\approx$ 3 fold (3.18)
<b>Nuclear morphology dependent on caspase activation</b>	Yes	Yes
<b>Macrophage response</b>	Weak	Strong

Thus, the external application of HC or similar SQTL in inflamed zones may induce a transient activation of the immune response but a final contribution to inflammation resolution by the clearance of apoptotic inflammatory cells and invading microorganisms. These features may contribute to the beneficial effects attributed to SQTL in the treatment of inflammation and in the wound healing process.



## **VIII. REFERENCES**

## VIII. REFERENCES

1. Chabner, B. A. and Roberts, T. G., Jr. (2005) Timeline: Chemotherapy and the war on cancer. *Nat. Rev. Cancer* **5**, 65-72
2. Allan, J. M. and Travis, L. B. (2005) Mechanisms of therapy-related carcinogenesis. *Nat. Rev. Cancer* **5**, 943-955
3. Kim, R. (2005) Recent advances in understanding the cell death pathways activated by anticancer therapy. *Cancer* **103**, 1551-1560
4. Herr, I. and Debatin, K. M. (2001) Cellular stress response and apoptosis in cancer therapy. *Blood* **98**, 2603-2614
5. Brown, J. M. and Attardi, L. D. (2005) The role of apoptosis in cancer development and treatment response. *Nat. Rev. Cancer* **5**, 231-237
6. Igney, F. H. and Krammer, P. H. (2002) Death and anti-death: tumour resistance to apoptosis. *Nat. Rev. Cancer* **2**, 277-288
7. Pettit, G. R. (1996) Progress in the discovery of biosynthetic anticancer drugs. *J. Nat. Prod.* **59**, 812-821
8. Mann, J. (2002) Natural products in cancer chemotherapy: past, present and future. *Nat. Rev. Cancer* **2**, 143-148
9. Urban, S., Hickford, S. J. H., Blunt, J. W., and Munro, M. H. G. (2000) Bioactive marine alkaloids. *Current Organic Chemistry* **4**, 765-807
10. Pettit, G. R., Inoue, M., Kamano, Y., Herald, D. L., Arm, C., Dufresne, C., Christie, N. D., Schmidt, J. M., Doubek, D. L., and Krupa, T. S. (1988) Isolation and Structure of the Powerful Cell-Growth Inhibitor Cephalostatin-1. *Journal of the American Chemical Society* **110**, 2006-2007
11. Pettit, G. R., Inoue, M., Kamano, Y., Dufresne, C., Christie, N., Niven, M. L., and Herald, D. L. (1988) Isolation and Structure of the Hemichordate Cell-Growth Inhibitors Cephalostatin-2, Cephalostatin-3, and Cephalostatin-4. *Journal of the Chemical Society-Chemical Communications* 865-867
12. Pettit, G. R., Kamano, Y., Dufresne, C., Inoue, M., Christie, N., Schmidt, J. M., and Doubek, D. L. (1989) Isolation and Structure of the Unusual Indian-Ocean Cephalodiscus-Gilchristi Components, Cephalostatins 5 and 6. *Canadian Journal of Chemistry-Revue Canadienne de Chimie* **67**, 1509-1513
13. Pettit, G. R., Kamano, Y., Inoue, M., Dufresne, C., Boyd, M. R., Herald, C. L., Schmidt, J. M., Doubek, D. L., and Christie, N. D. (1992) Antineoplastic Agents .214. Isolation and Structure of Cephalostatins 7-9. *Journal of Organic Chemistry* **57**, 429-431

14. Pettit, G. R., Xu, J. P., Williams, M. D., Christie, N. D., Doubek, D. L., Schmidt, J. M., and Boyd, M. R. (1994) Isolation and Structure of Cephalostatin-10 and Cephalostatin-11. *Journal of Natural Products* **57**, 52-63
15. Pettit, G. R., Ichihara, Y., Xu, J. P., Boyd, M. R., and Williams, M. D. (1994) Isolation and Structure of the Symmetrical Disteroidal Alkaloids Cephalostatin-12 and Cephalostatin-13. *Bioorganic & Medicinal Chemistry Letters* **4**, 1507-1512
16. Pettit, G. R., Xu, J. P., Ichihara, Y., Williams, M. D., and Boyd, M. R. (1994) Antineoplastic Agents .285. Isolation and Structures of Cephalostatin-14 and Cephalostatin-15. *Canadian Journal of Chemistry-Revue Canadienne de Chimie* **72**, 2260-2267
17. Pettit, G. R., Xu, J. P., Schmidt, J. M., and Boyd, M. R. (1995) Isolation and Structure of the Exceptional Pterobranchia Human Cancer Inhibitors Cephalostatin-16 and Cephalostatin-17. *Bioorganic & Medicinal Chemistry Letters* **5**, 2027-2032
18. Pettit, G. R., Tan, R., Xu, J. P., Ichihara, Y., Williams, M. D., and Boyd, M. R. (1998) Antineoplastic agents. 398. Isolation and structure elucidation of cephalostatins 18 and 19. *Journal of Natural Products* **61**, 955-958
19. [http://www.graptolite.net/pterobranchia/C\\_densus.html](http://www.graptolite.net/pterobranchia/C_densus.html) 2006-02-07.
20. Dirsch, V. M., Muller, I. M., Eichhorst, S. T., Pettit, G. R., Kamano, Y., Inoue, M., Xu, J. P., Ichihara, Y., Wanner, G., and Vollmar, A. M. (2003) Cephalostatin 1 selectively triggers the release of Smac/DIABLO and subsequent apoptosis that is characterized by an increased density of the mitochondrial matrix. *Cancer Res.* **63**, 8869-8876
21. Lacour, T. G., Guo, C. X., Bhandaru, S., Boyd, M. R., and Fuchs, P. L. (1998) Interphylal product splicing: The first total syntheses of cephalostatin 1, the north hemisphere of ritterazine G, and the highly active hybrid analogue, ritterostatin G(N)1(N). *Journal of the American Chemical Society* **120**, 692-707
22. <http://dtp.nci.nih.gov/dtpstandard/servlet/MeanGraph?searchtype=NSC&searchlist=363979&outputformat=HTML&outputmedium=page&chemnameboolean=AND&debugswitch=false&assaytype=&testshortname=NCI+Cancer+Screen+Current+Data&dataarraylength=70&endpt=GI50&button=Mean+Graph&highconc=-6.0> 2006-02-07.
23. Schmidt, T. J. (1999) Toxic activities of sesquiterpene lactones: Structural and biochemical aspects. *Current Organic Chemistry* **3**, 577-608
24. Kupchan, S. M., Eakin, M. A., and Thomas, A. M. (1971) Tumor Inhibitors .69. Structure-Cytotoxicity Relationships Among Sesquiterpene Lactones. *Journal of Medicinal Chemistry* **14**, 1147-&

25. Lee, K. H., Huang, E. S., PIANTADO.C, Pagano, J. S., and Geissman, T. A. (1971) Cytotoxicity of Sesquiterpene Lactones. *Cancer Research* **31**, 1649-&
26. Zhang, S., Won, Y. K., Ong, C. N., and Shen, H. M. (2005) Anti-cancer potential of sesquiterpene lactones: bioactivity and molecular mechanisms. *Curr. Med. Chem. Anti.-Canc. Agents* **5**, 239-249
27. Schmidt, T. J. and Heilmann, J. (2002) Quantitative structure-cytotoxicity relationships of sesquiterpene lactones derived from partial charge ( $\bar{Q}$ )-based fractional accessible surface area descriptors (Q\_frASAs). *Quantitative Structure-Activity Relationships* **21**, 276-287
28. Lyss, G., Knorre, A., Schmidt, T. J., Pahl, H. L., and Merfort, I. (1998) The anti-inflammatory sesquiterpene lactone helenalin inhibits the transcription factor NF-kappaB by directly targeting p65. *J. Biol. Chem.* **273**, 33508-33516
29. Gertsch, J., Sticher, O., Schmidt, T., and Heilmann, J. (2003) Influence of helenanolide-type sesquiterpene lactones on gene transcription profiles in Jurkat T cells and human peripheral blood cells: anti-inflammatory and cytotoxic effects. *Biochem. Pharmacol.* **66**, 2141-2153
30. Klaas, C. A., Wagner, G., Sosa, S., Della Loggia, R., Bomme, U., Pahl, H. L., and Merfort, I. (2002) Studies on the anti-inflammatory activity of phytopharmaceuticals prepared from Arnica flowers. *Planta Medica* **68**, 385-391
31. Hall, I. H., Starnes, C. O., Jr., Lee, K. H., and Waddell, T. G. (1980) Mode of action of sesquiterpene lactones as anti-inflammatory agents. *J. Pharm. Sci.* **69**, 537-543
32. Siedle, B., Gustavsson, L., Johansson, S., Murillo, R., Castro, V., Bohlin, L., and Merfort, I. (2003) The effect of sesquiterpene lactones on the release of human neutrophil elastase. *Biochem. Pharmacol.* **65**, 897-903
33. Siedle, B., Garcia-Pineres, A. J., Murillo, R., Schulte-Monting, J., Castro, V., Rungeier, P., Klaas, C. A., Da Costa, F. B., Kisiel, W., and Merfort, I. (2004) Quantitative structure-activity relationship of sesquiterpene lactones as inhibitors of the transcription factor NF-kappaB. *J. Med. Chem.* **47**, 6042-6054
34. <http://www.bi.ku.dk/tavler/thumbs/557,01.jpg> 2006-02-07.
35. <http://botanical.com/botanical/mgmh/a/arnic058.html> 2006-02-07.
36. <http://www.j-lorber.de/jl/hson/arnikabluete-kl.jpg> 2006-02-07.
37. Schmidt, T. J. (1997) Helenanolide-type sesquiterpene lactones--III. Rates and stereochemistry in the reaction of helenalin and related helenanolides with sulphhydryl containing biomolecules. *Bioorg. Med. Chem.* **5**, 645-653
38. Hehner, S. P., Hofmann, T. G., Droge, W., and Schmitz, M. L. (1999) The antiinflammatory sesquiterpene lactone parthenolide inhibits NF-

- kappa B by targeting the I kappa B kinase complex. *J. Immunol.* **163**, 5617-5623
39. Garcia-Pineres, A. J., Castro, V., Mora, G., Schmidt, T. J., Strunck, E., Pahl, H. L., and Merfort, I. (2001) Cysteine 38 in p65/NF-kappaB plays a crucial role in DNA binding inhibition by sesquiterpene lactones. *J. Biol. Chem.* **276**, 39713-39720
40. Lee, K. H., Hall, I. H., Mar, E. C., Starnes, C. O., Elgebaly, S. A., Waddell, T. G., Hadgraft, R. I., Ruffner, C. G., and Weidner, I. (1977) Antitumor Agents .20. Sesquiterpene Antitumor Agents - Inhibitors of Cellular-Metabolism. *Science* **196**, 533-536
41. Belzacq, A. S., El Hamel, C., Vieira, H. L., Cohen, I., Haouzi, D., Metivier, D., Marchetti, P., Brenner, C., and Kroemer, G. (2001) Adenine nucleotide translocator mediates the mitochondrial membrane permeabilization induced by lonidamine, arsenite and CD437. *Oncogene* **20**, 7579-7587
42. Beekman, A. C., Woerdenbag, H. J., vanUden, W., Pras, N., Konings, A. W. T., Wikstrom, H. V., and Schmidt, T. J. (1997) Structure - Cytotoxicity relationships of some helenanolide-type sesquiterpene lactones. *Journal of Natural Products* **60**, 252-257
43. Dirsch, V. M., Stuppner, H., and Vollmar, A. M. (2001) Helenalin triggers a CD95 death receptor-independent apoptosis that is not affected by overexpression of Bcl-x(L) or Bcl-2. *Cancer Res.* **61**, 5817-5823
44. Assuncao, G. C. and Linden, R. (2004) Programmed cell deaths. Apoptosis and alternative deathstyles. *Eur. J. Biochem.* **271**, 1638-1650
45. Chipuk, J. E. and Green, D. R. (2005) Do inducers of apoptosis trigger caspase-independent cell death? *Nat. Rev. Mol. Cell Biol.* **6**, 268-275
46. Kerr, J. F., Wyllie, A. H., and Currie, A. R. (1972) Apoptosis: a basic biological phenomenon with wide-ranging implications in tissue kinetics. *Br. J. Cancer* **26**, 239-257
47. Leist, M. and Jaattela, M. (2001) Four deaths and a funeral: from caspases to alternative mechanisms. *Nat. Rev. Mol. Cell Biol.* **2**, 589-598
48. Zhang, B., Arany, Z., Mann, D., Rhee, J. G., and Fenton, R. G. (2005) Partitioning apoptosis: a novel form of the execution phase of apoptosis. *Apoptosis*. **10**, 219-231
49. Fink, S. L. and Cookson, B. T. (2005) Apoptosis, pyroptosis, and necrosis: mechanistic description of dead and dying eukaryotic cells. *Infect. Immun.* **73**, 1907-1916
50. Broker, L. E., Krut, F. A., and Giaccone, G. (2005) Cell death independent of caspases: a review. *Clin. Cancer Res.* **11**, 3155-3162
51. Jaattela, M. and Tschoopp, J. (2003) Caspase-independent cell death in T lymphocytes. *Nat. Immunol.* **4**, 416-423

52. Jaattela, M. (2004) Multiple cell death pathways as regulators of tumour initiation and progression. *Oncogene* **23**, 2746-2756
53. Nicotera, P. and Melino, G. (2004) Regulation of the apoptosis-necrosis switch. *Oncogene* **23**, 2757-2765
54. <http://medinfo.ufl.edu/pa/chuck/fall/handouts/injury.htm> 2006-02-07.
55. Danial, N. N. and Korsmeyer, S. J. (2004) Cell death: critical control points. *Cell* **116**, 205-219
56. Philchenkov, A. A. (2003) Caspases as regulators of apoptosis and other cell functions. *Biochemistry (Mosc.)* **68**, 365-376
57. Lavrik, I. N., Golks, A., and Krammer, P. H. (2005) Caspases: pharmacological manipulation of cell death. *J. Clin. Invest* **115**, 2665-2672
58. Chang, D. W., Ditsworth, D., Liu, H., Srinivasula, S. M., Alnemri, E. S., and Yang, X. (2003) Oligomerization is a general mechanism for the activation of apoptosis initiator and inflammatory procaspases. *J. Biol. Chem.* **278**, 16466-16469
59. Donepudi, M. and Grutter, M. G. (2002) Structure and zymogen activation of caspases. *Biophys. Chem.* **101-102**, 145-153
60. Fuentes-Prior, P. and Salvesen, G. S. (2004) The protein structures that shape caspase activity, specificity, activation and inhibition. *Biochem. J.* **384**, 201-232
61. Shi, Y. (2002) Mechanisms of caspase activation and inhibition during apoptosis. *Mol. Cell* **9**, 459-470
62. Fischer, U., Janicke, R. U., and Schulze-Osthoff, K. (2003) Many cuts to ruin: a comprehensive update of caspase substrates. *Cell Death. Differ.* **10**, 76-100
63. Shi, Y. (2004) Caspase activation: revisiting the induced proximity model. *Cell* **117**, 855-858
64. Tinel, A. and Tschoopp, J. (2004) The PIDDosome, a protein complex implicated in activation of caspase-2 in response to genotoxic stress. *Science* **304**, 843-846
65. Martinon, F. and Tschoopp, J. (2004) Inflammatory caspases: linking an intracellular innate immune system to autoinflammatory diseases. *Cell* **117**, 561-574
66. Martinon, F., Burns, K., and Tschoopp, J. (2002) The inflammasome: a molecular platform triggering activation of inflammatory caspases and processing of proIL-beta. *Mol. Cell* **10**, 417-426
67. Riedl, S. J. and Shi, Y. (2004) Molecular mechanisms of caspase regulation during apoptosis. *Nat. Rev. Mol. Cell Biol.* **5**, 897-907

68. Zaffaroni, N., Pennati, M., and Daidone, M. G. (2005) Survivin as a target for new anticancer interventions. *J. Cell Mol. Med.* **9**, 360-372
69. Zhou, Q. and Salvesen, G. S. (2000) Viral caspase inhibitors CrmA and p35. *Methods Enzymol.* **322**, 143-154
70. Ferri, K. F. and Kroemer, G. (2001) Organelle-specific initiation of cell death pathways. *Nat. Cell Biol.* **3**, E255-E263
71. Ravagnan, L., Roumier, T., and Kroemer, G. (2002) Mitochondria, the killer organelles and their weapons. *J. Cell Physiol* **192**, 131-137
72. Hengartner, M. O. (2000) The biochemistry of apoptosis. *Nature* **407**, 770-776
73. Sitia, R. and Braakman, I. (2003) Quality control in the endoplasmic reticulum protein factory. *Nature* **426**, 891-894
74. Dobson, C. M. (2003) Protein folding and misfolding. *Nature* **426**, 884-890
75. Rao, R. V., Ellerby, H. M., and Bredesen, D. E. (2004) Coupling endoplasmic reticulum stress to the cell death program. *Cell Death. Differ.* **11**, 372-380
76. Schroder, M. and Kaufman, R. J. (2005) ER stress and the unfolded protein response. *Mutat. Res.* **569**, 29-63
77. Breckenridge, D. G., Germain, M., Mathai, J. P., Nguyen, M., and Shore, G. C. (2003) Regulation of apoptosis by endoplasmic reticulum pathways. *Oncogene* **22**, 8608-8618
78. Oyadomari, S., Araki, E., and Mori, M. (2002) Endoplasmic reticulum stress-mediated apoptosis in pancreatic beta-cells. *Apoptosis*. **7**, 335-345
79. Kadowaki, H., Nishitoh, H., and Ichijo, H. (2004) Survival and apoptosis signals in ER stress: the role of protein kinases. *J. Chem. Neuroanat.* **28**, 93-100
80. Momoi, T. (2004) Caspases involved in ER stress-mediated cell death. *J. Chem. Neuroanat.* **28**, 101-105
81. Goldberg, A. L. (2003) Protein degradation and protection against misfolded or damaged proteins. *Nature* **426**, 895-899
82. Oyadomari, S. and Mori, M. (2004) Roles of CHOP/GADD153 in endoplasmic reticulum stress. *Cell Death. Differ.* **11**, 381-389
83. Zinszner, H., Kuroda, M., Wang, X., Batchvarova, N., Lightfoot, R. T., Remotti, H., Stevens, J. L., and Ron, D. (1998) CHOP is implicated in programmed cell death in response to impaired function of the endoplasmic reticulum. *Genes Dev.* **12**, 982-995

84. Rao, R. V., Castro-Obregon, S., Frankowski, H., Schuler, M., Stoka, V., del Rio, G., Bredesen, D. E., and Ellerby, H. M. (2002) Coupling endoplasmic reticulum stress to the cell death program. An Apaf-1-independent intrinsic pathway. *J. Biol. Chem.* **277**, 21836-21842
85. Morishima, N., Nakanishi, K., Takenouchi, H., Shibata, T., and Yasuhiko, Y. (2002) An endoplasmic reticulum stress-specific caspase cascade in apoptosis. Cytochrome c-independent activation of caspase-9 by caspase-12. *J. Biol. Chem.* **277**, 34287-34294
86. Rao, R. V., Hermel, E., Castro-Obregon, S., del Rio, G., Ellerby, L. M., Ellerby, H. M., and Bredesen, D. E. (2001) Coupling endoplasmic reticulum stress to the cell death program. Mechanism of caspase activation. *J. Biol. Chem.* **276**, 33869-33874
87. Hitomi, J., Katayama, T., Eguchi, Y., Kudo, T., Taniguchi, M., Koyama, Y., Manabe, T., Yamagishi, S., Bando, Y., Imaizumi, K., Tsujimoto, Y., and Tohyama, M. (2004) Involvement of caspase-4 in endoplasmic reticulum stress-induced apoptosis and A $\beta$ -induced cell death. *J. Cell Biol.* **165**, 347-356
88. Bando, Y., Katayama, T., Taniguchi, M., Ishibashi, T., Matsuo, N., Ogawa, S., and Tohyama, M. (2005) RA410/Sly1 suppresses MPP+ and 6-hydroxydopamine-induced cell death in SH-SY5Y cells. *Neurobiol. Dis.* **18**, 143-151
89. Dahmer, M. K. (2005) Caspases-2, -3, and -7 are involved in thapsigargin-induced apoptosis of SH-SY5Y neuroblastoma cells. *J. Neurosci. Res.* **80**, 576-583
90. Rizzuto, R., Pinton, P., Ferrari, D., Chami, M., Szabadkai, G., Magalhaes, P. J., Di Virgilio, F., and Pozzan, T. (2003) Calcium and apoptosis: facts and hypotheses. *Oncogene* **22**, 8619-8627
91. Hajnoczky, G., Davies, E., and Madesh, M. (2003) Calcium signaling and apoptosis. *Biochem. Biophys. Res. Commun.* **304**, 445-454
92. Orrenius, S., Zhivotovsky, B., and Nicotera, P. (2003) Regulation of cell death: the calcium-apoptosis link. *Nat. Rev. Mol. Cell Biol.* **4**, 552-565
93. Wang, H. G., Pathan, N., Ethell, I. M., Krajewski, S., Yamaguchi, Y., Shibusaki, F., McKeon, F., Bobo, T., Franke, T. F., and Reed, J. C. (1999) Ca<sup>2+</sup>-induced apoptosis through calcineurin dephosphorylation of BAD. *Science* **284**, 339-343
94. Suzuki, K., Hata, S., Kawabata, Y., and Sorimachi, H. (2004) Structure, activation, and biology of calpain. *Diabetes* **53 Suppl 1**, S12-S18
95. Friedrich, P. (2004) The intriguing Ca<sup>2+</sup> requirement of calpain activation. *Biochem. Biophys. Res. Commun.* **323**, 1131-1133
96. Khorchid, A. and Ikura, M. (2002) How calpain is activated by calcium. *Nat. Struct. Biol.* **9**, 239-241

97. Wang, K. K. (2000) Calpain and caspase: can you tell the difference? *Trends Neurosci.* **23**, 20-26
98. Yamashima, T. (2004) Ca<sup>2+</sup>-dependent proteases in ischemic neuronal death: a conserved 'calpain-cathepsin cascade' from nematodes to primates. *Cell Calcium* **36**, 285-293
99. Nakagawa, T. and Yuan, J. (2000) Cross-talk between two cysteine protease families. Activation of caspase-12 by calpain in apoptosis. *J. Cell Biol.* **150**, 887-894
100. Rudner, J., Jendrossek, V., and Belka, C. (2002) New insights in the role of Bcl-2 Bcl-2 and the endoplasmic reticulum. *Apoptosis*. **7**, 441-447
101. Thomenius, M. J. and Distelhorst, C. W. (2003) Bcl-2 on the endoplasmic reticulum: protecting the mitochondria from a distance. *J. Cell Sci.* **116**, 4493-4499
102. Scorrano, L., Oakes, S. A., Opferman, J. T., Cheng, E. H., Sorcinelli, M. D., Pozzan, T., and Korsmeyer, S. J. (2003) BAX and BAK regulation of endoplasmic reticulum Ca<sup>2+</sup>: a control point for apoptosis. *Science* **300**, 135-139
103. Demaurex, N. and Distelhorst, C. (2003) Cell biology. Apoptosis--the calcium connection. *Science* **300**, 65-67
104. Morishima, N., Nakanishi, K., Tsuchiya, K., Shibata, T., and Seiwa, E. (2004) Translocation of Bim to the endoplasmic reticulum (ER) mediates ER stress signaling for activation of caspase-12 during ER stress-induced apoptosis. *J. Biol. Chem.* **279**, 50375-50381
105. Kamada, S., Washida, M., Hasegawa, J., Kusano, H., Funahashi, Y., and Tsujimoto, Y. (1997) Involvement of caspase-4(-like) protease in Fas-mediated apoptotic pathway. *Oncogene* **15**, 285-290
106. Young, T., Mei, F., Liu, J., Bast, R. C., Kurosky, A., and Cheng, X. (2005) Proteomics analysis of H-RAS-mediated oncogenic transformation in a genetically defined human ovarian cancer model. *Oncogene*
107. Chawla-Sarkar, M., Lindner, D. J., Liu, Y. F., Williams, B. R., Sen, G. C., Silverman, R. H., and Borden, E. C. (2003) Apoptosis and interferons: role of interferon-stimulated genes as mediators of apoptosis. *Apoptosis*. **8**, 237-249
108. Yang, X., Wang, J., Liu, C., Grizzle, W. E., Yu, S., Zhang, S., Barnes, S., Koopman, W. J., Mountz, J. D., Kimberly, R. P., and Zhang, H. G. (2005) Cleavage of p53-vimentin complex enhances tumor necrosis factor-related apoptosis-inducing ligand-mediated apoptosis of rheumatoid arthritis synovial fibroblasts. *Am. J. Pathol.* **167**, 705-719
109. Martin, C. A. and Panja, A. (2002) Cytokine regulation of human intestinal primary epithelial cell susceptibility to Fas-mediated apoptosis. *Am. J. Physiol Gastrointest. Liver Physiol* **282**, G92-G104

110. Pelletier, N., Casamayor-Palleja, M., De, L. K., Mondiere, P., Saltel, F., Jurdic, P., Bella, C., Genestier, L., and Defrance, T. (2006) The endoplasmic reticulum is a key component of the plasma cell death pathway. *J. Immunol.* **176**, 1340-1347
111. Zhivotovsky, B. and Orrenius, S. (2005) Caspase-2 function in response to DNA damage. *Biochem. Biophys. Res. Commun.* **331**, 859-867
112. Wang, Q., Maniati, M., Jabado, O., Pavlaki, M., Troy, C. M., Greene, L. A., and Stefanis, L. (2006) RAIDD is required for apoptosis of PC12 cells and sympathetic neurons induced by trophic factor withdrawal. *Cell Death Differ.* **13**, 75-83
113. Wang, L., Miura, M., Bergeron, L., Zhu, H., and Yuan, J. (1994) Ich-1, an Ice/ced-3-related gene, encodes both positive and negative regulators of programmed cell death. *Cell* **78**, 739-750
114. Troy, C. M., Rabacchi, S. A., Friedman, W. J., Frappier, T. F., Brown, K., and Shelanski, M. L. (2000) Caspase-2 mediates neuronal cell death induced by beta-amyloid. *J. Neurosci.* **20**, 1386-1392
115. Hood, J. L., Logan, B. B., Sinai, A. P., Brooks, W. H., and Roszman, T. L. (2003) Association of the calpain/calpastatin network with subcellular organelles. *Biochem. Biophys. Res. Commun.* **310**, 1200-1212
116. Hood, J. L., Brooks, W. H., and Roszman, T. L. (2004) Differential compartmentalization of the calpain/calpastatin network with the endoplasmic reticulum and Golgi apparatus. *J. Biol. Chem.* **279**, 43126-43135
117. Missiaen, L., Van Acker, K., Van Baelen, K., Raeymaekers, L., Wuytack, F., Parys, J. B., De Smedt, H., Vanoevelen, J., Dode, L., Rizzuto, R., and Callewaert, G. (2004) Calcium release from the Golgi apparatus and the endoplasmic reticulum in HeLa cells stably expressing targeted aequorin to these compartments. *Cell Calcium* **36**, 479-487
118. Mancini, M., Machamer, C. E., Roy, S., Nicholson, D. W., Thornberry, N. A., Casciola-Rosen, L. A., and Rosen, A. (2000) Caspase-2 is localized at the Golgi complex and cleaves golgin-160 during apoptosis. *J. Cell Biol.* **149**, 603-612
119. Lauber, K., Blumenthal, S. G., Waibel, M., and Wesselborg, S. (2004) Clearance of apoptotic cells: getting rid of the corpses. *Mol. Cell* **14**, 277-287
120. de Almeida, C. J. and Linden, R. (2005) Phagocytosis of apoptotic cells: a matter of balance. *Cell Mol. Life Sci.* **62**, 1532-1546
121. Bratton, D. L., Fadok, V. A., Richter, D. A., Kailey, J. M., Guthrie, L. A., and Henson, P. M. (1997) Appearance of phosphatidylserine on apoptotic cells requires calcium-mediated nonspecific flip-flop and is enhanced by loss of the aminophospholipid translocase. *J. Biol. Chem.* **272**, 26159-26165

122. Williamson, P. and Schlegel, R. A. (2002) Transbilayer phospholipid movement and the clearance of apoptotic cells. *Biochim. Biophys. Acta* **1585**, 53-63
123. Hamon, Y., Chambenoit, O., and Chimini, G. (2002) ABCA1 and the engulfment of apoptotic cells. *Biochim. Biophys. Acta* **1585**, 64-71
124. Turner, C., Devitt, A., Parker, K., MacFarlane, M., Giuliano, M., Cohen, G. M., and Gregory, C. D. (2003) Macrophage-mediated clearance of cells undergoing caspase-3-independent death. *Cell Death. Differ.* **10**, 302-312
125. Egger, L., Schneider, J., Rheme, C., Tapernoux, M., Hacki, J., and Borner, C. (2003) Serine proteases mediate apoptosis-like cell death and phagocytosis under caspase-inhibiting conditions. *Cell Death. Differ.* **10**, 1188-1203
126. Cocco, R. E. and Ucker, D. S. (2001) Distinct modes of macrophage recognition for apoptotic and necrotic cells are not specified exclusively by phosphatidylserine exposure. *Mol. Biol. Cell* **12**, 919-930
127. Eda, S., Yamanaka, M., and Beppu, M. (2004) Carbohydrate-mediated phagocytic recognition of early apoptotic cells undergoing transient capping of CD43 glycoprotein. *J. Biol. Chem.* **279**, 5967-5974
128. Beppu, M., Ando, K., Saeki, M., Yokoyama, N., and Kikugawa, K. (2000) Binding of oxidized Jurkat cells to THP-1 macrophages and antiband 3 IgG through sialylated poly-N-acetyllactosaminyl sugar chains. *Arch. Biochem. Biophys.* **384**, 368-374
129. Kagan, V. E., Gleiss, B., Tyurina, Y. Y., Tyurin, V. A., Elenstrom-Magnusson, C., Liu, S. X., Serinkan, F. B., Arroyo, A., Chandra, J., Orrenius, S., and Fadeel, B. (2002) A role for oxidative stress in apoptosis: oxidation and externalization of phosphatidylserine is required for macrophage clearance of cells undergoing Fas-mediated apoptosis. *J. Immunol.* **169**, 487-499
130. Kagan, V. E., Fabisiak, J. P., Shvedova, A. A., Tyurina, Y. Y., Tyurin, V. A., Schor, N. F., and Kawai, K. (2000) Oxidative signaling pathway for externalization of plasma membrane phosphatidylserine during apoptosis. *FEBS Lett.* **477**, 1-7
131. Arroyo, A., Modriansky, M., Serinkan, F. B., Bello, R. I., Matsura, T., Jiang, J., Tyurin, V. A., Tyurina, Y. Y., Fadeel, B., and Kagan, V. E. (2002) NADPH oxidase-dependent oxidation and externalization of phosphatidylserine during apoptosis in Me2SO-differentiated HL-60 cells. Role in phagocytic clearance. *J. Biol. Chem.* **277**, 49965-49975
132. Fadok, V. A., Bratton, D. L., and Henson, P. M. (2001) Phagocyte receptors for apoptotic cells: recognition, uptake, and consequences. *J. Clin. Invest* **108**, 957-962
133. Henson, P. M., Bratton, D. L., and Fadok, V. A. (2001) Apoptotic cell removal. *Curr. Biol.* **11**, R795-R805

134. Fadok, V. A. and Chimini, G. (2001) The phagocytosis of apoptotic cells. *Semin. Immunol.* **13**, 365-372
135. Moreira, M. E. and Barcinski, M. A. (2004) Apoptotic cell and phagocyte interplay: recognition and consequences in different cell systems. *An. Acad. Bras. Cienc.* **76**, 93-115
136. Gregory, C. D. and Devitt, A. (2004) The macrophage and the apoptotic cell: an innate immune interaction viewed simplistically? *Immunology* **113**, 1-14
137. Fadeel, B. (2003) Programmed cell clearance. *Cell Mol. Life Sci.* **60**, 2575-2585
138. Fadok, V. A., Bratton, D. L., Rose, D. M., Pearson, A., Ezekowitz, R. A., and Henson, P. M. (2000) A receptor for phosphatidylserine-specific clearance of apoptotic cells. *Nature* **405**, 85-90
139. Li, M. O., Sarkisian, M. R., Mehal, W. Z., Rakic, P., and Flavell, R. A. (2003) Phosphatidylserine receptor is required for clearance of apoptotic cells. *Science* **302**, 1560-1563
140. Henson, P. M., Bratton, D. L., and Fadok, V. A. (2001) The phosphatidylserine receptor: a crucial molecular switch? *Nat. Rev. Mol. Cell Biol.* **2**, 627-633
141. Hoffmann, P. R., deCathelineau, A. M., Ogden, C. A., Leverrier, Y., Bratton, D. L., Daleke, D. L., Ridley, A. J., Fadok, V. A., and Henson, P. M. (2001) Phosphatidylserine (PS) induces PS receptor-mediated macropinocytosis and promotes clearance of apoptotic cells. *J. Cell Biol.* **155**, 649-659
142. Hanayama, R., Tanaka, M., Miwa, K., Shinohara, A., Iwamatsu, A., and Nagata, S. (2002) Identification of a factor that links apoptotic cells to phagocytes. *Nature* **417**, 182-187
143. Hanayama, R., Tanaka, M., Miyasaka, K., Aozasa, K., Koike, M., Uchiyama, Y., and Nagata, S. (2004) Autoimmune disease and impaired uptake of apoptotic cells in MFG-E8-deficient mice. *Science* **304**, 1147-1150
144. Scott, R. S., McMahon, E. J., Pop, S. M., Reap, E. A., Caricchio, R., Cohen, P. L., Earp, H. S., and Matsushima, G. K. (2001) Phagocytosis and clearance of apoptotic cells is mediated by MER. *Nature* **411**, 207-211
145. Fadok, V. A., Warner, M. L., Bratton, D. L., and Henson, P. M. (1998) CD36 is required for phagocytosis of apoptotic cells by human macrophages that use either a phosphatidylserine receptor or the vitronectin receptor (alpha v beta 3). *J. Immunol.* **161**, 6250-6257
146. Fadok, V. A. and Henson, P. M. (2003) Apoptosis: giving phosphatidylserine recognition an assist--with a twist. *Curr. Biol.* **13**, R655-R657

147. Roos, A., Xu, W., Castellano, G., Nauta, A. J., Garred, P., Daha, M. R., and van Kooten, C. (2004) Mini-review: A pivotal role for innate immunity in the clearance of apoptotic cells. *Eur. J. Immunol.* **34**, 921-929
148. Gershov, D., Kim, S., Brot, N., and Elkon, K. B. (2000) C-Reactive protein binds to apoptotic cells, protects the cells from assembly of the terminal complement components, and sustains an antiinflammatory innate immune response: implications for systemic autoimmunity. *J. Exp. Med.* **192**, 1353-1364
149. Nauta, A. J., Raaschou-Jensen, N., Roos, A., Daha, M. R., Madsen, H. O., Borrias-Essers, M. C., Ryder, L. P., Koch, C., and Garred, P. (2003) Mannose-binding lectin engagement with late apoptotic and necrotic cells. *Eur. J. Immunol.* **33**, 2853-2863
150. Vandivier, R. W., Ogden, C. A., Fadok, V. A., Hoffmann, P. R., Brown, K. K., Botto, M., Walport, M. J., Fisher, J. H., Henson, P. M., and Greene, K. E. (2002) Role of surfactant proteins A, D, and C1q in the clearance of apoptotic cells in vivo and in vitro: calreticulin and CD91 as a common collectin receptor complex. *J. Immunol.* **169**, 3978-3986
151. Leverrier, Y. and Ridley, A. J. (2001) Requirement for Rho GTPases and PI 3-kinases during apoptotic cell phagocytosis by macrophages. *Curr. Biol.* **11**, 195-199
152. Brown, S., Heinisch, I., Ross, E., Shaw, K., Buckley, C. D., and Savill, J. (2002) Apoptosis disables CD31-mediated cell detachment from phagocytes promoting binding and engulfment. *Nature* **418**, 200-203
153. Huynh, M. L., Fadok, V. A., and Henson, P. M. (2002) Phosphatidylserine-dependent ingestion of apoptotic cells promotes TGF-beta1 secretion and the resolution of inflammation. *J. Clin. Invest* **109**, 41-50
154. Voll, R. E., Herrmann, M., Roth, E. A., Stach, C., Kalden, J. R., and Girkontaite, I. (1997) Immunosuppressive effects of apoptotic cells. *Nature* **390**, 350-351
155. Fadok, V. A., Bratton, D. L., Konowal, A., Freed, P. W., Westcott, J. Y., and Henson, P. M. (1998) Macrophages that have ingested apoptotic cells in vitro inhibit proinflammatory cytokine production through autocrine/paracrine mechanisms involving TGF-beta, PGE2, and PAF. *J. Clin. Invest* **101**, 890-898
156. McDonald, P. P., Fadok, V. A., Bratton, D., and Henson, P. M. (1999) Transcriptional and translational regulation of inflammatory mediator production by endogenous TGF-beta in macrophages that have ingested apoptotic cells. *J. Immunol.* **163**, 6164-6172
157. Xiao, Y. Q., Malcolm, K., Worthen, G. S., Gardai, S., Schiemann, W. P., Fadok, V. A., Bratton, D. L., and Henson, P. M. (2002) Cross-talk between ERK and p38 MAPK mediates selective suppression of pro-inflammatory cytokines by transforming growth factor-beta. *J. Biol. Chem.* **277**, 14884-14893

158. Camenisch, T. D., Koller, B. H., Earp, H. S., and Matsushima, G. K. (1999) A novel receptor tyrosine kinase, Mer, inhibits TNF-alpha production and lipopolysaccharide-induced endotoxic shock. *J. Immunol.* **162**, 3498-3503
159. Park, J. S., Svetkauskaite, D., He, Q., Kim, J. Y., Strassheim, D., Ishizaka, A., and Abraham, E. (2004) Involvement of toll-like receptors 2 and 4 in cellular activation by high mobility group box 1 protein. *J. Biol. Chem.* **279**, 7370-7377
160. Vandivier, R. W., Fadok, V. A., Hoffmann, P. R., Bratton, D. L., Penvari, C., Brown, K. K., Brain, J. D., Accurso, F. J., and Henson, P. M. (2002) Elastase-mediated phosphatidylserine receptor cleavage impairs apoptotic cell clearance in cystic fibrosis and bronchiectasis. *J. Clin. Invest* **109**, 661-670
161. Fadok, V. A., Bratton, D. L., Guthrie, L., and Henson, P. M. (2001) Differential effects of apoptotic versus lysed cells on macrophage production of cytokines: role of proteases. *J. Immunol.* **166**, 6847-6854
162. Kurosaka, K., Watanabe, N., and Kobayashi, Y. (1998) Production of proinflammatory cytokines by phorbol myristate acetate-treated THP-1 cells and monocyte-derived macrophages after phagocytosis of apoptotic CTLL-2 cells. *J. Immunol.* **161**, 6245-6249
163. Kawagishi, C., Kurosaka, K., Watanabe, N., and Kobayashi, Y. (2001) Cytokine production by macrophages in association with phagocytosis of etoposide-treated P388 cells in vitro and in vivo. *Biochim. Biophys. Acta* **1541**, 221-230
164. Kurosaka, K., Watanabe, N., and Kobayashi, Y. (2001) Production of proinflammatory cytokines by resident tissue macrophages after phagocytosis of apoptotic cells. *Cell Immunol.* **211**, 1-7
165. Misawa, R., Kawagishi, C., Watanabe, N., and Kobayashi, Y. (2001) Infiltration of neutrophils following injection of apoptotic cells into the peritoneal cavity. *Apoptosis*. **6**, 411-417
166. Savill, J., Dransfield, I., Gregory, C., and Haslett, C. (2002) A blast from the past: clearance of apoptotic cells regulates immune responses. *Nat. Rev. Immunol.* **2**, 965-975
167. Hirt, U. A. and Leist, M. (2003) Rapid, noninflammatory and PS-dependent phagocytic clearance of necrotic cells. *Cell Death. Differ.* **10**, 1156-1164
168. Reddy, S. M., Hsiao, K. H., Abernethy, V. E., Fan, H., Longacre, A., Lieberthal, W., Rauch, J., Koh, J. S., and Levine, J. S. (2002) Phagocytosis of apoptotic cells by macrophages induces novel signaling events leading to cytokine-independent survival and inhibition of proliferation: activation of Akt and inhibition of extracellular signal-regulated kinases 1 and 2. *J. Immunol.* **169**, 702-713
169. Pope, R. M. (2002) Apoptosis as a therapeutic tool in rheumatoid arthritis. *Nat. Rev. Immunol.* **2**, 527-535

170. Maderna, P. and Godson, C. (2003) Phagocytosis of apoptotic cells and the resolution of inflammation. *Biochim. Biophys. Acta* **1639**, 141-151
171. Freire-de-Lima, C. G., Nascimento, D. O., Soares, M. B., Bozza, P. T., Castro-Faria-Neto, H. C., de Mello, F. G., DosReis, G. A., and Lopes, M. F. (2000) Uptake of apoptotic cells drives the growth of a pathogenic trypanosome in macrophages. *Nature* **403**, 199-203
172. Hotchkiss, R. S., Chang, K. C., Grayson, M. H., Tinsley, K. W., Dunne, B. S., Davis, C. G., Osborne, D. F., and Karl, I. E. (2003) Adoptive transfer of apoptotic splenocytes worsens survival, whereas adoptive transfer of necrotic splenocytes improves survival in sepsis. *Proc. Natl. Acad. Sci. U. S. A* **100**, 6724-6729
173. Docke, W. D., Randow, F., Syrbe, U., Krausch, D., Asadullah, K., Reinke, P., Volk, H. D., and Kox, W. (1997) Monocyte deactivation in septic patients: restoration by IFN-gamma treatment. *Nat. Med.* **3**, 678-681
174. Bondanza, A., Rovere, P., Borri, A., Caremoli, E. R., Guidetti, A., Citterio, G., Consogno, G., Zimmermann, V. S., Rugarli, C., and Manfredi, A. A. (2001) Cytokine secretion associated with the clearance of apoptotic bodies in renal cell carcinoma patients. *Int. J. Cancer* **91**, 713-717
175. Bergsmedh, A., Szeles, A., Henriksson, M., Bratt, A., Folkman, M. J., Spetz, A. L., and Holmgren, L. (2001) Horizontal transfer of oncogenes by uptake of apoptotic bodies. *Proc. Natl. Acad. Sci. U. S. A* **98**, 6407-6411
176. Willuhn, G., Kresken, J., and Leven, W. (1990) Further Helenanolides from the Flowers of Arnica-Chamissonis Subsp Foliosa. *Planta Medica* **56**, 111-114
177. Castro, V., Murillo, R., Klaas, C. A., Meunier, C., Mora, G., Pahl, H. L., and Merfort, I. (2000) Inhibition of the transcription factor NF-kappa B by sesquiterpene lactones from Podachaenium eminens. *Planta Medica* **66**, 591-595
178. Castro, V., Rungeler, P., Murillo, R., Hernandez, E., Mora, G., Pahl, H. L., and Merfort, I. (2000) Study of sesquiterpene lactones from Milleria quinqueflora on their anti-inflammatory activity using the transcription factor NF-kappa B as molecular target. *Phytochemistry* **53**, 257-263
179. Hofmann, T. G., Moller, A., Hehner, S. P., Welsch, D., Droge, W., and Schmitz, M. L. (2001) CD95-induced JNK activation signals are transmitted by the death-inducing signaling complex (DISC), but not by Daxx. *Int. J. Cancer* **93**, 185-191
180. [http://www.ueb.cas.cz/.../Basic\\_principles.htm](http://www.ueb.cas.cz/.../Basic_principles.htm) 2006-01-12.
181. <http://www.petermac.org/pdf/Intro%20to%20Flow%20Cytometry%20.pdf> 2006-01-12.
182. Nicoletti, I., Migliorati, G., Pagliacci, M. C., Grignani, F., and Riccardi, C. (1991) A rapid and simple method for measuring thymocyte apoptosis by

- propidium iodide staining and flow cytometry. *J. Immunol. Methods* **139**, 271-279
183. López-Antón, N., Hermann, C., Murillo, R., Merfort, I., Vollmar, A. M., and Dirsch, V. M. Sesquiterpene lactone-induced cell death modulates human macrophage response dependent on their reactive groups. (*Submitted*)
184. Bergmeyer, H. U. (1974) Methods of Enzymatic Analysis. Academic, New York.
185. [http://www.zeiss.de/C1256CFB00332E16/0/1A64C9DC85D5FD63C1256CFC0026FF71/\\$file/45-0008\\_d.pdf](http://www.zeiss.de/C1256CFB00332E16/0/1A64C9DC85D5FD63C1256CFC0026FF71/$file/45-0008_d.pdf) 2006-01-12.
186. Stennicke, H. R., Deveraux, Q. L., Humke, E. W., Reed, J. C., Dixit, V. M., and Salvesen, G. S. (1999) Caspase-9 can be activated without proteolytic processing. *J. Biol. Chem.* **274**, 8359-8362
187. Bradford, M. M. (1976) A rapid and sensitive method for the quantitation of microgram quantities of protein utilizing the principle of protein-dye binding. *Anal. Biochem.* **72**, 248-254
188. Laemmli, U. K. (1970) Cleavage of structural proteins during the assembly of the head of bacteriophage T4. *Nature* **227**, 680-685
189. McManus, M. T. and Sharp, P. A. (2002) Gene silencing in mammals by small interfering RNAs. *Nat. Rev. Genet.* **3**, 737-747
190. [http://www.invivogen.com/PDF/psiRNA-h7SKneo\\_TDS.pdf](http://www.invivogen.com/PDF/psiRNA-h7SKneo_TDS.pdf) 2006-02-08.
191. Sambrook, J., Fritsch, E. F., and Maniatis, T. (1989) Molecular Cloning : A Laboratory Manual. Second edition. Cold Spring Harbour Laboratory press., New York.
192. Ndolo, T., Dhillon, N. K., Nguyen, H., Guadalupe, M., Mudryj, M., and Dandekar, S. (2002) Simian immunodeficiency virus Nef protein delays the progression of CD4+ T cells through G1/S phase of the cell cycle. *J. Virol.* **76**, 3587-3595
193. MÜLLER, I. M. "Characterisation of apoptosis signal transduction induced by the marine compound cephalostatin 1 in leukemic cells". Dissertation. LMU München. Department of Pharmacy, Munich, 2004
194. Paschen, W. (2003) Endoplasmic reticulum: a primary target in various acute disorders and degenerative diseases of the brain. *Cell Calcium* **34**, 365-383
195. Xue, X., Piao, J. H., Nakajima, A., Sakon-Komazawa, S., Kojima, Y., Mori, K., Yagita, H., Okumura, K., Harding, H., and Nakano, H. (2005) Tumor necrosis factor alpha (TNFalpha) induces the unfolded protein response (UPR) in a reactive oxygen species (ROS)-dependent fashion, and the UPR counteracts ROS accumulation by TNFalpha. *J. Biol. Chem.* **280**, 33917-33925

196. Fribley, A., Zeng, Q., and Wang, C. Y. (2004) Proteasome inhibitor PS-341 induces apoptosis through induction of endoplasmic reticulum stress-reactive oxygen species in head and neck squamous cell carcinoma cells. *Mol. Cell Biol.* **24**, 9695-9704
197. Nawrocki, S. T., Carew, J. S., Pino, M. S., Highshaw, R. A., Dunner, K., Jr., Huang, P., Abbruzzese, J. L., and McConkey, D. J. (2005) Bortezomib sensitizes pancreatic cancer cells to endoplasmic reticulum stress-mediated apoptosis. *Cancer Res.* **65**, 11658-11666
198. Nawrocki, S. T., Carew, J. S., Dunner, K., Jr., Boise, L. H., Chiao, P. J., Huang, P., Abbruzzese, J. L., and McConkey, D. J. (2005) Bortezomib inhibits PKR-like endoplasmic reticulum (ER) kinase and induces apoptosis via ER stress in human pancreatic cancer cells. *Cancer Res.* **65**, 11510-11519
199. Landowski, T. H., Megli, C. J., Nullmeyer, K. D., Lynch, R. M., and Dorr, R. T. (2005) Mitochondrial-mediated disregulation of Ca<sup>2+</sup> is a critical determinant of Velcade (PS-341/bortezomib) cytotoxicity in myeloma cell lines. *Cancer Res.* **65**, 3828-3836
200. Tobiume, K., Matsuzawa, A., Takahashi, T., Nishitoh, H., Morita, K., Takeda, K., Minowa, O., Miyazono, K., Noda, T., and Ichijo, H. (2001) ASK1 is required for sustained activations of JNK/p38 MAP kinases and apoptosis. *EMBO Rep.* **2**, 222-228
201. Fischer, H., Koenig, U., Eckhart, L., and Tschachler, E. (2002) Human caspase 12 has acquired deleterious mutations. *Biochem. Biophys. Res. Commun.* **293**, 722-726
202. Garcia-Calvo, M., Peterson, E. P., Leiting, B., Ruel, R., Nicholson, D. W., and Thornberry, N. A. (1998) Inhibition of human caspases by peptide-based and macromolecular inhibitors. *J. Biol. Chem.* **273**, 32608-32613
203. Read, S. H., Baliga, B. C., Ekert, P. G., Vaux, D. L., and Kumar, S. (2002) A novel Apaf-1-independent putative caspase-2 activation complex. *J. Cell Biol.* **159**, 739-745
204. O'Reilly, L. A., Ekert, P., Harvey, N., Marsden, V., Cullen, L., Vaux, D. L., Hacker, G., Magnusson, C., Pakusch, M., Cecconi, F., Kuida, K., Strasser, A., Huang, D. C., and Kumar, S. (2002) Caspase-2 is not required for thymocyte or neuronal apoptosis even though cleavage of caspase-2 is dependent on both Apaf-1 and caspase-9. *Cell Death. Differ.* **9**, 832-841
205. Takeda, K., Matsuzawa, A., Nishitoh, H., and Ichijo, H. (2003) Roles of MAPKKK ASK1 in stress-induced cell death. *Cell Struct. Funct.* **28**, 23-29
206. Yoneda, T., Imaizumi, K., Oono, K., Yui, D., Gomi, F., Katayama, T., and Tohyama, M. (2001) Activation of caspase-12, an endoplasmic reticulum (ER) resident caspase, through tumor necrosis factor receptor-associated factor 2-dependent mechanism in response to the ER stress. *J. Biol. Chem.* **276**, 13935-13940

207. Fadok, V. A., de Cathelineau, A., Daleke, D. L., Henson, P. M., and Bratton, D. L. (2001) Loss of phospholipid asymmetry and surface exposure of phosphatidylserine is required for phagocytosis of apoptotic cells by macrophages and fibroblasts. *J. Biol. Chem.* **276**, 1071-1077
208. Jersmann, H. P., Ross, K. A., Vivers, S., Brown, S. B., Haslett, C., and Dransfield, I. (2003) Phagocytosis of apoptotic cells by human macrophages: analysis by multiparameter flow cytometry. *Cytometry* **51A**, 7-15
209. Anderson, H. A., Maylock, C. A., Williams, J. A., Paweletz, C. P., Shu, H., and Shacter, E. (2003) Serum-derived protein S binds to phosphatidylserine and stimulates the phagocytosis of apoptotic cells. *Nat. Immunol.* **4**, 87-91
210. Marsden, V. S., O'Connor, L., O'Reilly, L. A., Silke, J., Metcalf, D., Ekert, P. G., Huang, D. C., Cecconi, F., Kuida, K., Tomaselli, K. J., Roy, S., Nicholson, D. W., Vaux, D. L., Bouillet, P., Adams, J. M., and Strasser, A. (2002) Apoptosis initiated by Bcl-2-regulated caspase activation independently of the cytochrome c/Apaf-1/caspase-9 apoptosome. *Nature* **419**, 634-637
211. Henderson, C. J., Aleo, E., Fontanini, A., Maestro, R., Paroni, G., and Brancolini, C. (2005) Caspase activation and apoptosis in response to proteasome inhibitors. *Cell Death. Differ.* **12**, 1240-1254
212. Ma, Y. and Hendershot, L. M. (2004) The role of the unfolded protein response in tumour development: friend or foe? *Nat. Rev. Cancer* **4**, 966-977
213. Mandic, A., Hansson, J., Linder, S., and Shoshan, M. C. (2003) Cisplatin induces endoplasmic reticulum stress and nucleus-independent apoptotic signaling. *J. Biol. Chem.* **278**, 9100-9106
214. Katayama, T., Imaizumi, K., Manabe, T., Hitomi, J., Kudo, T., and Tohyama, M. (2004) Induction of neuronal death by ER stress in Alzheimer's disease. *J. Chem. Neuroanat.* **28**, 67-78
215. McCullough, K. D., Martindale, J. L., Klotz, L. O., Aw, T. Y., and Holbrook, N. J. (2001) Gadd153 sensitizes cells to endoplasmic reticulum stress by down-regulating Bcl2 and perturbing the cellular redox state. *Mol. Cell Biol.* **21**, 1249-1259
216. Lu, P. D., Jousse, C., Marciniak, S. J., Zhang, Y., Novoa, I., Scheuner, D., Kaufman, R. J., Ron, D., and Harding, H. P. (2004) Cytoprotection by pre-emptive conditional phosphorylation of translation initiation factor 2. *EMBO J.* **23**, 169-179
217. Berridge, M. J., Bootman, M. D., and Roderick, H. L. (2003) Calcium signalling: dynamics, homeostasis and remodelling. *Nat. Rev. Mol. Cell Biol.* **4**, 517-529
218. Berridge, M. J., Lipp, P., and Bootman, M. D. (2000) The versatility and universality of calcium signalling. *Nat. Rev. Mol. Cell Biol.* **1**, 11-21

219. Voorhees, P. M., Dees, E. C., O'Neil, B., and Orlowski, R. Z. (2003) The proteasome as a target for cancer therapy. *Clin. Cancer Res.* **9**, 6316-6325
220. Adams, J. (2004) The development of proteasome inhibitors as anticancer drugs. *Cancer Cell* **5**, 417-421
221. Kadowaki, H., Nishitoh, H., Urano, F., Sadamitsu, C., Matsuzawa, A., Takeda, K., Masutani, H., Yodoi, J., Urano, Y., Nagano, T., and Ichijo, H. (2005) Amyloid beta induces neuronal cell death through ROS-mediated ASK1 activation. *Cell Death Differ.* **12**, 19-24
222. Obeng, E. A. and Boise, L. H. (2005) Caspase-12 and caspase-4 are not required for caspase-dependent endoplasmic reticulum stress-induced apoptosis. *J. Biol. Chem.* **280**, 29578-29587
223. Di, S. F., Ferraro, E., Tufi, R., Achsel, T., Piacentini, M., and Cecconi, F. (2005) ER stress induces apoptosis by an apoptosome-dependent but caspase 12-independent mechanism. *J. Biol. Chem.* **281**, 2693-2700
224. Rao, R. V., Peel, A., Logvinova, A., del Rio, G., Hermel, E., Yokota, T., Goldsmith, P. C., Ellerby, L. M., Ellerby, H. M., and Bredesen, D. E. (2002) Coupling endoplasmic reticulum stress to the cell death program: role of the ER chaperone GRP78. *FEBS Lett.* **514**, 122-128
225. Rao, R. V., Poksay, K. S., Castro-Obregon, S., Schilling, B., Row, R. H., del, R. G., Gibson, B. W., Ellerby, H. M., and Bredesen, D. E. (2004) Molecular components of a cell death pathway activated by endoplasmic reticulum stress. *J. Biol. Chem.* **279**, 177-187
226. Lassus, P., Opitz-Araya, X., and Lazebnik, Y. (2002) Requirement for caspase-2 in stress-induced apoptosis before mitochondrial permeabilization. *Science* **297**, 1352-1354
227. Lamkanfi, M., D'hondt, K., Vande, W. L., van Gurp, M., Denecker, G., Demeulemeester, J., Kalai, M., Declercq, W., Saelens, X., and Vandenebeele, P. (2005) A novel caspase-2 complex containing TRAF2 and RIP1. *J. Biol. Chem.* **280**, 6923-6932
228. Alessio, M., De Monte, L., Scirea, A., Gruarin, P., Tandon, N. N., and Sitia, R. (1996) Synthesis, processing, and intracellular transport of CD36 during monocytic differentiation. *J. Biol. Chem.* **271**, 1770-1775
229. Nishimura, N., Harada-Shiba, M., Tajima, S., Sugano, R., Yamamura, T., Qiang, Q. Z., and Yamamoto, A. (1998) Acquisition of secretion of transforming growth factor-beta 1 leads to autonomous suppression of scavenger receptor activity in a monocyte-macrophage cell line, THP-1. *J. Biol. Chem.* **273**, 1562-1567
230. Eda, S., Beppu, M., Yokoyama, N., and Kikugawa, K. (2001) Novel lectin-like proteins on the surface of human monocytic leukemia cell line THP-1 cells that recognize oxidized cells. *Arch. Biochem. Biophys.* **385**, 186-193

231. Kask, L., Trouw, L. A., Dahlback, B., and Blom, A. M. (2004) The C4b-binding protein-protein S complex inhibits the phagocytosis of apoptotic cells. *J. Biol. Chem.* **279**, 23869-23873
232. Tyurina, Y. Y., Serinkan, F. B., Tyurin, V. A., Kini, V., Yalowich, J. C., Schroit, A. J., Fadeel, B., and Kagan, V. E. (2004) Lipid antioxidant, etoposide, inhibits phosphatidylserine externalization and macrophage clearance of apoptotic cells by preventing phosphatidylserine oxidation. *J. Biol. Chem.* **279**, 6056-6064
233. Suzuki, I., Kondoh, M., Nagashima, F., Fujii, M., Asakawa, Y., and Watanabe, Y. (2004) A comparison of apoptosis and necrosis induced by ent-kaurene-type diterpenoids in HL-60 cells. *Planta Med.* **70**, 401-406
234. Nagashima, F., Kasai, W., Kondoh, M., Fujii, M., Watanabe, Y., Braggins, J. E., and Asakawa, Y. (2003) New ent-kaurene-type diterpenoids possessing cytotoxicity from the New Zealand liverwort *Jungermannia* species. *Chem. Pharm. Bull. (Tokyo)* **51**, 1189-1192
235. Geske, F. J., Monks, J., Lehman, L., and Fadok, V. A. (2002) The role of the macrophage in apoptosis: hunter, gatherer, and regulator. *Int. J. Hematol.* **76**, 16-26
236. Lucas, M., Stuart, L. M., Savill, J., and Lacy-Hulbert, A. (2003) Apoptotic cells and innate immune stimuli combine to regulate macrophage cytokine secretion. *J. Immunol.* **171**, 2610-2615
237. Merfort, I. (2003) [Arnica: new insights on the molecular mode of action of a traditional medicinal plant]. *Forsch. Komplementarmed. Klass. Naturheilkd.* **10 Suppl 1**, 45-48

## **IX. APPENDIX**

## IX. APPENDIX

### 1 ALPHABETICAL LIST OF COMPANIES

Agfa	Cologne, Germany
Amaxa	Cologne, Germany
Amersham Biosciences	Freiburg, Germany
BD Biosciences	Heidelberg, Germany
Beckman Coulter	Krefeld, Germany
Biomers.net	Ulm, Germany
Bio-Rad	Munich, Germany
Biotrend	Cologne, Germany
Biozol	Eching, Germany
Calbiochem	Schwalbach, Germany
Cell Signalling/New England Biolabs	Frankfurt/Main, Germany
DakoCytomation	Hamburg, Germany
Dianova	Hamburg, Germany
Gerhardt	Königswinter, Germany
Gibco/Invitrogen	Karlsruhe, Germany
Invivogen	San Diego California, USA
MBL	Woburn, Massachusetts, USA
Medigenomics	Martinsried, Germany
Merck	Darmstadt, Germany
Molecular Probes/Invitrogen	Karlsruhe, Germany
PAA Laboratories	Cölbe, Germany
PAN Biotech	Aidenbach, Germany
Perkin Elmer	Überlingen, Germany
Promega	Mannheim, Germany
Qiagen	Hilden, Germany
Roche	Mannheim, Germany
Roth	Karlsruhe, Germany
Shimadzu	Duisburg, Germany
Sigma-Aldrich	Taufkirchen, Germany
Tecan	Crailsheim, Germany
TILL Photonics	Gräfelfing, Germany
Zeiss	Oberkochen, Germany

## **2 PUBLICATIONS**

### **2.1 ABSTRACTS**

López-Antón, N., Rudy, A., Barth, N., Müller, I.M., Schmitz, M.L., Pettit, G.R., Dirsch, V.M., Vollmar, A.M.

Cephalostatin 1 activates an ER stress-specific and apoptosome-independent apoptotic signal pathway.

Jahrestagung der Deutschen Pharmazeutischen Gesellschaft, October 5-8, 2005, Mainz, Germany.

Lopez N., Merfort I., Castro V., Vollmar A.M., Dirsch V.M.

Variations in the mode of cell death induced by sesquiterpene lactones influence the response of macrophages.

45<sup>th</sup> Spring Meeting of the Deutsche Gesellschaft für experimentelle und klinische Pharmakologie und Toxikologie, March 9-11, 2004, Mainz, Germany.

Naunyn-Schmiedeberg's Archive of Pharmacology, Vol. 369, Suppl. 1.

### **2.2 ORIGINAL PUBLICATIONS**

N. López-Antón, A. Rudy, N. Barth, M.L. Schmitz, G.R. Pettit, K. Schulze-Osthoff, V.M. Dirsch, A.M. Vollmar.

The marine product cephalostatin 1 activates an ER stress-specific and apoptosome-independent apoptotic signalling pathway.

*Submitted*

N. López-Antón, C. Hermann, R. Murillo, I. Merfort, A.M. Vollmar, V.M. Dirsch.

Sesquiterpene lactone-induced cell death modulates human macrophage response dependent on their reactive groups.

*Submitted*

### 3 CURRICULUM VITAE

#### Persönliche Daten

Name	Nancy López Antón
Geburtsdatum	11.09.1978
Geburtsort	Sabadell (Barcelona, Spanien)
Staatsangehörigkeit	Spanisch
Familienstand	Ledig

#### Schulbildung

09/1984 – 06/1992	CP Serraparera, Cerdanyola del Vallès [Grundschule]
09/1992 – 06/1996	IB Pere Calders, Bellaterra – Cerdanyola del Vallès [Gymnasium]
06/1996	PAAU an der Universitat Autònoma de Barcelona, Bellaterra – Cerdanyola del Vallès [Hochschulzulassungsprüfung vgl. mit Abitur]

#### Studium, Promotion

09/1996 – 09/2001	Studium der Pharmazie, Universitat de Barcelona – Fakultät für Pharmazie  Praktisches Semester in der T. Álvarez-Apotheke, Cerdanyola del Vallès
09/2002 – 02/2006	Promotion am Lehrstuhl von Prof. Dr. A. M. Vollmar, Zentrum für Pharmaforschung, Department Pharmazie, LMU München

#### **4 ACKNOWLEDGEMENTS**

First and foremost, I want to thank Prof. Dr. Angelika M. Vollmar for giving me the opportunity to perform this doctoral thesis in her research group. I am deeply grateful for her permanent professional as well as personal support and encouragement.

Furthermore, I would like to thank Prof. Dr. Verena M. Dirsch for her constant support, expert guidance and patience throughout the course of this work.

Special thanks go to my thesis committee, especially PD. Dr. C. Culmsee for acting as second examiner.

Many thanks go to PD. Dr. S. Zahler for his expert guidance and patience, foremost in the calcium measures and the use of the confocal microscope.

I am very much obliged to Dr. Nicole Barth for her permanent and unlimited helpfulness. Her experience and aid was critical for the successful carrying out of the siRNA experiments.

I am deeply grateful to all the members of the working group for the great work atmosphere and for always being ready to help. Special thanks go to H-P, Ursula, Thomas and Irina for their warm reception in the laboratory. My dearest thanks go to my lab colleagues Thomas and Irina for their friendship and enjoyable company as well as Kathi, Anita and Anja for the great time in- and outside the laboratory. Particularly, I am deeply indebted to Anja for her patience and support in Mainz.

Last, but not least I want to thank David for his never-ending comprehension and encouragement and my family for their support over the distance.

